Flexible and Stretchable Energy Storage: Recent Advances and Future Perspectives

*Wei Liu, Min-Sang Song, Biao Kong, and Yi Cui**

Energy-storage technologies such as lithium-ion batteries and supercapacitors have become fundamental building blocks in modern society. Recently, the emerging direction toward the ever-growing market of flexible and wearable electronics has nourished progress in building multifunctional energy-storage systems that can be bent, folded, crumpled, and stretched while maintaining their electrochemical functions under deformation. Here, recent progress and well-developed strategies in research designed to accomplish flexible and stretchable lithium-ion batteries and supercapacitors are reviewed. The challenges of developing novel materials and configurations with tailored features, and in designing simple and large-scaled manufacturing methods that can be widely utilized are considered. Furthermore, the perspectives and opportunities for this emerging field of materials science and engineering are also discussed.

1. Introduction

Ever-increasing energy demands and depleting fossil fuel resources require the exploration of sustainable energy-conversion and energy storage systems that are reliable, low-cost and environmentally friendly, which is one of the key challenges that our society is facing. We have seen very impressive progress in developing electrochemical energy-storage systems such as lithium-ion batteries (LIBs) and supercapacitors (SCs) for the applications ranging from portable devices and electric vehicles to grid-scale energy-storage systems over the last two to three decades.[1] In recent years, owing to the perspective and expectation toward high-tech designs and products with more advanced functions and technological innovations by consumers in our modern society, exploring applicable devices and opening up novel application opportunities is consistently and significantly considered. Electronic devices that can be flexible, bendable, foldable and stretchable, such as wearable electronics, electronic papers, smart clothes, electronic skins, displays, bendable smart phones and implantable medical devices, have been required urgently.[2] As a result, to power these devices, there is a persistent need for developing equally flexible[3] and stretchable[4] energy-storage systems that can be conformal with deformation while retaining their electrochemical functions.

LIBs are one of the most ideal candidates of power sources for electronic devices owing to high energy density and power density, and cycle life.[5] In comparison to LIBs, SCs endow high power density and moderate energy density, which have also attracted growing attention in recent years.[6] Conventional LIBs and SCs are typically rigid and heavy, due to the currently used fabrication processes based on slurry-casting method and traditional configuration. The conventional electrode is prepared by coating slurry containing active materials, conductive materials (carbon black) and polymer binder on current collector and followed by drying and pressing. The electrode materials are therefore easily detached from the current collector, and it is difficult for metallic current collectors to recover to their original shape by repeated bending/releasing, which in turn deteriorates the electrochemical performance. The delaminated electrode materials are even able to penetrate separator and subsequently cause short circuit and thermal runaway. LIBs and SCs consist several main components including cathode and anode, separator/electrolyte, current collector and package materials.[7] All of the components are required to be capable to be deformed with a compatible feature for flexible and stretchable LIBs and SCs. Since the conventional components are not deformable enough, it is highly desirable that all of them should be replaced by the deformable new ones. Currently, the investigation of flexible and stretchable LIBs and SCs face three key challenges: i) design and fabrication of flexible and stretchable electrodes; ii) electrochemical performance stability at dynamic status; iii) high energy density and power density. The development in the field of flexible and stretchable energy-storage systems is still at the early stage of lab research. Hence, exploring novel approaches for flexible and stretchable energy storage remains an urgently academic and industrial challenge.[8]

Dr. W. Liu, Dr. M.-S. Song, Dr. B. Kong, Prof. Y. Cui
Department of Materials Science and Engineering
Stanford University
Stanford, CA 94305, USA
E-mail: yicui@stanford.edu
Dr. M.-S. Song
Energy Material Lab
Material Research Center
Samsung Advanced Institute of Technology
Samsung Electronics
130 Samsung-ro, Yeongtong-gu, Suwon-si
Gyeonggi-do 16678, Republic of Korea
Prof. Y. Cui
Stanford Institute for Materials and Energy Sciences
SLAC National Accelerator Laboratory
Menlo Park, CA 94205, USA

DOI: 10.1002/adma.201603436

Here, the very recent advances that have been made in design concepts, fabrication methods, and electrochemical and mechanical performances for flexible and stretchable energy-storage devices, especially focusing on LIBs and SCs, are extensively covered. There has been considerable research on flexible energy-storage systems over more than one decade, while the stretchable batteries and SCs have not attracted much attention since 2009.[4b,9] We therefore first highlight the latest achievements of flexible batteries and SCs since 2010, dividing by sections of electrode, electrolyte, integrated battery systems and other batteries beyond LIBs. We follow with a detailed presentation on stretchable LIBs and SCs by the same dividing chapters as the sections of flexible LIBs and SCs. In the last section we describe an overview of the recent achievements and challenges on flexible and stretchable energy-storage systems with a discussion of the perspectives and opportunities. A timeline summarizing the main milestones are illustrated in **Figure 1**, which indicates the history of the development of stretchable SCs and batteries.

2. Flexible Energy Storage

To power wearable electronic devices, the energy-storage systems require flexible, high energy density, excellent long-term stability as well as good rate capability, lightweight and low cost.[3b] Although a considerable effort has been devoted to investigate flexible energy-storage systems such as LIBs and SCs, this field remains at the early stages of development, where the electrochemical performances of the currently reported flexible LIBs and SCs is far from the level of conventional rigid devices and the requirements of practical applications. Because LIBs and SCs usually consist of several components including anode, cathode, separator, electrolyte, current collector and package, all of the components must be capable to be deformed with compatibility for flexible LIBs and SCs. As a result, the major strategies focus on the following aspects: i) preventing of leakage and internal short-circuits during repeatable bending or folding, for the case of using liquid electrolyte that can be simply injected into sealed package; ii) maintaining good contact between each component; iii) high energy density and long cycle life without decay during operation at bending or folding, which is the most challenging.

2.1. Flexible Lithium-Ion Batteries

Since first introduced in 1991, LIBs have been attracted growing attention and have been extensively applied as power source for portable electronic devices, electric vehicles as well as large-scaled energy-storage systems, owing to high energy density, long-term cycle life, good stability and high operating voltage.[5] Accordingly, LIBs is one of the most ideal candidates for flexible energy-storage systems for the applications of wearable devices, bendable displays, implanted medical devices and so on. However, currently, the most developed batteries are rigid and heavy due to the commonly used fabrication method and the metallic current collectors. Therefore, to further expand the practical applications of LIBs in flexible electronic devices, a large number of approaches of batteries with flexible, bendable and foldable ability have been reported, which are mainly on the various designs on electrode configuration or integrated battery system and nanostructured materials with excellent electrochemical and mechanical performances, as is aforementioned. In this section, we will highlight recent progress in

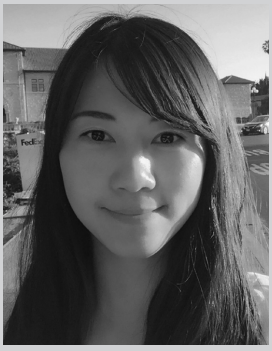

Wei Liu received her B.S. in materials physics from Beijing Normal University in 2008 and her Ph.D. in materials science and engineering from Tsinghua University in 2013. She is currently a postdoctoral scholar at Stanford University. Her research interests cover the areas of materials science, nanotechnology, and solid-state ionics, with a focus on studies of lithium batteries and fuel cells.

Min-Sang Song is currently a visiting scientist at Stanford University, as well as chief researcher at the Energy Material Lab at Samsung Advanced Institute of Technology (SAIT). He received his Ph.D. degree in Materials Science and Engineering at the Korea Advanced Institute of Science and Technology (KAIST) in 2007. From 2008 to present, he worked as a research member at SAIT. His research interests include electrode materials and cell design/fabrication in energy-storage devices, such as lithium-ion batteries, flexible/stretchable batteries, and lithium–sulfur batteries.

Yi Cui is a professor at Stanford University and SLAC National Accelerator Laboratory. He received his B.S. from the University of Science and Technology of China in 1998 and his Ph.D. from Harvard University in 2002. He was a Miller Postdoctoral Fellow at the University of California, Berkeley and joined in Stanford as a faculty member in 2005. His current research is on nanomaterials design for energy and environment. He is a co-director of the Bay Area Photovoltaic Consortium.

Adv. Mater. **2016**,
DOI: 10.1002/adma.201603436

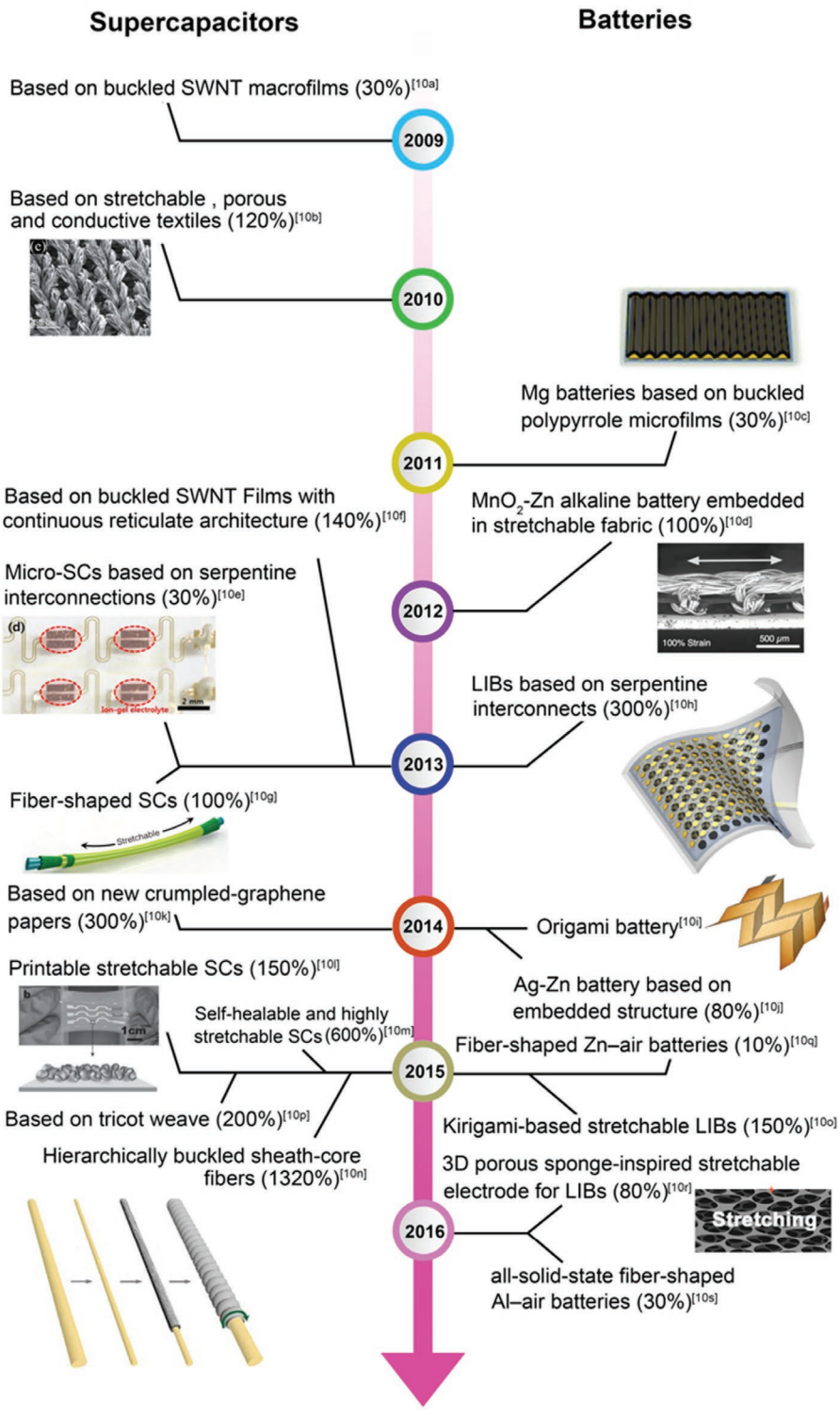

Figure 1. A brief chronology of the development of stretchable energy-storage systems. Images reproduced with permission as follows: "Based on stretchable, porous and conductive textiles": reproduced with permission[10b] Copyright 2010, American Chemical Society. "Micro-SCs based on serpentine interconnections": reproduced with permission.[10e] Copyright 2013, American Chemical Society. "Mg batteries based on buckled polypyrrole microfilms": reproduced with permission.[10c] Copyright 2011, Wiley-VCH. "MnO_2–Zn alkaline battery embedded in stretchable fabric": reproduced with permission.[10d] Copyright 2012, Wiley-VCH. "Fiber-shaped SCs": reproduced with permission.[10g] Copyright 2013, Wiley-VCH. "Printable stretchable SCs": reproduced with permission.[10l] Copyright 2015, Wiley-VCH. "3D porous sponge-inspired stretchable electrode for LIBs": reproduced with permission.[10r] Copyright 2016, Wiley-VCH. "LIBs based on serpentine interconnects": reproduced with permission.[10h] Copyright 2013, Macmillan Publishers Limited. "Origami battery": reproduced with permission.[10] Copyright 2014, Macmillan Publishers Limited. "Hierarchically buckled sheath–core fibers."[10n] Copyright 2015, American Association for the Advancement of Science.

flexible electrodes with various configurations and flexible solid electrolytes for LIBs, as well as integrated battery systems and the batteries beyond LIBs, since 2010.

2.1.1. Flexible Electrodes

One of the most crucial keys is developing flexible electrodes for LIBs, due to the intrinsic flexible feature for separator and package materials. The traditional method for preparation of cathode and anode materials is mainly based on slurry coating on metallic current collector. Electrode slurry usually contains active material, conductive material (carbon black) and polymer binder (poly(vinylidene fluoride), carboxymethyl cellulose, styrene butadiene rubber), in which active material is the dominant content. As a result, based on the traditional manufacture method, the electrode materials are easy to be detached from current collector by repeatable deformation. Hence, diverse methods are currently carried out to explore flexible electrode materials with high electronic/ionic conductivity and without significant electrochemical performance decay during bending or folding, as alternatives to the conventional electrodes used in flexible LIBs. The multilayers of separator sandwiched by two electrodes presents the general stack in LIBs, using two-dimensional (2D) through-plane electrode structure, where various configuration designs have been demonstrated to achieve flexibility, including paper-like, textile, sponge, wire-shape structure, etc. Moreover, novel electrode architectures such as 2D in-plane electrode and three-dimensional (3D) electrode have also been adopted in flexible batteries, showing improved electrochemical and mechanical performances. Various electrode structures together with flexible designs will be discussed in the following sections in sequence.

2.1.2. Flexible 2D Electrode Configuration

Paper-Like Configuration: In the most recent development of flexible LIBs, electrode materials of paper-like structure based on either freestanding membrane or coated on flexible substrate have been widely reported. The paper-like structure can provide flexible, thin and lightweight features, large-scale, energy-efficient productions, and high surface area for reagents to be stored. 3D porous paper-like structure also allows fast access of electrons and ions transport across the entire structure. In addition, the paper-like energy-storage systems hold great promise to be fully integrated with flexible electronics devices. Materials including carbon materials (carbon nanotubes (CNTs), carbon nanofibers (CNFs), graphene), conductive polymers and composite materials are commonly used as conductive network or current collector.[11]

CNTs are seamless cylindrical nanostructure of one or more layer of one-atom-thick sheets of carbon (graphene) with open or closed ends, which have extremely interesting properties of high electronic conductivity and flexibility. CNTs therefore are valuable for various applications of materials science and technology.[12] Yi Cui's group at Stanford University is the pioneer of flexible LIBs. Cui and co-workers[13] demonstrated flexible paper LIBs using paper as separators and freestanding conductive paper (CNT thin films) as current collectors, as shown in **Figure 2**a. CNT thin films were coated on a stainless-steel substrate based on a solution process and then electrode materials were applied to the CNT film. Finally, the double layer $LiCoO_2$ (LCO)/CNT or $Li_4Ti_5O_{12}$ (LTO)/CNT film could be lifted off. The LIB materials and current collectors were integrated onto a paper through an easy lamination process. This novel paper battery showed high electrochemical performance and mechanical properties. Figure 2b displays the voltage profile at first cycle of the flexible paper LIB, indicating high specific capacity of about 130 mA h g^{-1}. High Coulombic efficiency and low discharge retention are also shown in Figure 2c. For practical applications, high energy density is required. Compared with previous reported work, this thin and flexible LIB with thickness of ≈300 μm showed a higher energy density of 108 mW h g^{-1}, based on the total mass. CNT-based composite materials have also attracted much attention as flexible electrodes for LIBs, which combine all features from each component. Later, Zheng et al. reported a three-dimensionally (3D) interconnected hybrid hydrogel system via a CNT–conductive-polymer network architecture for flexible LIB electrodes.[14] As shown in Figure 2d, super-long CNTs with diameters of 30–80 nm and length of up to 1 mm and active nanoparticle materials were well dispersed in poly(3,4-ethylenedioxythiophene) doped with poly(4-styrenesulfonate) (PEDOT:PSS). The authors believed that unlike previously reported conducting polymers that are fragile and are not compatible with aqueous solution, the current studied interpenetrating network of the CNT–conducting-polymer hydrogel exhibited high conductivity as well as good mechanical properties. As a result, high electrochemical performance with good mechanical ability was found, which indicates that the flexible TiO_2 electrodes achieved a capacity of 76 mA h g^{-1} and the flexible SiNP-based electrodes showed a high areal capacity of 2.2 mA h cm^{-2} at 0.1C rate, as shown in Figure 2f. This novel paper-like batteries based on CNT–conductive-polymer network can be afforded for practical applications. Based on CNTs and their composites, paper-like structural electrodes for flexible LIBs have been proposed in many related reports.[15]

Meanwhile, in recent years, for flexible electrodes, carbon related materials such as graphene that is a new class of two-dimensional (2D) carbon nanostructure of one-atom-thick sheets with a covalently bonded honeycomb arrangement, has also attracted great attention owing to its high electronic and ionic conductivity, chemical stability, flexibility, and mechanical properties.[16] Graphene paper was first adopted in LIBs by Wallace and co-workers.[17] They synthesized stable graphene aqueous dispersions from commercially available, low cost graphite. The ultrastrong and highly conductive paper-like membrane was prepared by vacuum filtration using the graphene aqueous dispersion, which showed a smooth surface with a shiny metallic luster on both sides. Recently, Chen and co-workers reported a paper-like high-performance flexible LIB electrode by combing centimeter-size high quality black phosphorus (BP) with highly conductive graphene sheets. This electrode based on BP-graphene hybrid paper showed highly flexible behavior and good electrochemical performances. A high specific capacity of 501 mA h g^{-1}, excellent rate capability, and prolonged cycling performance at a current density of 500 mA g^{-1} have been achieved.[18]

Adv. Mater. 2016,
DOI: 10.1002/adma.201603436

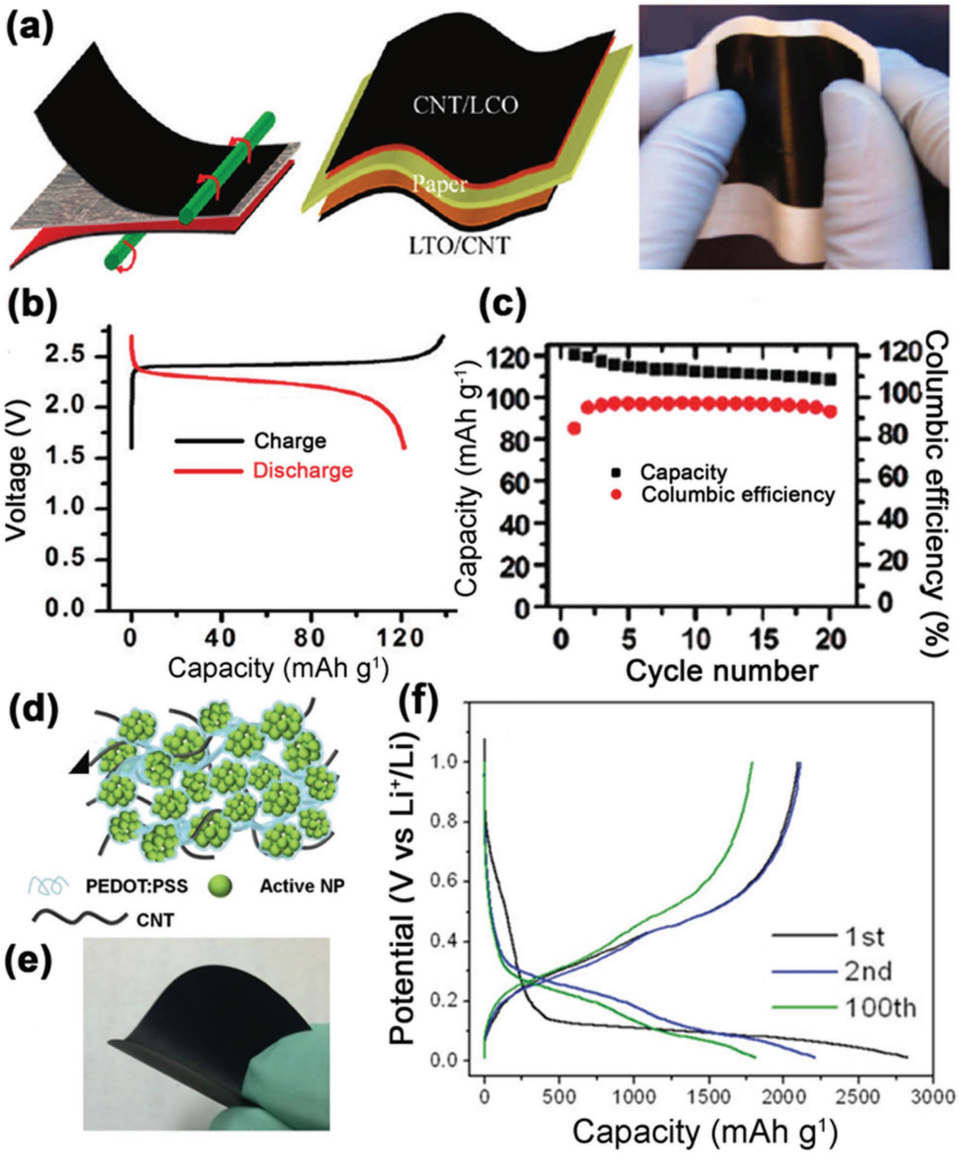

Figure 2. a) Schematic of the lamination process and picture of the paper-like LIB before encapsulation for measurement. b) Galvanostatic charging/discharging curves of a laminated LTO–LCO paper battery. c) Cycling performance of LTO–LCO full cells. a–c) Reproduced with permission.[13] Copyright 2010, American Chemical Society. d) Schematic of the electrode materials using active nanoparticles, CNT and PEDOT:PSS. e) Photograph of the flexible TiO_2–PEDOT:PSS–CNT film. f) Cycle galvanostatic charge/discharge curves of an electrode at C/10. d–f) Reproduced with permission.[14] Copyright 2014, Wiley–VCH.

Furthermore, graphite oxide (GO) and reduced graphite oxide (rGO) have also been used in a large number of applications, which are layered carbon materials with oxygen functional groups and defects.[19] Wang et al.[20] demonstrated a self-supporting binder-free Si-based anode by the encapsulation of SiNWs with dual layers of an overlapping graphene sheath that prevented the direct exposure of the encapsulated silicon to the electrolyte and an rGO overcoat, as a mechanically strong and flexible matrix to accommodate the volume change during charge/discharge. Flexible Co_3O_4/rGO composite aerogels as binder-free anodes, where the Co_3O_4 nanoparticles are integrated in an interconnected rGO network were reported recently.[21]

Additionally, interesting work on freestanding silicon nanowire (SiNW) paper with the combination of macroscopic flexibility and transparency features, which is used as Si anode in LIBs, was reported by Pang et al.[22] They demonstrated a simple syntheses by gas flow directed assembly of interconnected SiNWs with 10 nm diameter by free-catalyst thermal evaporation using a vertical high frequency induction furnace. After coating a layer of graphene, this Si anode showed high electrochemical performances of 5336 and 2699 mA h g^{-1} for charge and discharge capacities at current density of 1A g^{-1} for the first cycle.

Therefore, considerable effort has been devoted on paper-like electrodes based on various carbon-based and polymer-based

highly conductive materials for LIBs with flexible, bendable or foldable ability.

Sponge/Porous Configuration: Apart from the most studied paper-like approaches, flexible electrodes inspired by 3D conductive interconnected network of foam or sponge structure have also been employed with varying degrees of success in using in flexible LIBs. Compared with conductive network structure discussed in previous section, the foam-like structure has an interconnected conductive network that can guarantee high electrical conductivity. The preparation of 3D graphene foams (GFs) by template-directed chemical vapor deposition (CVD) was first demonstrated by Cheng's group.[23] The GFs consist of an interconnected flexible network of graphene, which have high electrical conductivity, lightweight and flexible feature. Based on this unique structure, several flexible electrodes for LIBs have been explored. Li et al.[24] reported flexible LTO/GF and $LiFePO_4$(LFP)/GF hybrid materials for LIBs by in situ hydrothermal deposition of active materials on GF followed by heating in Ar atmosphere, using GF as current collector.

Various flexible anode materials have also been demonstrated.[24,25] Ruoff's group[25e] reported a 3D nitrogen-doped porous graphene/graphite foam by simply in situ activation of N-doped graphene on a GF scaffold, and a flexible electrode based on nitrogen-doped graphene/SnO_2 foam with an integrated macroscale film and interconnected micro-/nanofoam architecture was also investigated recently.[25a,d] Porous α-Fe_2O_3 nanorods onto CNT–GF showed >1000 mA h g^{-1} capacities at 200 mA g^{-1} up to 300 cycles without obvious fading.[25c] A sponge-like anode of CNT–graphene–Si composites with improved electrochemical performances for LIBs have also been reported. The assembly of CNTs and graphene created void that allows the volume expansion of Si, while maintains fast electron transport.[25h] In addition, porous CNT sponge-like structure was also adopted as the backbone on which active electrode materials were deposited.[26]

Textile Configuration: A textile or cloth is a thin, flexible sheet of material formed by weaving or knotting natural or artificial fibers (yarn or thread), which is a promising candidate for energy-storage sytems.[27] Carbon fiber textile or cloth with 3D network architecture shows high electronic conductivity and mechanical properties, which can be adopted as soft collector by a replacement of the traditional metal current collector. In recent years, many researchers prepared flexible conductive textile by coating preexisting cotton or polyester textile (woven or non-woven, knitted) with various conductive carbon or active electrode materials for flexible or stretchable batteries or SCs.[10b,28] Cui's group was the pioneer in the study of flexible batteries and SCs in textile structure.[10b,28] In 2010, Cui's group first demonstrated flexible and stretchable pseudocapacitor textiles.[10b] The textile conductor is simply prepared by dispersing CNTs ink in water on a polyester fiber textile, which is highly conductive (electronic conductivity is 1300 S cm^{-1}) and porous. Therefore, this conductive textile is an ideal candidate as current collector for flexible electrodes. Later in 2011, Li-ion textile batteries with high areal mass loading using this 3D porous textile conductor as current collector were reported.[28a] The area mass loading is 140 170 mg cm^{-2}, which is about 7–8 times higher than traditional LIBs.

In addition, carbon fiber cloth can be obtained by carbonization of polymer-based cloth with high electronic conductivity. Flexible LTO and $LiMn_2O_4$ (LMO)/carbon composites textiles were reported. TiO_2/MnO_2 nanosheets were first deposited on the highly flexible carbon textiles by electrostatic interaction and then were transformed in situ into LTO/LMO by chemical lithiation. This resulting 3D porous textile electrode showed various advantages including the reduced Li^+/e^- diffusion length, the easy access of electrolyte ions, delivers excellent rate capability and good cyclic stability. An interesting work reported by Lui et al.[29] demonstrated a flexible and 3D ordered macroporous TiO_2 electrode using a polystyrene colloidal crystal template on carbon cloth, which showed significant improvements over conventional nanoparticle electrodes without the use of binder or other additive. Zhong Lin Wang's group[30] designed a self-charging power system by integrating a whole-textile triboelectric nanogenerator with a flexible LIB. The current collectors were synthesized by electroless plating Ni on insulating polyester fabrics.

2.1.3. Flexible 3D Electrode Configuration

The kinetic problems associated with the solid-state transport of Li-ion into electrodes materials have an effect on the electrochemical performance of batteries. For current traditional LIBs with planar electrodes, the transport of Li-ions is reduced by the dense structure of the electrodes. Therefore, developing novel electrode materials and structures with high active specific surface area and high ion/electronic conductivity is the main challenge. As a result, various 3D electrode design using nanostructure materials with advanced properties of optimizing the ionic/electronic current paths, large surface area, better permeability, have been widely exploited in LIBs with high specific capacity and good rate capability.[31] In addition, conventional electrodes require polymer binder and carbon black to mix together with active electrode powders, which not only reduces the percentage of active materials but also introduces undesirable interfaces in the electrodes. Hence, many types of 3D architecture electrodes have been described as alternatives to conventional electrodes in batteries to achieve better performances. 3D architectures such as aligned array, wire-shaped structure, porous scaffolds, and so on have been reported, as shown in **Figure 3**. General speaking, the electrode with sponge and textile configuration are also 3D architectures that can offer fast pathway for Li-ions and electrons.

Array Configuration: Aligned array of nanostructured materials have applied in LIBs, owing to its high specific surface area, reduced conduction pathway and enhanced mechanical performance. Cui's group developed Si nanowires as anode, which could improve the accommodation with large volume changes to avoid the initiation of fracture, unlike the conventional bulk or micrometer-sized materials, and also could increase electrically contact and efficient charge transport.[35] However, flexibility was not indicated. In addition, aligned arrays of CNTs have particularly attracted much attention used in soft batteries as their 3D architecture offers both flexibility and mechanical robustness.[36] Ajayan's group demonstrated a flexible CNT–copper oxide–poly(vinylidene fluoride) (CNT–Cu_2O–PVDF)

DOI: 10.1002/adma.201603436

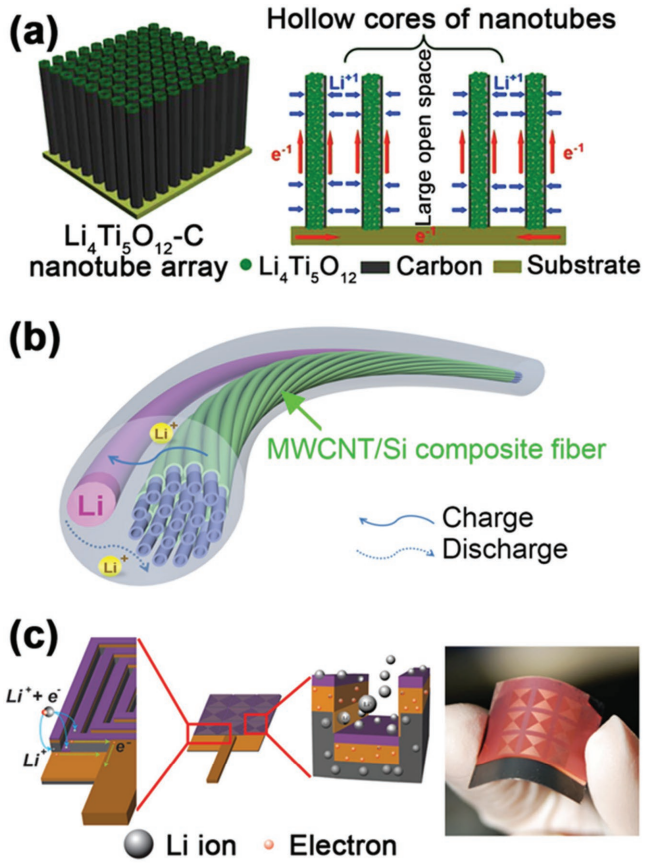

Figure 3. Various 3D electrode configurations. a) Schematic representation of well-aligned LTO-C Nanotube Arrays and diffusion of Li-ions and electrons during discharge/charge processes of the self-supported electrode. Reproduced with permission.[32] Copyright 2014, American Chemical Society. b) Schematic illustration of a half LIB based on the aligned MWCNT/Si. Reproduced with permission.[33] Copyright 2014, Wiley-VCH. c) A schematic illustration of Li-ion charging into the graphite/Si composite interdigital electrode. Reproduced with permission.[34] Copyright 2014, Wiley-VCH.

free-standing membrane, which is adopted as an electrode-separator material for LIBs.[36] Aligned CNTs were synthesized on a steel substrate by a chemical vapor deposition (CVD) process and were then coated with Cu_2O using electrodeposition. The poly(vinylidene fluoride-hexafluoropropylene) (PVDF-HFP)–SiO_2 composite polymer electrolyte was infiltrated to embed the hybrid nanoarray. The electrolyte membrane was porous by phase inversion to increase its uptake of the liquid electrolyte and improve ionic conductivity. The freestanding and flexible electrode was obtained by peeling from the substrate. The result revealed that this hybrid electrode showed an enhanced discharge capacity (2.3 mA h cm^{-2}) in comparison to pure CNTs (1.2 mA h cm^{-2}). This design sheds light on a used approach for the applications requiring lightweight and miniaturized batteries.

Furthermore, several work demonstrated 3D array structured electrodes for LIBs based on various materials, including Co_3O_4 nanowires arrays,[37] SnO_2/Fe_2O_3 composite nanotube array,[38] TiO_2–C/MnO_2 core–double-shell nanowires array[39] and LTO–C nanotube arrays.[32] As shown in Figure 3a, Liu et al.[32] developed a flexible and self-supported LTO–C nanotube array with high conductivity architectures for application in LIBs. ZnO hexagonal nanorod arrays were used as template to prepare TiO_2 nanotube arrays first and then LTO nanotube arrays were obtained by chemical lithiation and post-annealing processes, and finally LTO–C nanotube arrays were prepared by carbonization of glucose that was adsorbed on the inner and outer surfaces of nanotubes. This LTO–C nanotube arrays exhibited good rate capability (121 mA h g^{-1}) and long cycle life, attributed to the increased electroactive interface for transfer of Li-ions during charge/discharge and much improved electronic conductivity via the both inner and outer surface-coating of carbon layers.

Wire-Shaped Configuration: The shape of batteries is a critical limiting factor for the application in practical devices. As is well known that our clothes can afford various deformations, such as folding, twisting and stretching, inspired by which building wire-shaped batteries have been explored. Like aligned array structure, wire-shaped configuration used for electrodes in LIBs also can supply advantages such as improved Li-ions and electrons.[40] Meanwhile, wire-shaped electrodes are omnidirectional flexibility and can be interconnected/woven in textile and then are installation freedom for electronic devices, which is over conventional sheet-like batteries.[41] The first cable-like LIB was reported by Kwon et al.,[42] which could be up to very high levels of flexibility that have never been approached before. This cable-type LIB basically comprises several anode strands that were coiled into a hollow spiral core, a modified poly(ethylene terephthalate) (PET) nonwoven as separator and a coating layer of cathode. Due to the large specific area of anode, this cable battery showed excellent charge/discharge behaviors and good capacity retention. However, the specific capacity of 1 mA h cm^{-1} is low and long cycle performance was not observed. In addition, this cable battery was relatively too big with a millimeter ranged diameter to be woven into various textile structures.

Huisheng Peng's group from Fudan University is the pioneer in the research of flexible and stretchable batteries, especially on wire-shaped structure. Peng and co-workers[33] believed that wire-shaped batteries could be scaled up for practical applications due to the well-developed textile technology. They indicated a new, twisted, aligned multiwalled carbon nanotube (MWCNT)/Si[33] and CNT/Si[43] composite fiber as anodes for flexible, wire-shaped LIBs. As shown in Figure 3b, Si was first deposited on the MWCNT sheet through an atomic layer deposition (ALD) method, which could not only exploit the high specific capacity of silicon and the good electrical conductivity of MWCNT, but also accommodate the volume change of the Si during charge/discharge by the designed space among the aligned composite nanotubes.[33] Then the composite nanotubes could be twisted to be a flexible composite fiber electrode. A high specific capacity of 1970 mA h g^{-1} at the 50th cycle was observed, which is higher than pure Si with 1648 mA h g^{-1} at the 30th cycle. Furthermore, Peng and co-workers[44] demonstrated MWCNT/LTO and MWCNT/LMO yarns coupled as anode and cathode for flexible and stretchable LIBs with stretchability of 100%. However, low specific capacity needs further improvement.

3D Current Collector and Interdigital Electrodes: Rapid trends in the miniaturization of electronic products (microelectronics),

especially in the portable electronic devices, have sparked considerable interest in the miniaturization and integration of the energy-storage systems.[31a] Several types of 3D nanoarchitectured electrodes have been indicated as alternatives to the traditional planar electrodes. The 3D structures are carefully fabricated to optimize the ion/electron transport paths. Generally, the 3D nanoarchitectured electrodes are designed according to various structures of current collectors with tolerance against folding/bending motions. In addition, the traditional co-facial structure for LIBs is not intrinsically propitious to deformation of bending or folding, due to different tensile/compressive stress for each layer during the motions, which leads to friction force against neighboring layers. Meanwhile, the configuration of multilayers of anode, separator or electrolyte and cathode stacked consecutively results in a limitation in lowering the cell thickness, for which a high energy density is difficultly achieved.

Pikul et al. demonstrated a high energy density and high-power-density microbattery constructed from interdigital 3D bicontinuous nanoporous electrodes. However, flexible electrodes in LIBs using 3D interdigitated have not been developed widely. As shown in Figure 3c, a novel method to combine graphite and silicon through a 3D-structured thin copper current collector via sputtering.[31a] The 3D structured current collector between the two anodic materials could enhance the synergistic merits of the respective materials, which enables an increased specific capacity and a high rate capability.

Therefore, besides the obvious rigid and brittle character of LIBs, the structure of current collector also plays an important role in determining the performance of electrodes, which is important technical direction for fabricating flexible battery. The 3D current collector with large specific surface area can provide an improved adhesion between electrode materials. Wang et al. successfully developed a lightweight, thin and flexible CNT current collector to replace the widely used heavy metal current collectors for LIBs, which had better wetting, stronger adhesion, improved mechanical stability, and reduced contact resistance at the electrode/CNT interface.[45] Besides carbon-based current collectors, traditional metal current collectors have also been investigated. Park et al.[46] reported flexible, honeycomb-patterned Cu and Al materials that were used as current collectors to achieve the optimal adhesion in the electrodes.

Furthermore, Jang Wook Choi's group[47] demonstrated a flexible, coplanar cell where anodes and cathodes were interdigitatedly on the same plane. The thickness of the full cell thickness is only 0.5 mm. The 2D in-plane electrode structure allows the modification of its pattern for sequential addition of a single-cell voltage, due to which 7.4 V by series connection of two 3.7 V cells was demonstrated in this work. Meanwhile, other energy conversion devices, such as inductive electromagnetic energy transfer or solar energy, are able to be integrated with this 2D in-plane battery.

2.1.4. Flexible Solid-State Electrolyte

LIBs have been intensively commercialized to meet the ever-growing demands of technologies ranging from portable devices, electric vehicles to grid-scale energy-storage systems. However, current widely used liquid electrolyte with leakage, flammability and poor chemical stability issues prevents the development of next-generation high-performance LIBs. By replacing the liquid electrolyte with a solid one that provides substantially improved safety.[48] In addition, to realize safety and flexible batteries with high performances and benign mechanical properties, exploring solid-state Li-ion electrolytes with freedom design are strongly desired. Furthermore, solid electrolytes could suppress the growth of lithium dendrites in Li metal batteries. Lithium metal as the anode is the ultimate negative electrode that really takes advantage of the high specific capacity of cathode (e.g., sulfur). However, using solid Li-ion electrolytes results in decreased capacity utilization and performance deterioration owing to the low ionic conductivity and high interfacial resistance in contact with electrodes, remaining the principle design challenge.

Currently, solid Li-ion electrolytes can be divided into two general types: inorganic materials and organic polymers. Compared with solid polymer electrolytes (10^{-7}–10^{-5} S cm^{-1}), most reported inorganic materials have higher ionic conductivity, which can reach 1.0×10^{-4} S cm^{-1} at room temperature (RT) for oxide electrolytes and even up to 1.0×10^{-2} S cm^{-1} for sulfides.[49]

Inorganic Electrolytes: Traditional all solid-state LIBs use rigid substrate, while by the replacement of flexible substrate can realized the batteries with bendable, foldable advances, using reel-to-reel manufacturing. An early work about flexible inorganic electrolyte was presented by Ihlefeld et al.,[50] which shows an integration of the Li-ion conductor lanthanum lithium tantalate ($La_{1/3-x}Li_{3x}TaO_3$) with a thin copper foil current collector, for a Li-free all-solid-state battery. However, the performance of battery using this electrolyte was lacked. Another work about a bendable all-solid-state bendable LIB was indicated by Koo et al.,[51] based on a thin layer of lithium phosphorus oxynitride (LiPON) with thickness of about 2 μm as the solid electrolyte. All components including current collector, LCO cathode, LiPON electrolyte and Li metal were then deposited on mica substrate, and then the multilayer was peeled off using sticky tapes and transferred onto a poly(dimethylsiloxane) (PDMS) sheet. This bendable, thin-film LIB indicated a highest 4.2 V charging voltage and 106 μA h cm^{-2} capacity at non-bending status and that decreases to 99 μA h cm^{-2} at bending radius of $R = 3.1$ mm.

In recent years, $Li_{10}GeP_2S_{12}$ with an unprecedented conductivity of 1.2×10^{-2} S cm^{-1} and Li_2S–P_2S_5 glass ceramics of 1.7×10^{-2} S cm^{-1} have been reported.[49a,52] However, these sulfides are either unstable with Li metal and with high voltage cathode materials or extremely hygroscopic, producing toxic H_2S in contact with moisture. In 2015, Sang-Young Lee's group[53] first report a bendable sulfide solid electrolytes reinforced by a mechanically compliant poly(paraphenylene terephthalamide) (PPTA) nonwoven (NW) scaffold. These bendable solid electrolytes were prepared via the doctor-blade method to coat the sulfide SE slurry on a Ni foil and then cold pressing onto the NW scaffold. They demonstrated two different electrolyte configurations of SE-NW-SE and NW-SE-NW, which showed ionic conductivity of 0.20 mS cm^{-1} and 0.16 mS cm^{-1}. The full all-solid-state battery consisting of LCO as the cathode and LTO as the anode showed first discharge capacities of 89 mA h g_{LCO}^{-1}

Adv. Mater. 2016,
DOI: 10.1002/adma.201603436

and energy density of 44 W h kg_{cell}^{-1}. Although this all-solid-state battery indicated lower energy density than commercialized LIBs (100–200 W h kg_{cell}^{-1}), further improvement in electrochemical performance can be expected by applying advanced electrode materials such as sulfur coupled with Li metal.

Solid Polymer Electrolytes: Solid polymer electrolytes (SPEs) present more structure flexibility as well as easier lamination stacking and hermetic sealing processes to meet the requirements of different cell applications, which much attention sustained over the past few decades has been devoted.[54] A pioneer work about flexible all-solid-state LIBs using SPEs was reported by Liu et al.,[55] which demonstrates a flexible and stretchable battery composed of strain free LFP cathode, LTO anode and a polyethylene oxide (PEO) electrolyte. The free-standing anode and cathode were prepared by casting solution of the mixture of LFP/LTO powder, carbon black and PEO as binder. A full battery could be fabricated either by assembling and pressing three layers of cathode, electrolyte an anode, or by pouring the solution of electrolyte and cathode in order on the anode layer. The resulting battery film could be cut into strips with 1 cm width and 10 cm length and then integrated into a textile form a flexible textile LIB. In this full battery, many polymer binder materials have to be used in order to obtain the desired flexible and stretchable features of the electrodes, therefore, the energy density is low meanwhile the electrochemical performance is poor due to the low ionic conductivity of SPEs.

Considerable efforts have been devoted on improving ionic conductivity of SPEs, including crosslinking, using diblock copolymer or adding plasticizers have been studied. However, these modifications not only reduce the ionic conductivity and the compatibility with Li anode, but also lead to poor mechanical properties and low flame resistivity.[56] Dispersing ceramic nanoparticles that provide competitive interactions within the polymer matrix is an effective approach, which increases ionic conductivity, meanwhile, improves electrochemical and mechanical stability.[57] Cui's group first demonstrated a composite polymer electrolyte with $Li_{0.33}La_{0.557}TiO_3$ nanowires, which shows three orders of magnitude enhancement of ionic conductivity compared with filler-free electrolyte, due to the fast ion transport on the surfaces of ceramic nanowires that act as conductive network.[58] This composite polymer electrolyte is a promising candidate used in flexible LIBs due to its flexible ability. Among the fillers, graphene oxide nanosheets have recently also been reported to be used in composite SPEs. Kammoun et al. demonstrated a flexible LIB, which shows a high operating voltage of 4.9 V, an areal capacity of 0.13 mA h cm^{-2} and an energy density of 4.8 mW h cm^{-3}. This flexible LIB was based on the solid polymer composite electrolyte consisted of PEO and 1 wt% GO nanosheets, which was able to afford 6000 bending cycles with high voltage retention of 93%.[59] This work presented a simple method of encapsulating multilayers by a lamination method that is cost-effective and scalable. Very recently, Liangbin Hu's group at the University of Maryland demonstrated a flexible solid composite PEO-based electrolyte based on a 3D lithium-ion conducting garnet nanowire network, with high capacity, high safety and good stability.[60] This flexible solid electrolyte showed a high ionic conductivity of 2.5×10^{-4} S cm^{-1} at room temperature, which indicates great potential to replace conventional flammable liquid electrolyte for LIBs.

However, most of the previous work on flexible batteries has still been based on traditional cell assembly processes including stacking electrode sheets and separator layer and packaging and then infection of liquid electrolyte if it is required. In order to address the traditional cell manufacturing-related issues including safety, poor low electrochemical performance and mechanical properties, new fabrication processes such as multistep spray painting and screen-printing processes have been recently investigated. With the rapid development of printing technology that is simple and reliable, printed batteries are an excellent and powerful alternative to conventional batteries for various applications that require thin, lightweight and flexibility.[61] Recently, Sang-Young Lee's group reported printable, flexible all-solid-state batteries, as shown in **Figure 4**.[62] This battery was fabricated via a stencil printing process with ultraviolet (UV) cross-linking. A solid composite electrolyte layer and its matrix-embedded electrodes were printed on arbitrary objects with complex geometries, which results in fully integrated, multilayer-structured printable all-solid-state batteries. The highly ion-conductive and flexible electrolyte used in this work has been indicated previously by this group, which can be conformable to 3D micropatterned structure of electrodes over large areas.[63] This solid electrolyte is a composite gel polymer electrolyte composed of a UV-cured ethoxylated trimethylolpropane triacrylate (ETPTA) polymer matrix, liquid electrolyte (1 M $LiPF_6$ in ethylene carbonate (EC)/propylene carbonate (PC)), and Al_2O_3 nanoparticles. This electrolyte matrix precursor was mixed with electrode active materials (LFP and LTO) powders to achieve a composite electrode (Figure 4a). The full cell presented normal charge/discharge profiles and also high capacity retention (≈90%) up to 30 cycles with discharge specific capacity of about 160 mA h g^{-1}. In addition, the letters-shaped full cell maintained its dimensional stability even after being mechanically bent and also showed no appreciable deterioration in the charge/discharge specific capacity (Figure 4b).

2.1.5. Beyond Flexible Li-Ion Batteries

Recently, there has been an ever-growing demand for high-energy-density energy-storage systems for mobile electronic devices with increased power consumption and electric vehicles with extended driving range, as well as grid-scale energy-storage systems. The improvement in the performance of active electrode materials has been the critical challenge, which is a result of the energy density of a rechargeable battery depending on the specific capacities and operating voltage. Hence, to largely increase the energy density, new redox chemistries between charge-carrier ions and host materials beyond the conventional lithium "intercalation" mechanism is mainly required.[6d,64] Advanced batteries beyond LIBs with new chemistries for charge-carrier ion storage have been developed rapidly. Li–O_2 and Li–S batteries using Li metal as anode have attracted much attention.[1a,6d] Li metal has been considered as one of the most ideal anodes as account of its high theoretical capacity (3860 mA h g^{-1}) and low redox potential and low relative density. Sulfur is one of the most promising active

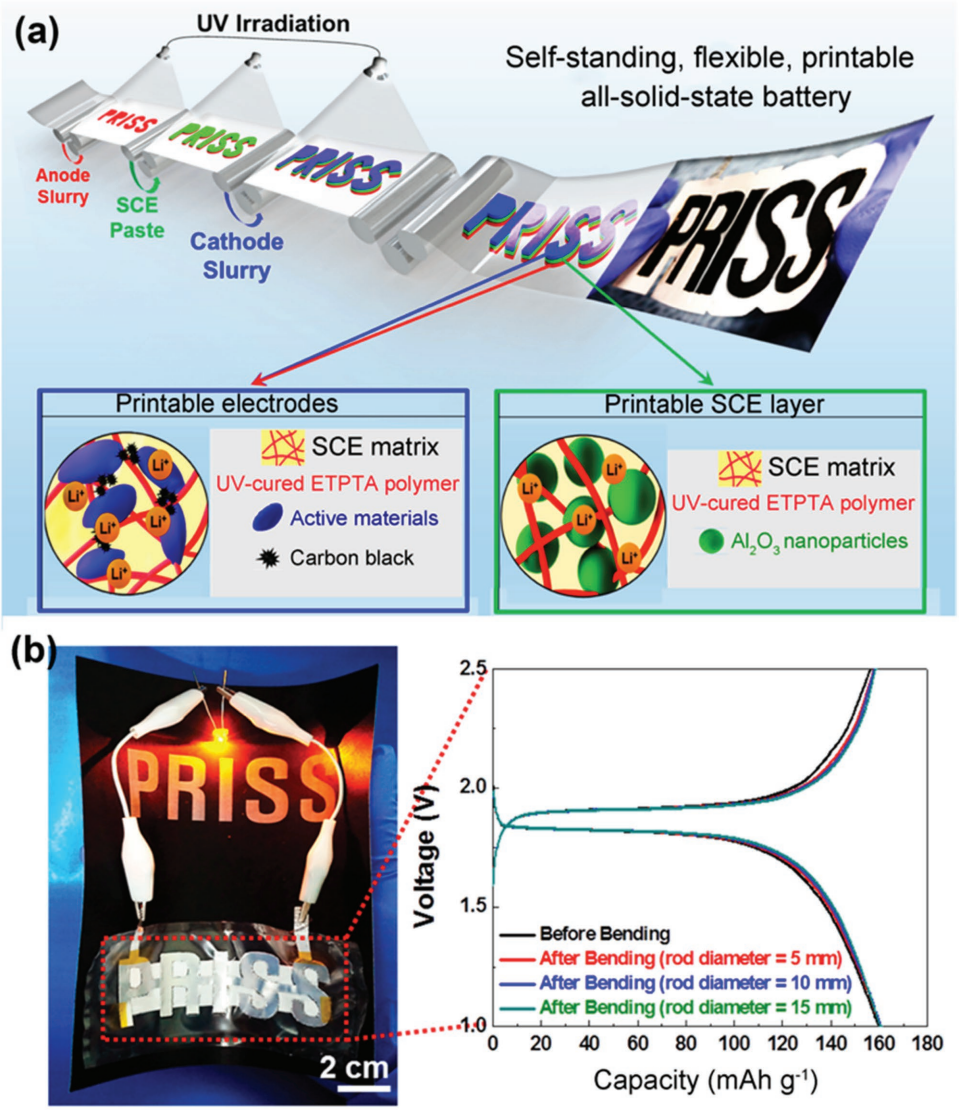

Figure 4. a) Schematic representation depicting the stepwise fabrication procedure for the printable solid-state batteries, wherein chemical structure of their major components and a photograph of the self-standing, flexible "PRISS" letters-shaped battery were provided. The stencil-printable electrodes were composed of electrode active materials powders, carbon black and SCE matrix. Between the stencil-printable electrodes, a stencil-printable SCE thin layer acting as a solid electrolyte was positioned. b) Photograph of "PRISS" letters-shaped battery and its charge/discharge profiles at current density of 0.05 C/0.05 C, which were measured under being completely wound along the rods having different diameters, not a planar configuration. a,b) Reproduced with permission.[62] Copyright 2015, American Chemical Society.

materials due to its high theoretical capacity (1675 mA h g^{-1}), low cost and natural abundance. Bruce et al.[1a] reported that the theoretical energy density for current used LIBs, Li–O_2 and Li–S batteries are 1015, 2199 and 3436 W h L^{-1}, respectively. Therefore, advanced Li–O_2 and Li–S batteries with flexible, bendable and foldable ability have been also developed, based on these approaches for flexible LIBs.

Hui-Ming Cheng's group is a pioneer on research of flexible Li–S batteries.[65] They demonstrated a binder-free, highly conductive and flexible membrane consisted with S–carbon nanotubes for Li–S batteries.[65a] They found that a flexible S-CNTs membrane could be synthesized by CVD of carbon and carbothermal reduction using a sulfate-containing anodic aluminum oxide (AAO) template, following by removal of AAO and an ethanol evaporation-induced assembly, which can sustain a 10 MPa stress with 9% strain. This S cathode can provide a capacity of 1438 mA h g^{-1} in sulfur and an overall capacity of 332 mA h g^{-1} in sulfur and carbon at 0.15 A g^{-1}. Cheng's group also developed sulfur cathode has been developed by using GF as a current collector and host for sulfur loading through simple slurry infiltration.[65b] The PDMS coating on the GF makes this interconnected network sufficiently robust, guaranteeing the stretchablilty of the cathode. The sulfur-PDMS/GF electrode possesses higher stretchability of 20% than the previous report[65a] with high rate performance and reversible capacity more than 450 mA h g^{-1}, and tiny capacity decay of 0.07% per cycle over 1000 cycles. Another approach of integrated structure of sulfur and graphene on a polypropylene (PP)

Adv. Mater. 2016,
DOI: 10.1002/adma.201603436

separator without PDMS has been proposed in order to preserve the high-energy density, while rendering the stretching of the electrode.[65c] The fracture stress and strain of the integrated electrode are around 30 MPa and 65%, respectively.

In 2015, Ju Li's group explored a flexible slurryless nano-Li_2S/reduced GO cathode paper (nano-Li_2S/rGO paper) by simple drop-coating.[66] The rGO paper was prepared by freeze-drying GO and a following heat treatment, and the nano-Li_2S loading was then achieved by drop coating on the rGO paper using anhydrous ethanol as the solvent. The discharge capacities at the first cycle of 1119 mA h g^{-1} (based on Li_2S) at a low rate of 0.1 C could be obtained. After cycling 200 times at 5 C, the capacity could still remain at 462.2 mA h g^{-1}. They believed the flexible nano-Li_2S/rGO paper could accommodate the stress generated from the large volume change during charge/discharge, therefore mechanical integrity of the electrode could be maintained, which results in good cyclability. In addition, a foldable Li–S battery with the highest areal capacity (≈3 mA h cm^{-2}) to date among foldable energy-storage devices was reported.[67] The main reason to achieve the folding along two mutually orthogonal directions is based on a special design: fully foldable and superelastic carbon nanotube current-collector films and impregnation of the active electrode materials into the current-collectors via a checkerboard pattern. Wang et al.[68] also demonstrated a flexible sulfur cathode, which is an integrated carbon/sulfur/carbon structure on polypropylene (PP) separator. This integrated sandwich-structured electrode delivered a high capacity of 730 mA h g^{-1} over 500 cycles, which is highly promising in flexible Li–S batteries for practical applications.

Near recently, besides Li–S batteries, flexible Li–O_2 batteries have also been investigated inspired by paper-like structure, textile and wire-shaped configuration. Liu et al.[69] proposed and demonstrated a novel, effective and scalable approach to fabricate a flexible paper–ink cathode for Li–O_2 batteries. A foldable Li–O_2 battery pack consisting of multiple parallel cells was also shown with increased energy density. A flexible Li–O_2 battery based on TiO_2 nanowire arrays (NAs) on carbon textiles (NAs/CT) as a freestanding cathode was also demonstrated.[70] The schematic illustration of synthesis process is shown in **Figure 5**a. Dense and homogenous TiO_2 seeds were first deposited onto the CF in order to protect the CT surface effectively. TiO_2 NAs could be grown in situ by the TiO_2 seeds-directed self-assembly method. The TiO_2 NAs/CT was applied as both cathode and current collector to replace the conventional rigid counterparts. The Li–O_2 battery device was constructed using the pristine CT or the TiO_2 NAs/CT cathode, a glass fiber separator, and Li anode (Figure 5b). Lithium triflate ($LiCF_3SO_3$) in tetraethylene glycol dimethyl ether (TEGDME) was used as the electrolyte. The results showed almost constant specific capacity after 100 cycles, revealing the good electrochemical stability for the flexible Li–O_2 battery. Figure 5c indicates that the electrochemical performance of this battery is hardly influenced by bending or twisting strains. The high flux of electron conduction throughout the cathode as well as the absent of the parasitic reaction caused by non-conductive polymeric binder, together with the flexible ability of the TiO_2 NAs/CT, can contribute to the high performances for this highly flexible Li–O_2 battery. In addition, a wire-shaped lithium–air battery has been indicated by Huisheng Peng's group.[71] They reported this battery could exhibit a discharge capacity of 12470 mA h g^{-1} with high stabililty for 100 cycles in air and it also showed well maintained electrochemical performances under bending. This flexible cable battery could be wearable and integrated into flexible textile for various electronic devices.

Additionally, other flexible batteries such as sodium-ion batteries (SIBs),[72] Zn–air batteries[73] and alkaline batteries[74] have also been studied. David et al.[72a] demonstrated the fabrication and electrochemical performance and mechanical properties of layered freestanding papers composed of acid-exfoliated few-layer molybdenum disulfide (MoS_2) and rGO flakes as a freestanding flexible electrode in LIBs. The results revealed a stable charge capacity of approximately 230 mA h g^{-1} with respect to

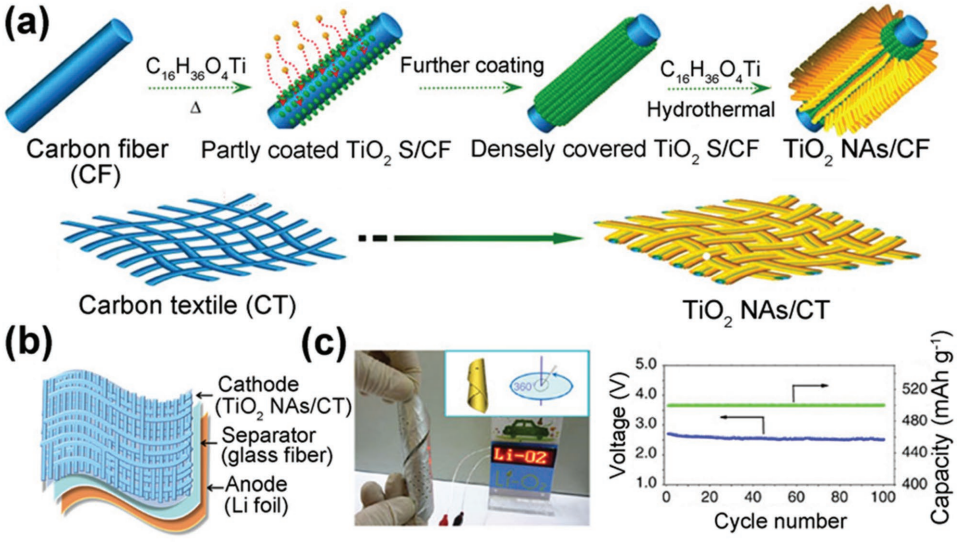

Figure 5. a) Schematic illustration for the preparation process of the TiO_2 NAs/CT. b) Schematic illustration of the flexible battery assembly. c) The twisting properties with the device twisted to 360° with the corresponding variation of discharge voltage vs cycle number of the Li–O_2 cells. a–c) Reproduced with permission.[70] Copyright 2015, Macmillan Publishers Limited.

total weight of the electrode with Coulombic efficiency reaching about 99%, which indicated good cycling ability.

Herein, from 2010, a large number of investigations and innovations about flexible energy-storage devices have been indicated mainly concentrated on designing and developing reliable nanoengineered electrode and electrolyte materials and optimal battery structural configurations. However, there is a long way to the commercialization of flexible batteries in practical applications and more effort is desired to be devoted to.

2.2. Flexible Supercapacitors

Also well-known as supercapacitors (SCs) or ultracapacitors, electrochemical capacitors (ECs) are power devices have attracted significant attention recently, owing to their high power, long cycle life, the ability to store and release the energy within a few seconds, and high reliability and good safety.[6a,b] Depending on the charge storage mechanism and used active materials, ECs can be distinguished generally into: electrochemical double layer capacitors (EDLCs) using carbon-based active materials with high surface area; pseudo-capacitors or redox SCs with fast and reversible surface or near-surface reactions for charge storage; hybrid capacitors using a capacitive or pseudo-capacitive electrode with a battery electrode together.[75] Owing to the requirement of powering wearable electronic devices, flexible, inexpensive, lightweight, environment-friendly SCs have been extensively developed. Various strategies have been studied for flexible SCs, which can be divided into the following three sections according to the methods of their stacks: flexible 2D through-plane electrode configuration; 2D in-plane electrode configuration; 3D electrode configuration.

2.2.1. Flexible 2D Through-Plane Electrode Configuration

Generally, SCs are cofacial planar-structured and they consist of the electrolyte/separator sandwiched by two electrodes. Like LIBs, based on the electrode as the key component, flexible SCs can also be designed as following structures.

Paper-Like Configuration: Same as flexible battery, SCs with paper-like configuration based on conductive carbon, polymer materials and composite materials are one of the most widely developed structures, due to lightweight, flexibility, and high conductivity. Nanostructured carbon materials including CNFs, CNTs, graphene, GO have been adopted in flexible paper-like SCs. The reports in the literature about flexible SCs based on CNFs will be reviewed first. Huang et al.[76] reported a 3D hybrid nanostructured electrode based on CNF paper (CFP) with large surface area and short diffusion path for electrons/ions for high-performance SCs. Cobalt and nickel double hydroxide (DH) nanosheets were electro-deposited on porous $NiCo_2O_4$ nanowires grown radially on CFP. The results demonstrated a high areal capacitance for this hybrid electrode of 2.3 F cm^{-2} at a current density of 2 mA cm^{-2} and high rate stability of less than 40% decay by increasing the current density from 2 to 150 mA cm^{-2}. The hybrid nanocomposite electrodes with $Co_{0.5}Ni_{0.5}$DHs delivered an energy density of ≈58.4 W h kg^{-1} at a power density of ≈41.3 kW kg^{-1}. In addition, a flexible and highly conductive $NiCo_2O_4$ single-crystalline nanotube arrays grown on the CFP was also demonstrated.[77]

Yi Cui's group from Stanford University is also a pioneer in the investigation of flexible SCs. Recently, they demonstrated a flexible all-solid-state SCs inspired by the structure of bamboos with a periodic distribution of interior holes along the length and graded pore structure at the cross section, as shown in **Figure 6**a and 6b.[78] This special structure not only can enhance electrochemical stability under mechanical deformations but also provide a high surface area accessible to the electrolyte and a fast ion-transport transport. The CNF network membrane could work as freestanding electrodes for an all solid-state SCs without extra support. The SC based on this flexible CNF electrode exhibited a high specific capacitance of 2.1 F cm^{-3} at 33 mA cm^{-3}. Additionally, the flexible all-solid state SC showed a stable cycle life in the potential range of 0–0.9 V at 67 mA cm^{-3} and retain 96% of the initial capacitance after 10 000 cycles, indicating excellent cycling stability. The specific power and energy densities for this bamboo-like CNFs are 61.3 kW kg^{-1} and 2.37 W h kg^{-1}, respectively. Figure 6c indicates that almost 100% capacitance retention ratio, calculated based on CV curves, was observed for the as-prepared device under continuous bent and twisted status (90°, 180°), and back to the initial status. A Ragone plot shown in Figure 6d demonstrates that the all-solid-state SC has the a extremely high volumetric power and energy density of 6.1 W cm^{-3} and 2.4 × 10^{-4} W h cm^{-3}, which is much larger than those typical all-solid-state ECs based on carbon materials. This nature-inspired work extends the research frontier on flexible all-solid-state SCs and opens up new paths to the development of their advanced applications.

Flexible SCs based on CNT materials have been also proposed. Flexible electrodes for SCs have been achieved either by coating CNTs on flexible substrates such as office papers[79] or by CNTs network film.[80] Xiao et al.[80] reported lightweight, thin, flexible mesoporous vanadium nitride (VN) nanowires (MVNNs)/CNT hybrid freestanding electrodes prepared by vacuum-filtering method. The all solid-state flexible SCs based on this freestanding MVNN/CNT hybrid electrodes with electrolyte of H_3PO_4/poly(vinyl alcohol) (PVA) showed a high volume capacitance of 7.9 F cm^{-3} and energy density of 0.54 mW h cm^{-3} and power density of 0.4 W cm^{-3} at a current density of 25 mA cm^{-3}. The synergistic effects by the high electrochemical performance of MVNNs, and the high conductivity and good mechanical properties of the CNTs could contribute the good properties.

Although improved electrochemical performance can be achieved by using CNTs-based electrode, the high cost of CNTs and the complex process in preparation of stable CNT dispersions have limited their practical applications. Owing to their special performances of strong mechanical property and high conductivity, graphene and GO paper have been used in various applications, which have been synthesized by the flow-directed assembly of individual GO/graphene sheet and are promising materials in energy-storage devices.[19b,81] An early work about SCs using ultrathin, transparent graphene films indicated 135 F g^{-1} for a film with about 25 nm thickness.[82] Later, mechanically pressing a graphene aerogel into a graphene paper was demonstrated.[83] The results indicated that the SCs based on graphene paper showed a high capacitance of 172 F g^{-1} at a

DOI: 10.1002/adma.201603436

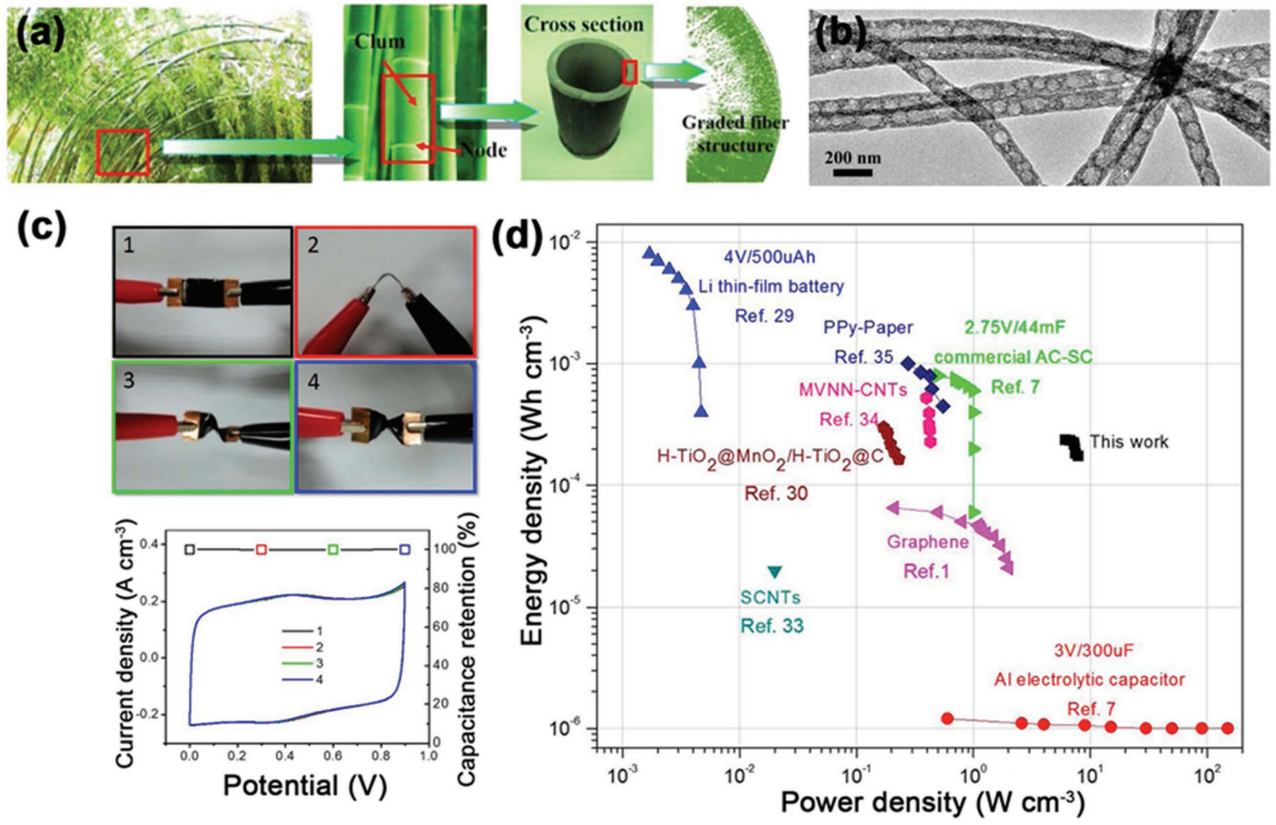

Figure 6. a) The graded structure of bamboos. b) TEM image for bamboo-like carbon nanofibers. c) Digital images of the flexible device bent by (1) 0° and (2) 90°, and twisted by (3) 90° and (4) 180° and the corresponding CV curves and capacitance retention tested at 100 mV s^{-1}. d) Ragone plot. a–d) Reproduced with permission.[78] Copyright 2015, American Chemical Society.

charge/discharge rate of 1 A g^{-1}, and a capacitance of 110 F g^{-1} can be obtained at a fast rate of 100 A g^{-1}. Therefore, the authors believed that this flexible graphene paper as electrodes for LIBs or SCs could show much higher performances compared to graphene paper fabricated by a flow-directed assembly method. The high mass yield of graphene sheets with high-quality for various practical applications in electronics, optoelectronics, and energy storage was subsequently reported by Parvez et al.[84] Using the graphene film, the flexible solid-state SCs delivered a high area capacitance of 11.3 mF cm^{-2} with a good rate capability of 5000 mV s^{-1}. In addition, many flexible SCs using GO paper have also been demonstrated.[85]

Moreover, carbon-based materials could be incorporated with pseudocapacitance materials including transition metal oxides[86] and polymers,[87] which is a promising strategy to further achieve enhanced electrochemical performances. Meng et al.[87] reported an ultrathin all-solid-state SC via a simple process. Two slightly separated polyaniline (PANI)-based electrodes were well solidified in the H_2SO_4–PVA gel electrolyte. It also indicated that this paper-like material could be modified into any shape, suitable for various applications. Even the SC was under a twisting state, it showed a high specific capacitance of 350 F g^{-1} for the electrode materials, good cycling stability over 1000 cycles.

Recently, in addition to carbon-based materials, polymer, metal oxides and composite materials, other novel materials such as MXenes[88] and molybdenum disulfide (MoS_2)[89] have also been attracted much attention and used in flexible SCs. MXenes is a new class of 2D materials, combining hydrophilic surfaces with metallic conductivity, which have shown promising performance as electrodes in both LIBs and SCs. Ling et al.[88] demonstrated the flexible and conductive $Ti_3C_2T_x$ MXene membranes with high capacitance. $Ti_3C_2T_x$/polymer composites was prepared by mixing $Ti_3C_2T_x$ MXene with polydiallyldimethylammonium chloride (PDDA) that is charged or PVA that is electrically neutral to form, which were pretty flexible and highly conductive. The SCs using MXene/PVA–KOH composite film showed an impressive volumetric capacitance of about 530 F cm^{-3} at 2 mV s^{-1}. Therefore, these layered materials (graphene, MXenes, MoS_2, vanadyl phosphate[90] and black phosphorous[91]) have shown great promise as electrodes in electrochemical energy-storage systems.

Sponge/Porous Configuration: Sponge structured material with 3D interconnected and porous network of both electron/ion pathways is emerged as a new direction used in various applications. Natural sponge is highly porous and a strong absorbing matrix with large internal specific surface area, which is a promising 3D scaffold for electrodes. In early work by Yi Cui's group, a commercial sponge with a high water absorption capacity was employed in flexible SCs.[92] Nanostructured MnO_2 was electrodeposited onto the conductive CNT-sponge skeleton as the electrode for the SC. A very high specific capacitance

of 1000 F g^{-1} could be obtained based on the mass of MnO_2 for the MnO_2–CNT-sponge SC. It also showed a high specific energy of 61 W h kg^{-1} and a specific power of 63 kW kg^{-1}.

Without the use of a polymer scaffold, a fully carbon-based sponge with flexibility and light weight such as CNT sponge and graphene foam (GF) have been recently prepared using CVD and employed as electrodes for LIBs and SCs.[24,93] Chen et al.[94] demonstrated a novel carbon foam (GF) with a 3D interconnected network synthesized by carbonizing melamine foam directly. For use as an electrode in SCs, it exhibited a specific capacitance higher than 250 F g^{-1} in 1M H_2SO_4 at a charge/discharge current density of 0.5 A g^{-1}. The nitrogen-doped carbons foam (NGF) based 3D electrode structure for SCs was also developed.[95] $NiCo_2S_4$ nanosheets have been successfully grown on NGF with strong adhesion by a hydrothermal method and a sulfidation process, which could be employed as the binder-free electrode for SCs. The resultant SC exhibited high rate capability of 877 F g^{-1} at 20 A g^{-1} and good cycling stability. They also displayed a asymmetric SC (ASC) with high performance assembled using $NiCo_2S_4$/NCF as the positive electrode and ordered mesoporous carbon (OMC) as the negative electrode, which exhibited a high energy density of 45.5 W h kg^{-1} at 512 W kg^{-1}.

In addition, 3D GF/CNT composite membrane with high flexibility and good mechanical properties was indicated to be a promising support candidate as flexible electrodes for SCS.[96] To demonstrate the concept of lightweight and flexible ASCs, researchers deposited MnO_2 and polypyrrole (Ppy) on the GF/CNT membrane. The ASCs assembled from GF/CNT/MnO_2 and GF/CNT/Ppy composite membrane with high mass loading of electroactive materials using an aqueous electrolyte were shown to work at an output voltage of 1.6 V, and delivered a high energy/power density of 22.8 W h kg^{-1} at 860 W kg^{-1} and 2.7 kW kg^{-1} at 6.2 W h kg^{-1}. The electrochemical performance could be further increased by less loading of active electrode materials, showing 10.3 kW kg^{-1} at 10.9 W h kg^{-1}.

Wu et al.[97] presented a new, green, and template-free route to prepare 3D sponge-like carbonaceous hydrogels and aerogels using crude biomass, watermelon as the carbon source. They synthesized the carbonaceous gel-based composite materials as electrodes for SCs by incorporating Fe_3O_4 nanoparticles into the carbonaceous gels networks and then calcination into magnetite carbon aerogels (MCAs). The MCAs exhibit a high capacitance of 333.1 F g^{-1} at a current density of 1 A g^{-1} in 6 M KOH solution. Good cycling stability with 96% capacitance retention after 1000 charge/discharge cycles was also observed for MCAs.

Textile Configuration: Flexible SCs can be achieved using textile electrodes containing a fibrous structural support that is highly flexible and mechanically robust, by a replacement of conventional metal current collector. The textile scaffold can be made of plastic, metal, CNT, graphene fiber/bundle/yarn, etc. The 3D network of textile is capable to provide a fast electronic/ionic conduction pathway and a high mass loading of active materials. Cui and co-workers[98] report a nanostructured material based on a highly conductive CNT textile fiber, which delivers an effective 3D framework for the electrodeposition of nanoscale MnO_2. The conductive textiles were prepared by coating CNTs on the surface of polyester fibers. Such structure greatly results in a fast ion transport in the electrode, which improves the electrochemical performances. For a given areal mass loading, the MnO_2 thickness on the conductive textile was much thinner compared with that on a flat metal substrate. Therefore, this porous textile structure allowed a high mass loading, up to 8.3 mg cm^{-2}, resulting in a large areal capacitance of 2.8 F cm^{-2} at a scan rate of 0.05 mV s^{-1}.

Meanwhile, it can be seen that the textile electrodes based on fibrous polymer supports result in a low weight and volume fraction for active electrode materials, which in turn decreases the specific capacitances of entire electrodes and SCs. Therefore, carbon-based fiber cloth with good flexibility and high conductivity shows an advantage for the electrodes in SCs. Lv et al.[99] demonstrated an advanced flexible integrated electrode for high-performance pseudocapacitors designed by growing N-doped CNT/Au-nanoparticles-doped-MnO_2 (NCTs/ANPDM) nanocomposite on carbon fabric. The free-standing ZnO nanorod arrays as templates were first grown on the carbon fabric by a hydrothermal synthesis method and then a thin amorphous N-doped carbon layer was formed on the surface of ZnO nanorods via the polymerization of dopamine and subsequently thermal carbonization processes. The carbon fabric coated with ZnO/N doped-C nanorods was used as a working electrode, and ANPDM could be successfully electrodeposited on their surfaces. Finally, the prepared ZnO/N-doped-C/ANPDM electrode was immersed in 3.0 M KOH solution to remove the ZnO nanorods template and formed the NCTs/ANPDM electrode. The solid-state ASC device using this flexible textile electrode achieved a high gravimetric capacitance and volumetric capacitance of 158 F g^{-1} and 131 mF cm^{-3} at a current density of 0.42 mA cm^{-3}. A prototype solid-state thin-film symmetric SC (SSC) device based on NCTs/ANPDM exhibited a large energy density of 51 W h kg^{-1} and superior cycling performance (93% after 5000 cycles). It was believed that the excellent electrical conductivity and well-ordered tunnels of NCTs together with Au nanoparticles of the electrode could provide a low internal resistance, a good ionic contact, and consequently enhance redox reactions for high specific capacitance of pure MnO_2 in aqueous electrolyte, even at high scan rates.

Dong et al.[100] proposed a new approach for the simultaneous preparation of flexible textile electrodes and fiber electrodes. The activated carbon fiber cloth (ACFC) was used as body materials to design ACFC/CNTs and ACFC/MnO_2/CNTs composites. The high electrical conductivity of CNTs, ultrahigh theoretical capacitance of MnO_2, and high electrochemical activity of ACFC body material, together endow the fabricated textile electrodes with excellent electrochemical properties, which demonstrated a high areal capacitance of 2542 mF cm^{-2}, an energy density of 56.9 μW h cm^{-2}, and a power density of 16287 μW cm^{-2}. Additionally, many reports in the literature discuss flexible SCs using carbon textile or cloth, showing excellent electrochemical performance and good mechanical property.[101]

2.2.2. Flexible 2D In-Plane Electrode Configuration

The recent boom in multifunction portable electronic equipment requires the rapid development of miniaturized

Adv. Mater. 2016,
DOI: 10.1002/adma.201603436

electrochemical energy-storage devices, for example, micro-SCs.[102] micro-SCs with interdigitated patterned electrodes can deliver very high power densities, several orders of magnitude higher than those of traditional batteries and SCs owing to the short ion transport distance.[103] Directly integrating the storage element as close as possible to the electronic circuit (on chip microdevices) represents a new direction, which provides excellent nano-/microscale peak power. Considerable efforts have been devoted to increase the energy and power densities of micro-SCs via the optimization of nanostructured electroactive materials and the development of thin film manufacture technologies as well as by the exploitation of novel device architectures. Fabrication thin film electrodes with a high electrical conductivity, highly electrochemically activated surface area, good interfacial integrity, and an elaborate device structure with short electron/ion transport distances have been the main approaches to achieve high performance for micro-SCs.[103] Generally, using flexible chips can result in the extra ability of flexibility. Wang et al.[104] first reported all-solid-state flexible micro-SCs on a PET chip based on a pattern of microelectrode consisted of PANI nanowire arrays through microfabrication technology and in situ chemical polymerization method. The flexible micro-SCs exhibited a high capacitance of 588 F cm^{-3} with a fast rate capability. In addition, these micro-SCs could be connected in series or parallel to further increase the output potential and/or current.

As is well known that control of structure and morphology is key for carbon-based electrodes to allow the effective permeation of the electrolyte to establish electrical double layers (EDLs) in SCs. Due to the 2D layered structure of graphene films, their large in-plane conductivities are expected to play a crucial role in the development of electrodes. The in-plane electrode structure provides a possibility to utilize this high conduction pathway for SCs. Ajayan's group demonstrated the utilization of pristine graphene using CVD method and multilayer graphene (reduced multilayer graphene oxide (RMGO)) as electrodes in an "in-plane" geometry in SCs.[105] The in-plane devices consisting of graphene and RMGO electrodes showed normalized capacitance by the geometrical area is 80 and 390 μF cm^{-2}, respectively. This flexible device could be easily adopted to various structural and hybrid designs for energy-storage devices.

Later, Wu et al.[103] reported graphene-based in-plane interdigital micro-SCs on arbitrary substrates. A thin membrane of GO was first obtained by spin-coating a GO slurry on a silicon substrate treated by O_2 plasma in advance. The GO film was then rapidly reduced by methane (CH_4)-plasma treatment, resulting in reduced graphene (MPG) film. Subsequently, well-developed lithography techniques were used to fabricate graphene based Au interdigital microelectrode patterns. The micro-SCs using H_2SO_4/PVA showed an area capacitance of 80.7 mF cm^{-2} and a stack capacitance of 17.9 F cm^{-3}. A power density of 495 W cm^{-3} and an energy density of 2.5 mW h cm^{-3} comparable to LIBs, were achieved. Such microdevices can operate at ultrahigh rate up to 1000 V s^{-1}, which is three orders of magnitude higher than that of conventional SCs. Moreover, the authors adopted this fabrication method to a PET substrate, which results in flexible micro-SCs, as shown in **Figure 7**a. The Au collectors could be removed by rinsing in KI/I_2 solution, resulting in a transparent characteristic of the fabricated microdevices (Figure 7b). This flexible SC showed an area capacitance of 78.9 mF cm^{-2} and a stack capacitance of 17.5 F cm^{-3} at 10 mV s^{-1}, which is comparable to the performance of the devices based on a rigid silicon substrate. A transparent all-solid-state SC using large-scale interdigitated pattern type electrodes of MnO_2 was also reported.[106] This SC showed a high capacitance of 405 F g^{-1} and flexibility of bending radius of 1.5 mm.

In addition, carbon-based composite materials have been also studied as electrodes in flexible SCs with in-plane electrode structure. Lin et al.[107] demonstrated a flexible 3D graphene/carbon nanotube carpets (G/CNTCs)-based micro-SCs, fabricated in situ on nickel electrodes. The micro-SCs using G/CNTCs showed a high volumetric energy density of 2.42 mW h cm^{-3} in the ionic liquid, more than two orders of magnitude higher compared with commercial Al electrolytic capacitors. In addition, an ultrahigh rate capability of 400 V s^{-1} could enable the microdevices to demonstrate a maximum power density of 115 W cm^{-3} using aqueous electrolyte.

It can be seen that the conventional fabrication techniques for micro-SCs mainly on photolithography technology or on oxidative channel-etching methods to fabricate the interdigitated electrode patterns on substrates, which are high cost and are therefore difficult to apply to the construction of cost-effective devices for commercial applications. Recently, directly printable in-plane micro-SCs on paper and ultrathin PET substrates have been demonstrated accordingly.[108] A hybrid ink composed of electrochemically exfoliated graphene (EG) and an electrochemically active PEDOT:PSS formulation was first prepared. By spray-coating the hybrid ink via a shadow mask with the designed device geometry, the direct printing of micro-SCs was obtained. Using paper as flexible substrate, the SCs showed an areal capacitance as high as 5.4 mF cm^{-2}, which is among the best reported performances of graphene-based micro-SCs. This flexible SC also exhibited a good rate capability with capacitance retention of 75% when operated from 10 to 1000 mV s^{-1}.

2.2.3. Flexible 3D Electrode Configuration

The configuration and nanostructure of the electrodes in SCs have greatly effect on the electrochemical performance. As a result of ion adsorption at the electrode/electrolyte interface for the SCs, 3D nanostructured materials can be designed to provide a high surface area and subsequently enhance specific capacitance. Meanwhile, optimizing the length of electron/ion conduction pathways can enhance the charge/discharge rate for SCs.[109] Various approaches to the modifications of 3D electrode structures without binder in flexible SCs have been reported to show increased electrochemical performances and mechanical properties. 3D architectures such as aligned array and wire-shaped structure for flexible SCs are reviewed as follows.

Array Configuration: Various flexible SCs based on aligned array of 3D nanostructured electrodes have showed improved performances compared with traditional planar configuration.[110] To achieve flexible electrodes in SCs, the arrays with high surface area can be either grown on polymer cloth/yarn, carbon-based textile or metal foil. An early work demonstrated a template-free method to prepare a large area of length-controllable

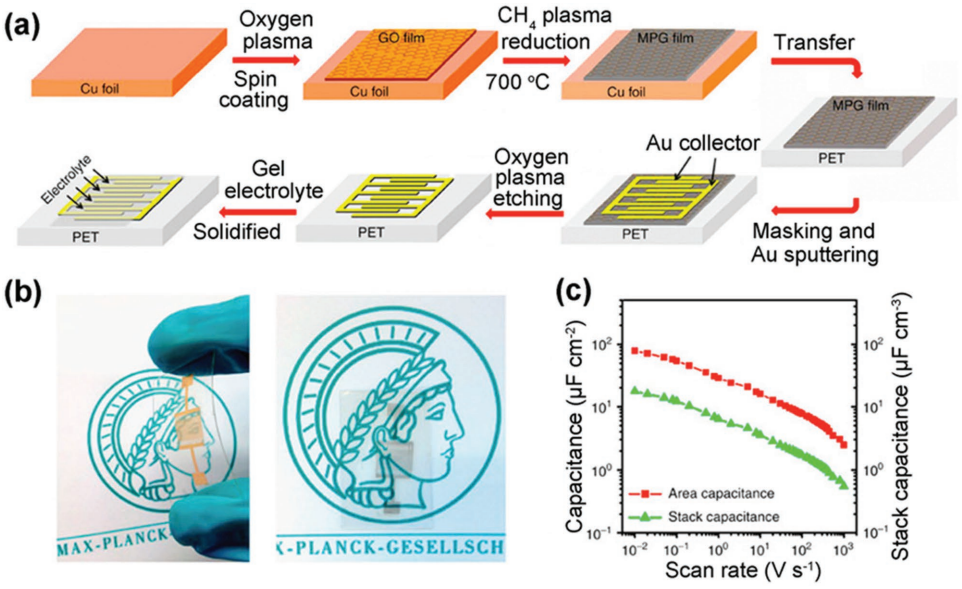

Figure 7. a) Schematic illustration of the fabrication process of flexible MPG-MSCs-PET. b) The MPG-MSCs-PET with and without Au collectors, demonstrating the flexible and transparent characteristics of the fabricated microdevices. c) Area capacitance and stack capacitance of the MPG-MSCs-PET. a,b) Reproduced with permission.[103] Copyright 2013, Macmillan Publishers Limited.

and well-aligned PPy nanowire arrays using an electrochemical polymerization.[111] The SCs using PPy NW arrays as electrode indicated a high capacitance of 566 F g^{-1} and 70% retaining of its initial capacitance over hundreds of charge/discharge cycles.

Figure 8a indicates that this advanced 3D nanostructure of ordered array can provide short penetrating paths and lower ion resistance for the diffusion of counter-ions to increase the availability in PPy NW arrays during the charge/discharge.

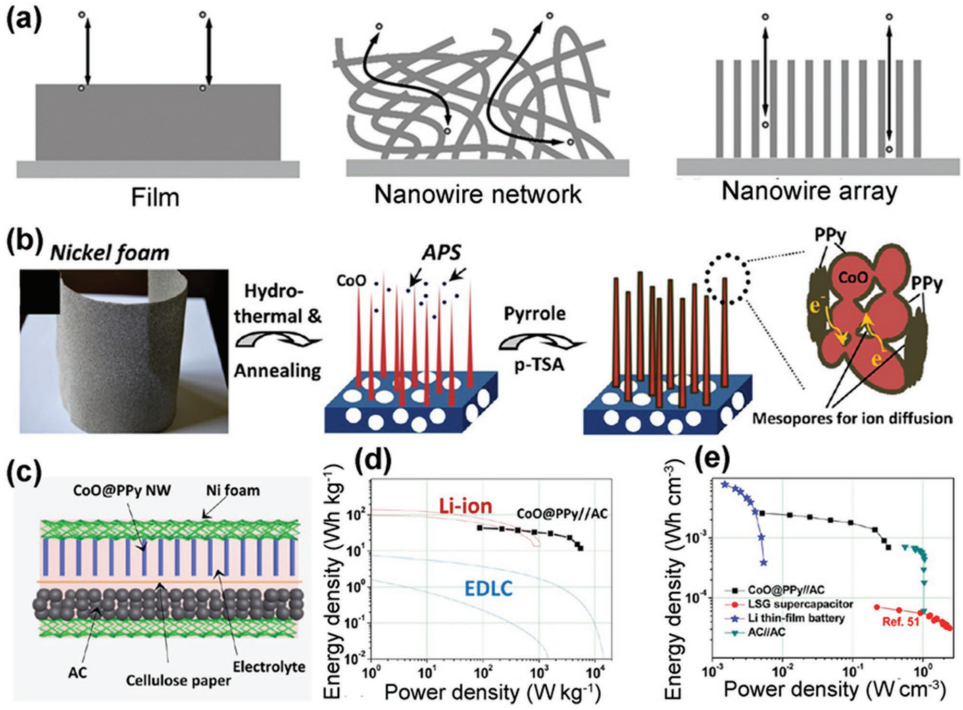

Figure 8. a) Schematic model of ion diffusion of film, random nanowire networks, and aligned nanowire arrays. Reproduced with permission.[111] Copyright 2010, the Royal Society of Chemistry. b) The preparation procedure and structure of the 3D hybrid nanowire electrode. c) Schematic illustration of the asymmetric SC structure. d) Ragone plot of the SC. EDLC and LIB are also included for comparison. e) Volumetric energy and powder densities of the SC compared with other data. b–e) Reproduced with permission.[112] Copyright 2010, American Chemical Society.

Adv. Mater. **2016**,
DOI: 10.1002/adma.201603436

Wang et al.[113] demonstrated a flexible SC based on cloth-supported single-walled carbon nanotubes (SWCNTs) and a conductive PANI nanowire array composite electrode. For a typical synthesis process, SWCNTs were first deposited on a flexible substrate of non-woven wiper cloth by dip coating with SWCNT ink, and PANI nanowire arrays then grown onto the surface of SWCNT/cloth via dilute polymerization. The prepared PANI/SWCNT/cloth composite electrode was used to assemble the flexible SCs directly, which had an improved specific capacitance of 410 F g^{-1} and good cycling stability. Later, the flexible ASCs with array structure based on highly conductive carbon cloth has been reported.[114] The flexible ASCs consisted acicular Co_9S_8 nanorod arrays as the positive electrode and Co_3O_4@RuO_2 nanosheet arrays as the negative electrode on woven carbon fabrics. The liquid-state and solid-state ASCs indicated high volumetric capacitance of 3.42 and 4.28 F cm^{-3}, energy density of 1.21 mW h cm^{-3} at 13.29 W cm^{-3} and 1.44 mW h cm^{-3} at 0.89 W cm^{-3}, respectively. Good rate capability and cycle stability for the flexible ASCs were also achieved. Moreover, the solid-state ASCs showed stable electrochemical performance at the normal, bent and twisted conditions.

Nickel foam is one of the best candidates as 3D current collector, owing to its large and uniform macropores and high electrical conductivity, which can guarantee efficient electrolyte penetration and fast ion conduction. Zhou et al.[112] developed a flexible electrode for SCs based on well-aligned CoO nanowire array with PPy uniformly immobilized onto each nanowire surface grown on 3D nickel foam, as shown in Figure 8b. A high specific capacitance of 2223 F g^{-1}, excellent rate capability and cycling stability (99.8% capacitance retention after 2000 cycles) were observed for the composite electrode benefit from the merits of the elegant synergy between CoO and PPy. An aqueous ASC device (Figure 8c) with a maximum voltage of 1.8 V using this hybrid array as the positive electrode and activated carbon membrane as the negative electrode was assembled, which showed high energy density of 43.5 W h kg^{-1}, high power density of 5500 W kg^{-1} 11.8 W h kg^{-1} and good cyclability of 20 000 times.

Wire-Shaped Configuration: Flexible SCs utilize 1D cylindrically wire-shaped electrodes have attracted growing interest and demonstrated great application potential in microscale energy-storage devices for in miniaturized and wearable electronics. Generally, the structures including two parallel fibers, two twisted fibers and one coaxial fiber have been studied for fiber-shaped SCs.[115] Zhong Lin Wang's group from Georgia Institute of Technology developed the first wire-shaped SC in 2011.[116] They demonstrated a high-efficiency fiber-based micro-SC with ZnO nanowires as electrodes using a flexible plastic wire or a Kevlar fiber as a substrate. This flexible fiber-shaped SC could be used in self-powering nanosystems, such as a power shirt using piezoelectric ZnO NWs grown radially around textile fibers. Liu et al.[117] reported a hierarchical graphene–metallic textile hybrid electrode consisted of graphene sheets immobilized on the surface of cotton yarns with Ni coating. Other work about flexible wire-shaped SCs based on polymer fibers has also been demonstrated.[118]

Besides polymer fibers or yards as flexible scaffold, a large number of reports in the literature discuss wire-shaped SCs based on carbon materials such as CNF, CNT, graphene, GO and composite materials. Later, Xiao et al.[119] in cooperation with Zhong Lin Wang to develop an all-solid-state flexible SC based on a carbon/MnO_2 (C/M) core–shell fiber using CF. MnO_2 was first grown on CF via a self-limiting electroless deposition method to obtain C/M core–shell fibers. The fibers were then closely and parallel located on a PET substrate with a gap of 1 mm, and a H_3PO_4/PVA gel electrolyte was subsequently coated on the fibers. The solid state SC was prepared by packaging after the gel solidified. A high rate capability with a scan rate up to 20 V s^{-1}, a high volume capacitance of 2.5 F cm^{-3}, and an energy density of 2.2×10^{-4} W h cm^{-3} could be achieved for the flexible, wire-shaped SC. Yongyao Xia's group demonstrated a highly flexible, all-solid-state, wire-shaped micro-SC fabricated by twisting a $Ni(OH)_2$-nanowire fiber and an ordered mesoporous carbon (OMC) fiber together using a gel polymer electrolyte to separate them.[120] This wire-shaped micro-SC displayed a high specific capacitance of 6.67 mF cm^{-1} (or 35.67 mF cm^{-2}) and a high specific energy density of 0.01 mW h cm^{-2} (or 2.16 mW h cm^{-3}), with 70% capacitance retention over 10 000 cycles.

Flexible graphene fiber (GF) presents for a new type of fiber for practical applications, which is a promising scaffold for electrodes in LIBs and SCs. Meng et al.[121] reported an all graphene core–sheath fiber. The core of GF was covered with a sheath of 3D porous graphene network. The all-solid-state fiber-like supercapacitors were obtained from two twined fiber electrodes covered with H_2SO_4/PVA gel electrolyte. This flexible wire-shaped SC could offer excellent electrochemical performances due the high electronic conductivity of the core graphene fiber and the large surface areas of 3D graphene network. The energy density and power density were $0.4–1.7 \times 10^{-7}$ W h cm^{-2} and $6–100 \times 10^{-6}$ W cm^{-2}, which are comparable to that of ZnO-nanowire-based fiber SC.[116] Moreover, this flexible wire-shaped SC had stable electrochemical performances under bending status. The fiber SC had a capacitance of ca. 19 μF cm^{-1} even in knotted state.

Recently, Zhong Lin Wang's and Liming Dai's group developed an approach of preparation 3D graphene–CNT hollow fibers, with radially aligned CNTs (RACNTs) seamlessly sheathed by a cylindrical graphene layer.[122] One-step CVD using an anodized aluminum oxide (AAO) wire template was performed. The synthetic process to the 3D graphene–RACNT hollow fibers is shown in **Figure 9**a. The all-solid-state wire-shaped SCs exhibited a surface specific capacitance of 89.4 mF cm^{-2} and a length specific capacitance of 23.9 mF cm^{-1}, due to the fibers with a controllable surface area, meso-/micropores, and high electrical conductivity. As shown in Figure 9c, the as-prepared fiber was very flexible, and it can be knotted and also can make into a sheet of weave. A solid-state fiber-like SC was prepared based on two twisted 3D graphene–RACNT fiber electrodes, using H_2SO_4/PVA gel as the solid electrolyte, which showed a specific capacitance of 3.33 mF cm^{-2} at the discharge current of 2.12 mA cm^{-2} (Figure 9b). Moreover, as illustrated in Figure 8d and 8e, these 3D graphene–RACNT wire SCs could be integrated into assemblies with various specific energy for diverse practical applications.

Huisheng Peng's group is also leading the development of wire-shaped SCs. Recently, they demonstrated flexible fiber tube electrodes including hollow rGO/conducting polymer

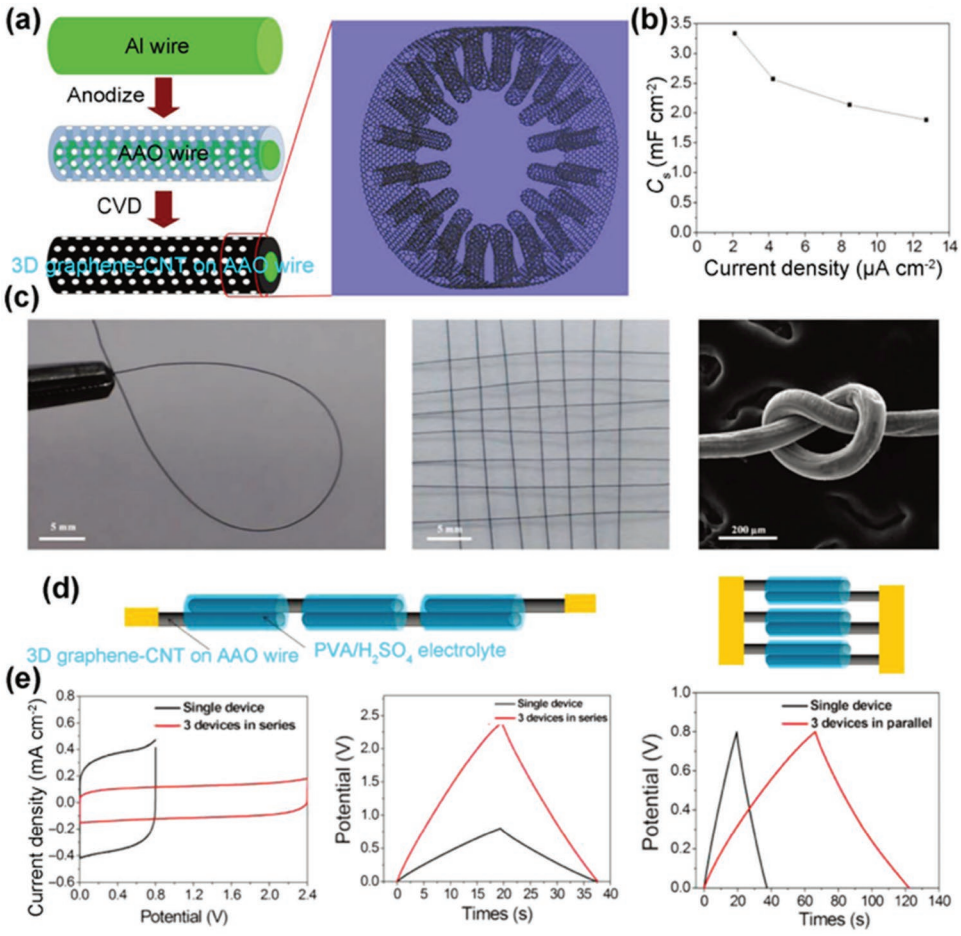

Figure 9. a) Schematic diagrams showing the synthesis of the 3D graphene–RACNT fiber. b) Surface-specific capacitance of the 3D graphene–RACNT wire electrode calculated from the galvanostatic charge/discharge curves. c) Photo of circle-shaped 3D graphene–RACNT fiber. Photo of weaved graphene–RACNT fibers. SEM image of a knot of the fiber. d) Schematic representation of an integrated SC in series and in parallel from three graphene–RACNT wire SCs. e) Galvanostatic charge–discharge curves and CV curves, respectively, for the series integrated graphene–RACNT wire SC and a single wire SC. Galvanostatic charge–discharge curves for the parallel integrated graphene–RACNT wire SC and a single wire SC. a–e) Reproduced with permission.[122] Copyright 2015, American Association for the Advancement of Science.

fibers (HCFs) and hollow bare rGO fibers (HPFs).[123] The symmetric fiber-like SCs consisted of two parallel HCF electrodes using H_3PO_4/PVA gel electrolyte showed a high specific areal capacitances of 304.5 mF cm^{-2} (or 143.3 F cm^{-3} or 63.1 F g^{-1}) at 0.08 mA cm^{-2}, corresponding to an energy density of 27.1 μW h cm^{-2} at a power density of 66.5 μW cm^{-2}. To the best of our knowledge, they represented the highest areal capacitance and areal energy density for the fiber SCs to date. Meanwhile, these wire-shaped SCs showed good stability with almost unchanged specific capacitance after bending for 500 times and 96% capacity retention over 10 000 cycles.

In practical application, the flexible SC devices undergo unavoidably various kinds of deformations including bending, folding, twisting. Therefore, long-term local strains by repeatable deformations lead to structure and functional failure. In order to solve this issue, Huang et al.[124] proposed a shape memory SC (SMSC) for the first time. A shape memory alloy of nickel-titanium (NiTi) was employed as the main skeleton and the current collector for the active electrode materials of MnO_2 and PPy. The SMSC was pretty flexible below its activation temperature. It could automatically recover its original shape and restore all deformations when it was heated over a trigger temperature. With the extra function of shape memory, all potential damage to the SCs could be nipped in the bud, which results in increased life span. The authors also demonstrated that with pre-designed shapes, the cloths based on the shape memory textiles could provide extra functionalities, for example, automatic cooling or temperature alarm other than energy storage, which enables various wearable electronic devices.

3. Stretchable Energy Storage

In the last decade, along with the rapid and wide development of flexible electronics, the field of stretchable electronics has also been investigated from the developing of fundamental enabling technologies, studying applicable devices, and broadening novel application opportunities.[4b] However, stretchable energy

DOI: 10.1002/adma.201603436

storage did not spring up as a new technology until 2009, to accommodate the ever-changing market ranging from medical implants to stretchable electronics,[10a] owing to the relative complicated configurations or the requirement of maintaining sufficiently high energy density at various stretched deformations. The stretchable energy-storage devices must accomodate large strain and shape deformations, such as bending, twisting, folding, and stretching. Therefore, in comparison to flexible devices, stretchable energy-storage devices, such as LIBs and SCs, claim higher requests to structure and material design. In general, two approaches have been focused on to develop stretchable energy storage: exploring novel materials that are intrinsically elastic to serve as key components (electrodes and electrolytes); designing novel structural for rigid components to realize device systems with stretchable ability. The former idea is much more difficult to be realized than the latter one. The recent important evolutions on stretchable batteries and SCs are highlighted in the following sections, respectively.

3.1. Stretchable Lithium-Ion Batteries

Although the recent notable advances in the flexible LIBs with reliable bendable characteristic have been achieved, the bending function have not yet met the requirement of the batteries for stretchable electronic devices that can be integrated into clothes[125] or conformally attached to the skin[126] because the batteries are also required to be stretched and deformed into arbitrary shapes according to dynamic motions of the stretchable electronic devices in order to sustain large strain induced by the devices while maintaining their electrochemical performances. Therefore, the development of stretchable LIBs is inevitable to power the stretchable devices. To realize the stretchable batteries, the current rigid key components of the lithium-ion batteries should be either: i) replaced by intrinsically stretchable materials or ii) made into stretchable forms by using new architecture for heterogeneous integration of rigid and soft materials,[4b] as is aforementioned. To date, a handful of reports in the literature have have demonstrated stretchable LIBs. In the following sections, recent important advances in stretchable electrodes, electrolyte, and integrated battery system on the basis of the above strategies are sequentially introduced and described to guide the route toward the stretchable LIBs with more improved performances and stretching reliability.

3.1.1. Stretchable Electrodes

Until now, the elastic organic materials that can replace the active materials (LCO and graphite) and carbon-based current conducting agent in the electrodes for the current LIBs have never been suggested due to their insufficient performances compared to the conventional materials.[127] Instead, many efforts have been made to achieve the stretchable electrodes by adopting the strategies for constructing the following main structures where rigid materials are incorporated with elastic ones: i) porous framework;[10r,128] ii) wavy design;[129] and iii) helically coiled spring configuration.[130]

Porous Framework: PDMS is a soft elastic polymer most widely used in stretchable applications due to its beneficial properties such as high mechanical stretchability, and chemical and thermal stability.[10a,131] The first study on the fabrication of the stretchable electrode using PDMS with pores has been reported in 2012 by Lee et al.[128a] In this study, a stretchable CNT/PDMS composite electrode as the anode for LIBs was prepared using porous PDMS obtained from the phase separation of poly(methyl methacrylate) (PMMA) in PDMS and then extraction of PMMA (Figure 11a). During this process, the porosity and stretchability of CNT/PDMS electrodes can be controlled by varying the ratio of PDMS/PMMA/block copolymer. The optimized porous electrode showed 190 mA h g^{-1} (based on the weight of CNT), that is, 670% higher capacity compared to nonporous one, proving the effectiveness of their strategy. The electrodes with moderate average pore sizes ranging from 30 to 50 μm achieved the stretchability of more than 70% based on a fracture strain. However, further optimization of pore structure is necessary to get higher capacity because only CNTs exposed on the surfaces of the pores can participate in the redox reaction with Li-ions in the liquid electrolyte penetrating into the pores.

Afterward, a further advance in the porous PDMS stretchable electrodes has been made by Liu et al.[10r] They reported stretchable electrodes using the 3D porous sponge-like PDMS scaffolds, based on sugar cubes as template for constructing pore structure (**Figure 10**b–e). Infiltration of PDMS into sugar cube pores and then, removal of sugar cube by dissolution in water enable simple and easy production of 3D porous PDMS scaffolds. A stretchable LTO anode and LFP cathode fabricated using 3D porous PDMS and a conventional electrode slurry showed high stretchability of more than 80% and excellent capacity retention of 82% and 91% for the LTO anode and the LFP cathode, respectively, over 500 stretch/release cycles, which represents a great improvement for stretchable electrodes for lithium-ion batteries. In addition, the LTO anode in 33% stretched state has only a slight capacity decay of 6% in comparison with unstretched one. A stable long-term cycle life of 70% capacity retention after 300 cycles was also observed in the stretchable full cell composed of the stretchable LTO anode and LFP cathode. However, although the excellent stretchable stability and reversibility of the electrodes has been achieved, the electrodes still need to be further developed due to their continuous decrease in performance with stretching, which is most likely due to an increase in resistance of the electrodes during stretching.

Unlike PDMS, PVDF has been rarely used as an elastic material for the stretchable applications due to its rigidity resulting from high young's modulus.[132] However, electrospun PVDF membrane with porous network can become stretchable because the nanofibers are very long and eventually form interconnected networks.[133] For the first time, Xiao et al. fabricated 3D stretchable silicon anode for LIBs by employing stretchable Ni/PVDF coaxial nanofiber membrane as current collector as well as substrate.[128b] A coaxial stretchable PVDF nanofiber membrane was first prepared by electrospinning, and then nickel and active amorphous silicon were coated one by one onto that to form a core–shell structure of Si/Ni/PVDF nanofiber membrane (Figure 10f–h). The resulting stretchable anode showed about 20% stretchability with high electrochemical performance of high capacity (3210 mA h g^{-1}), long cycle life (56.9% capacity retention after 1000 cycles), and good rate capability. However, the 20% stretchability is not enough to be

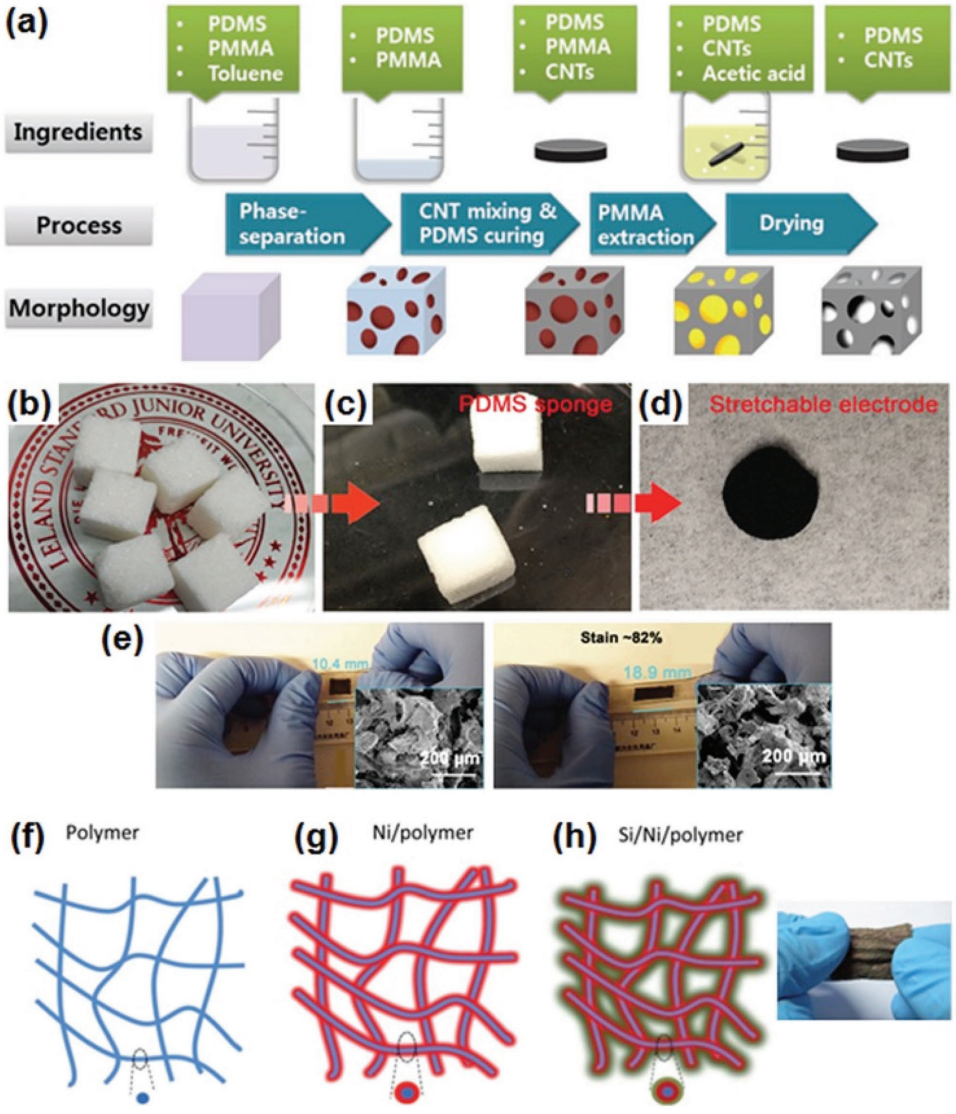

Figure 10. a) Schematic representation of the preparation procedure for the porous PDMS–CNT nanocomposites. a) Reproduced with permission.[128a] Copyright 2012, Wiley-VCH. Schematic illustration for the synthesis of the stretchable electrode for LIBs. Digital photographs of: b) sugar cubes, c) PDMS sponge, and d) stretchable electrode. e) Digital photographs show the electrode with stretchability of 82%. The inset images show SEM images of the electrode in unstretched state and stretched state, respectively. b–e) Reproduced with permission.[10r] Copyright 2016, Wiley-VCH. f–h) Schematic illustration of preparation procedure for the coaxial Si/Ni/PVDF flexible nanofiber membrane. The inset image shows the stretched Si/Ni/PVDF membrane. f–h) Reproduced with permission.[128b] Copyright 2014, the Royal Society of Chemistry.

applied to the stretchable devices, and therefore, more efforts should be made to improve the stretchability.

Wavy Configuration: Wave design is the representative well-known strategy to make stretchable substrates in the field of stretchable electronics.[4b,134] The key advantage of this strategy is that deposition of rigid materials on pre-strained elastic substrate and subsequent release of prestrain can make thin layer of any rigid materials stretchable. However, in spite of this advantage, to the best of our knowledge, there has been so far only one study on wave structured electrodes for the stretchable LIBs in the literature.

Very recently, wavy stretchable electrodes with a gum-like stretchability were reported by Weng et al.[129] Aligned CNT sheets, a blend of active material (LMO or LTO) and CNTs, and another CNT sheet were coated on the CNT sheet sequentially. Un-curing PDMS fluid was then poured onto the sandwich structure, which was then placed onto a 450% pre-strained PDMS substrate. Finally, curing PDMS and releasing the pre-strain by removal of the Cu foil were carried out to make wave structured electrode.(**Figure 11**a–d) The fabricated wavy electrodes with the sandwich configuration demonstrated as high stretchability as 400% (Figure 11e,f) and almost unchanged capacity after 500 stretching cycles with a strain of 400%. More importantly, there was no noticeable increase in resistance of the electrodes during stretching, which enabled retaining the electrochemical performance of the electrodes even at high

Adv. Mater. **2016**,
DOI: 10.1002/adma.201603436

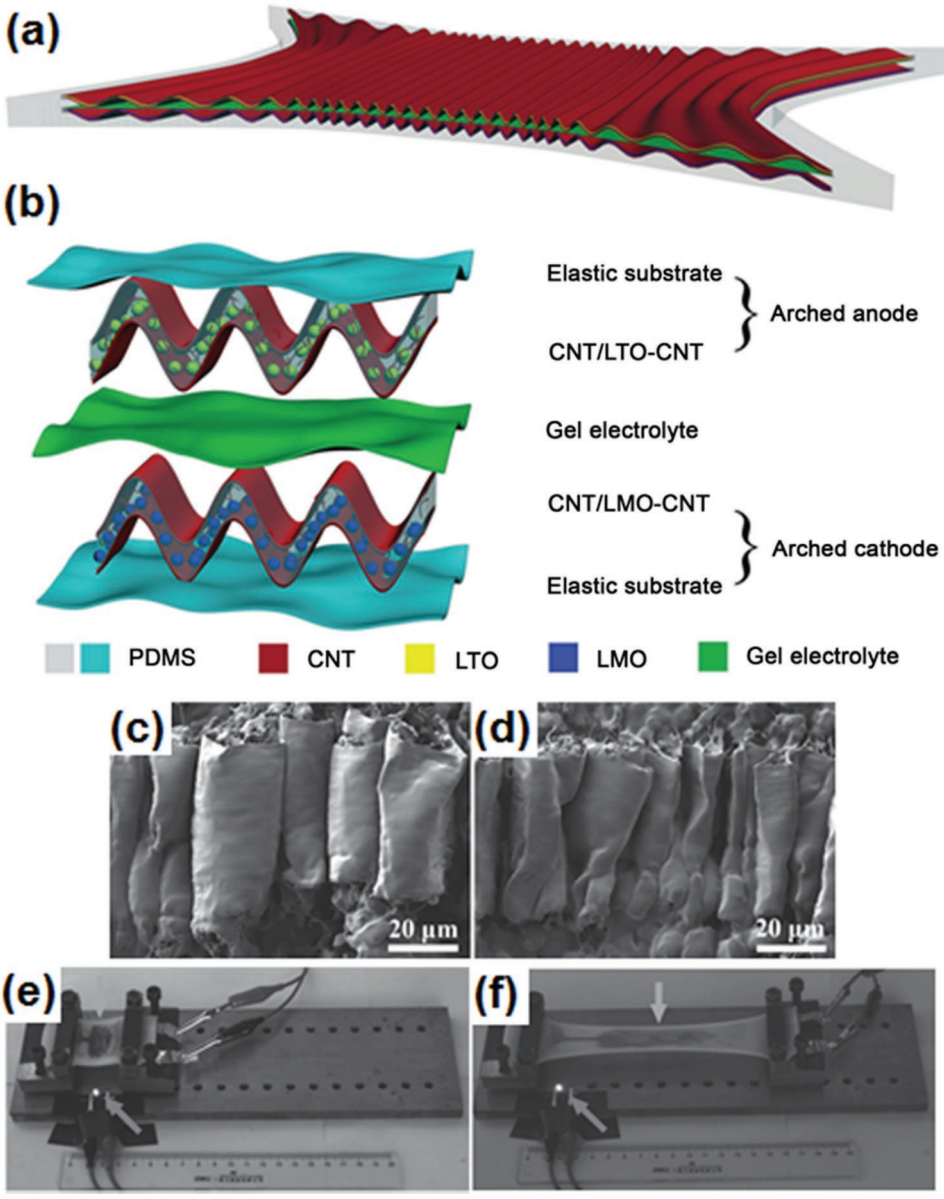

Figure 11. a,b) Schematic illustration of a stretchable battery (a) and its multilayered structure (b). c,d) SEM images of the arched structure before (c) and after (d) 1000 stretching cycles at a 400% strain, respectively. e,f) A gum-like LIB fixed on a moving stage lights up an LED before (e) and under 400% (f) stretching strain. a–f) Reproduced with permission.[129] Copyright 2015, Wiley-VCH.

stretched state of 400%. Although the excellent performances obviously originated from the wavy structure, it should be noted that the wavy electrode without the sandwich structure showed much lower performance. The improvements attained in this study are quite important for the stretchable LIBs to be practical ones. However, abrupt degradation in performance of the electrodes with areal active material loading density of more than 6 mg cm^{-2} has to be overcome for further increase in the energy density.

Helically Coiled Spring Configuration: Recently a few attempts have been made to fabricate stretchable electrodes with helically coiled spring configuration for the stretchable LIBs.[130] The first demonstration of a super-stretchy fiber-shaped electrode with spring configuration was given in 2014.[130a] They achieved the spring structured electrodes with the remarkable super-stretchability of 600% and quite stable electrochemical performances under stretching (**Figure 12**a–c). The fiber-shaped electrodes were first prepared by fabricating two MWCNT sheets incorporated with active materials (LMO and LTO) and then scrolling into fibers, which were further wound onto an elastic PDMS fiber to work as the spring structured stretchable electrodes. The stretchable batteries with high performance under stretching could be also fabricated by winding the prepared LMO and LTO fiber electrodes as cathode and anode, respectively, onto PDMS fiber in parallel with a gap of 1 mm to avoid short circuit and then coating gel electrolyte, using PDMS to seal the battery. If low loading amount of active materials in the electrodes, large parallel gap between the cathode and anode in

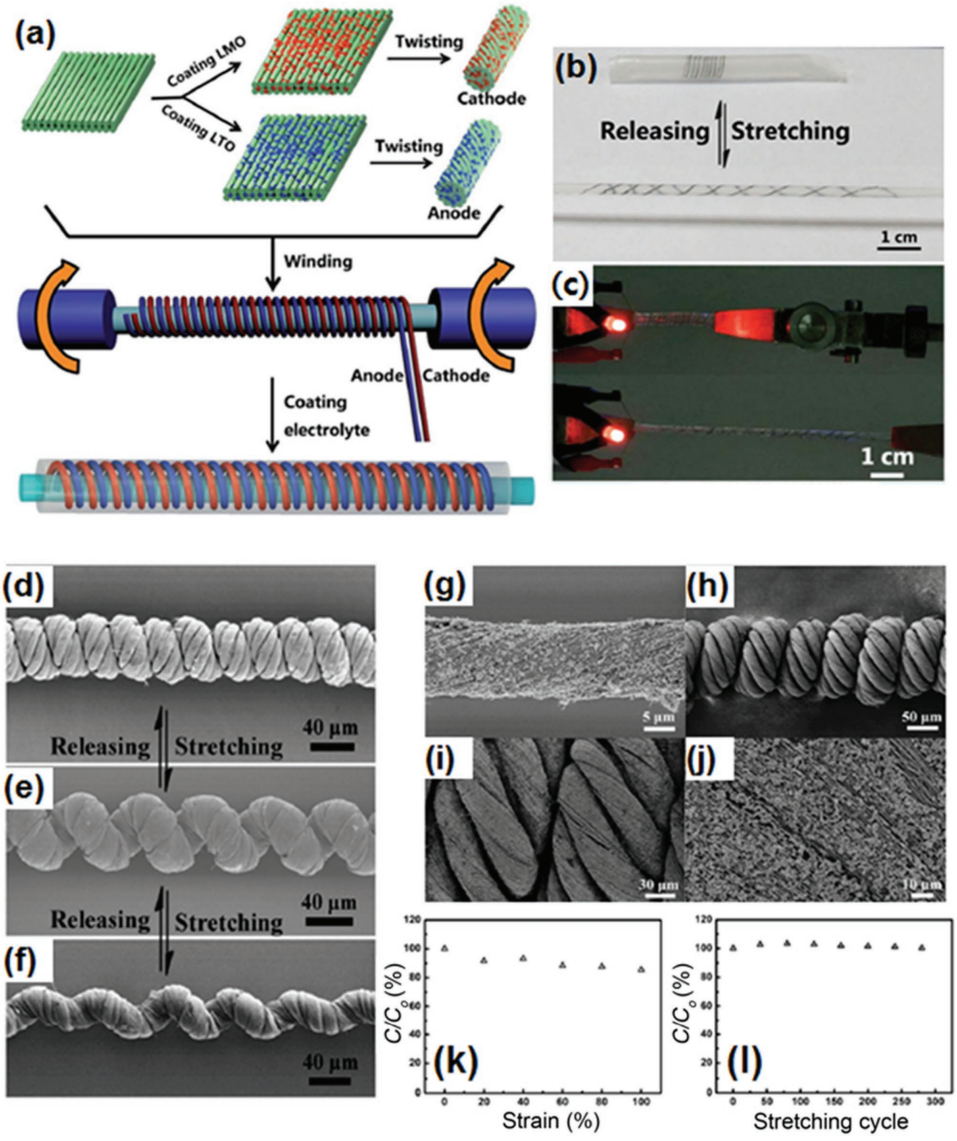

Figure 12. a) Schematic illustration of the fabrication of the stretchable LIB based on the MWCNT/LMO fiber as the positive electrode and MWCNT/LTO fiber as the negative electrode. Photographs of: b) a stretchable fiber-shaped battery under a 600% strain and c) a stretchable fiber-shaped battery powering a LED before and after stretching by 200% strain. a–c) Reproduced with permission.[130a] Copyright 2014, the Royal Society of Chemistry. d–j) SEM images of a springlike CNT fiber at different strains of 0% (d), 50% (e), and 100% (f). g–j) SEM images of a CNT/LTO composite fiber (g), a springlike CNT/LTO composite fiber (h–j) at different magnifications. k,l) Specific capacitance vs strain (k) and stretching cycles (l). d–l) Reproduced with permission.[130b] Copyright 2014, Wiley-VCH.

the spring configuration, and relatively high volume portion of PDMS fiber in the battery were further optimized, the energy density of the super-stretchy batteries with spring configuration would be much higher.

Afterwards, with a view to addressing the previous energy density problem, the same research group has reported advanced springlike fiber electrodes without PDMS fibers, leading to significant increase in energy density.[130b] They comprised overtwisted aligned MWCNTs with uniform coiled loops and the same active materials (LMO and LTO), providing the electrode with a high stretchability larger than 300% (Figure 12d–j). Compared with the previous work,[130a] the PDMS-free springlike electrodes lead to reduction in the volume and the weight of the battery by about 400% and 300%, respectively, with the enhanced linear specific capacity by 600%. The battery using springlike electrodes was highly stretchable, and it remained 85% capacity under a 100% strain (Figure 12k). In addition, the capacity reduced by less than 1% after repeated 300 stretching/releasing cycles at 50% strain (Figure 12l). This study successfully addressed the low energy density problem resulting from large volume of inactive elastic polymer substrate in the stretchable fiber battery shown in the previous study while still attaining the excellent stretchability and performance. Since there are no binder, conducting agent, and metal current collector in the springlike electrode, given presenting a comparison in energy density of the springlike

and the conventional electrodes based on the total electrode mass including current collector, it would be more helpful to assess the increase in the energy density achieved in this study considering its practical criteria for use in the future stretchable electronic devices which may need energy density comparable to that of the conventional electrodes in the current LIBs.

3.1.2. Stretchable Solid-State Electrolytes for Lithium-Ion Batteries

Obviously, the use of liquid electrolytes in traditional LIBs presents the largest obstacle to variation in the cell design with advanced feature of high flexibility or stretchability, for which, considerable efforts have been devoted to replace liquid electrolytes with solid ion electrolytes that are shape-conformable, in recent decades. More importantly, a solid electrolyte that provides substantially improved safety, which is beyond the ability of current widely used liquid electrolyte with leakage, flammability and poor chemical stability issues that prevents the development of next-generation high-performance LIBs.[135] However, recently, most stretchable LIBs were demonstrated to use gel electrolyte and the development of stretchable solid electrolyte have been not rapidly carried out.

Compared with inorganic electrolytes, SPEs present more structure flexibility as well as easier lamination stacking, which are more potential in stretchable LIBs. Recently, Porcarelli et al.[136] designed a super soft polymer electrolyte network that was architectured from a thermoplastic polymer matrix of known molecular weight using the rapid and cost-effective in situ photopolymerization technique. The UV-induced (co) polymerization could promote an effective interlinking between PEO chains plasticized by tetraglyme at various lithium salt concentrations. This interlinked PEO-based solid polymer electrolytes showed an ionic conductivity values exceeding 0.1 mS cm^{-1} at 25 °C are obtained, along with a wide electrochemical stability window larger than 5 V and an excellent lithium-ion transference number (>0.6). Moreover, this solid polymer electrolyte was highly elastic, which offers good prospects in stretchable all-solid-state LIBs.

A current strong interest has been focused on ionic liquids (ILs), motivated by their unique combination of properties, as safe electrolytes for the application in electrochemical devices. Wang et al.[137] demonstrated a gum-like hybrid electrolyte that can be applied in flexible/stretchable LIBs, as shown in **Figure 13**. This hybrid electrolyte endowed double percolation network structure: a percolation network of a liquid electrolyte supported by a network of solid particles, and a strong entanglement network of polymer electrolyte (poly(ethylene oxide), PEO, with $LiClO_4$). The thermally sensitive particles wax particles were used as the core. It found that the hybrid electrolytes indicated gum-like when the content of the liquid phase was more

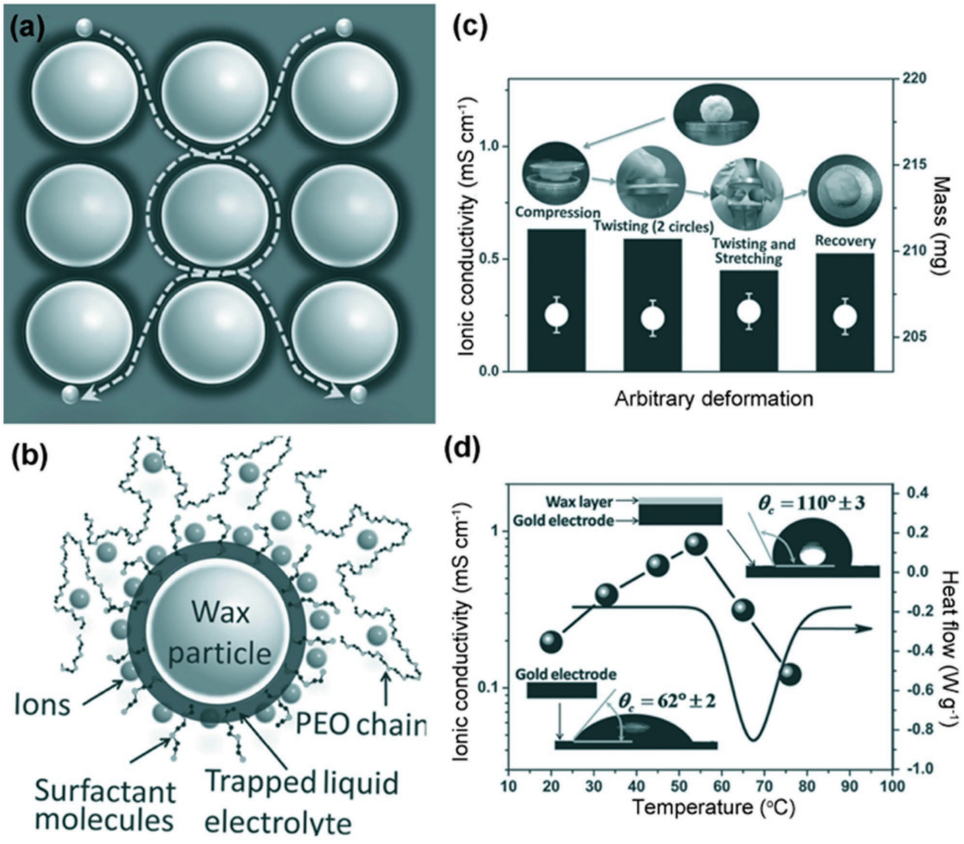

Figure 13. a) Schematic illustration of the network structures designed for the gummy electrolyte. b) Details of the core–shell particles. c) Performance stability of the gummy electrolyte against arbitrary deformation. d) Temperature-dependent of the ionic conductivity for the gummy electrolyte. The inset photographs are the contact angle testing of the electrode surface before and after the high temperature testing. a–d) Reproduced with permission.[137] Copyright 2013, Wiley-VCH.

than ca. 40 wt%. The gum-like hybrid electrolyte with liquid electrolyte content of ca. 50 wt% showed a high ionic conductivity (ca. 3×10^{-4} S cm^{-1} at room temperature) and excellent mechanical performance, which could be used in advanced batteries with improved safety and flexibility/stretchability. In addition, the battery using this hybrid electrolyte indicated improved safety: the melting layer of the thermally sensitive particles could stop the electrochemical reaction due to the decreased ionic conductivity when the temperature reached the melting point of the wax particles, so the battery temperature can remain in a safe range (Figure 13d). Zhang et al.[138] also reported a stretchable solid electrolyte using ionic liquid. The stretchable SPEs comprised of lithium bis(fluorosulfonyl) imide ($Li[N(SO_2F)_2]$, LiFSI) and polymeric ionic liquid (i.e., poly[*N*,*N*-dimethyl-*N*-[2-(methacryloyloxy) ethyl]-*N*-[2-(2-methoxyethoxy) ethyl]ammonium] bis(fluorosulfonyl) imide, $P[C_5O_2N_{MA,11}]FSI$). The maximum ionic conductivity for SPEs is 1.4×10^{-5} S cm^{-1} at 30 °C. Moreover, the SPE can afford 500% strain.

It is worth noting that the characteristics of ionic conductivity of polymer electrolytes during tensile deformation are not well recognized. Kelly et al.[139] reported the effects of tensile strain on the ionic conductivity of the PEO film through an in situ study. The results showed that both in-plane and through-plane ion conductivities of PEO undergo a similar and steady ion conductivity growth during axial deformation, achieving an approximate 4-fold increase in ion conductivity at a 15% strain. The authors believed that this phenomenon was mainly attributed to the disentanglement of polymer chains during tensile deformation and the subsequently reduction of the degree of tortuosity in the path of ion transport.

3.1.3. Stretchable Integrated Battery Systems

Various strategies have been adopted to achieve the stretchable key components such as electrode and electrolyte in LIBs. While fabrication of fully integrated energy-storage devices with high bendability, twistability and stretchability is also an effective idea to reach system-level deformability in practical application with standard manufacture technologies. A work from Rogers' group[10h] caused a stir in the field of stretchable batteries, which demonstrated a segmented design in the active electrode materials, with unusual 'self-similar' interconnect structures between them, and using silicone elastomers as substrates, with The schematic illustration in **Figure 14**a of the pouch cells consisting arrays of small-scaled storage components connected by conductive frameworks with highly stretchable feature. The current collectors consist of patterned circular disks of aluminum and copper were first fabricated by photolithography. The patterned layers of PI encapsulate interconnecting traces between these disks were then prepared by photolithography and oxygen plasma etching. Thin, low modulus sheets of silicone elastomer form top and bottom substrates were used to support these structures and other components of the batteries. A square array of 100 disks of electrode connected in parallel was covered by elastomer sheets. In order to avoid short circuit and to eliminate the requirement for a separator, there were spatial offsets between the molded pads of the laminated LCO and LTO. A gel electrolyte was later injected into the gap. Acryloxy perfluoropolyether elastomer was used as stretchable package materials. The highly stretchable LIBs showed excellent electrochemical performances and mechanical properties. Figure 14c indicates that the voltage profiles of the electrodes under 300% uniaxial strain (red) indicated good stability for the stretchable battery, showing a stable capacity density of ≈1.1 mA h cm^{-2}. As shown in Figure 14e, this battery could provide sufficient power to light up light-emitting diodes, even at a stretching status of up to 300%. However, this stretchable battery exhibited a capacity decay over only 20 cycles (Figure 14d), which is due to some combination of reaction with moisture in the packaging materials, and electrical conduction discontinuity of slurry particles. Therefore, improvement in the stretchable batteries based on self-similar serpentine interconnects should be considered.

Origami[10i] and kirigami[10o] are the ancient arts based on folding and cutting 2D paper into deformable 3D structure, which are able to realize a high level of stretchability. Song et al.[10i] demonstrated an origami LIB that can be highly deformed by folding and twisting. The LCO/LTO electrodes were prepared on to paper current collectors by standard slurry coating, and the packaging is aluminized polyethylene (PE). The assembled full battery was folded according to the desired origami patterns (Miura-ori pattern in **Figure 15**a) in an ambient environment. The origami LIB with Miura-ori pattern showed many identical parallelogram faces that were connected by "mountain" and "valley" creases, which could be either almost fully compressible in one direction or foldable in two directions. A high level of deformability could be achieved, while the main parts of the parallelogram faces remained undeformed and rigid configuration. However, the foldability of the origami LIBs is restricted and uneven surfaces could be introduced by repeatable folding which restrict their practical applications. Hence, later, this group developed kirigami LIBs, showing large stretchability higher than 150%.[10o] Conventional materials including graphite and LCO with standardized battery manufacturing could be applied to fabricate the planar LIBs. As shown in Figure 15b, three kirigami patterns were presented with a zigzag-cut pattern, a cut-N-twist pattern, and a cut-N-shear pattern. Figure 15c displays the LIB under its fully stretched state, indicating that the kirigami LIB could reach larger than 100% stretchability. This kirigami LIB showed good and stable electrochemical performances at deformed status, shown in Figure 15d. Over 85% capacity retention and Coulombic efficiency of 99.8% over 100 cycles could be achieved for the kirigami LIB under alternative states of compact and stretched states.

3.1.4. Beyond Stretchable Li-Ion Batteries

One significant challenge in the field of LIBs is to search for next generation systems with higher energy density in order to meet the current demands for longer operation time of electronic applications including electric vehicle which are powered by the conventional LIBs based on lithium–metal-oxide cathode materials and carbonaceous anode materials.[65a,140] From this point of view, Li–S system has attracted much attention because of its significant theoretical capacity. As mentioned in Section 2.1.5, various flexible Li–S batteries with good electrochemical performances

Adv. Mater. **2016**,
DOI: 10.1002/adma.201603436

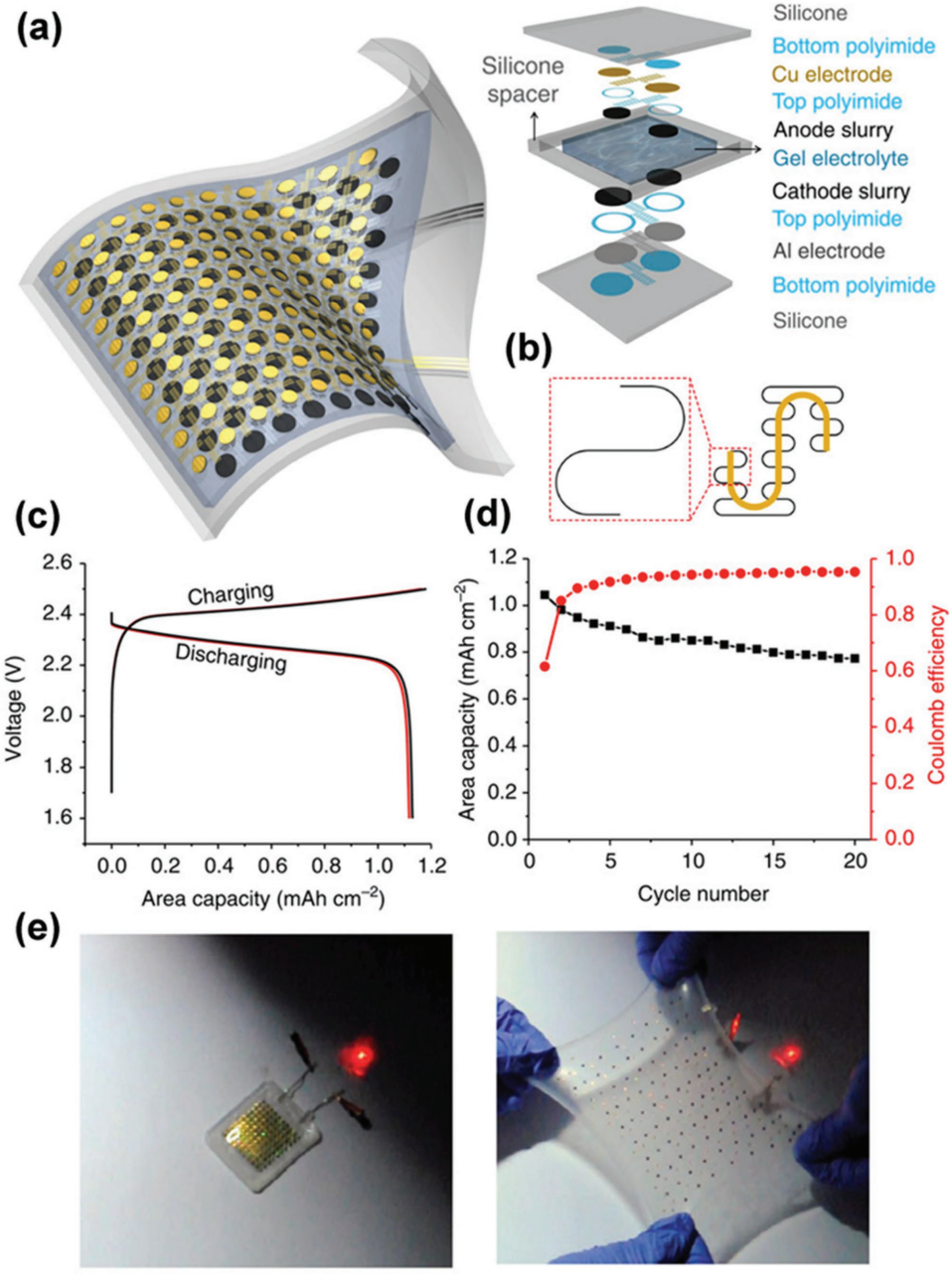

Figure 14. a) Schematic illustration of the structure for the stretchable LIB. b) The 'self-similar' serpentine geometries for the interconnects (black: 1st level serpentine; yellow: 2nd level serpentine). c) Galvanostatic charging/discharging of the battery without (black) and with 300% uniaxial strain (red). d) Capacity retention and Coulombic efficiency vs cycle number. e) Photo showing the stretchable battery powering a red LED under biaxially 300% strain. a–e) Reproduced with permission.[10h] Copyright 2013, Macmillan Publishers Limited.

have been developed, however, the development of highly stretchable Li–S is still remaining challenge.

Moreover, stretchable metal–air batteries, such as zinc–air batteries[10q] and aluminum–air batteries,[10s] have also attracted much attention due to their high capacity and long-term stability for wearable electronic devices. Very recently, Peng's group developed an all-solid-state aluminum–air battery based on fiber-shaped structure (**Figure 16**), which showed a specific capacity of 935 mA h g^{-1} and an energy density of 1168 W h kg^{-1}.[10s] As shown in Figure 16b,c, it can be seen that the output voltage of the aluminum–air battery remained unchanged under bent and stretchable states. In addition, as the common feature for the fiber-shaped battery, this flexible and stretchable could be woven into textile for practical application.

3.2. Stretchable Supercapacitors

The development of sustainable and environmental friendly energy for a low carbon footprint triggered main changes

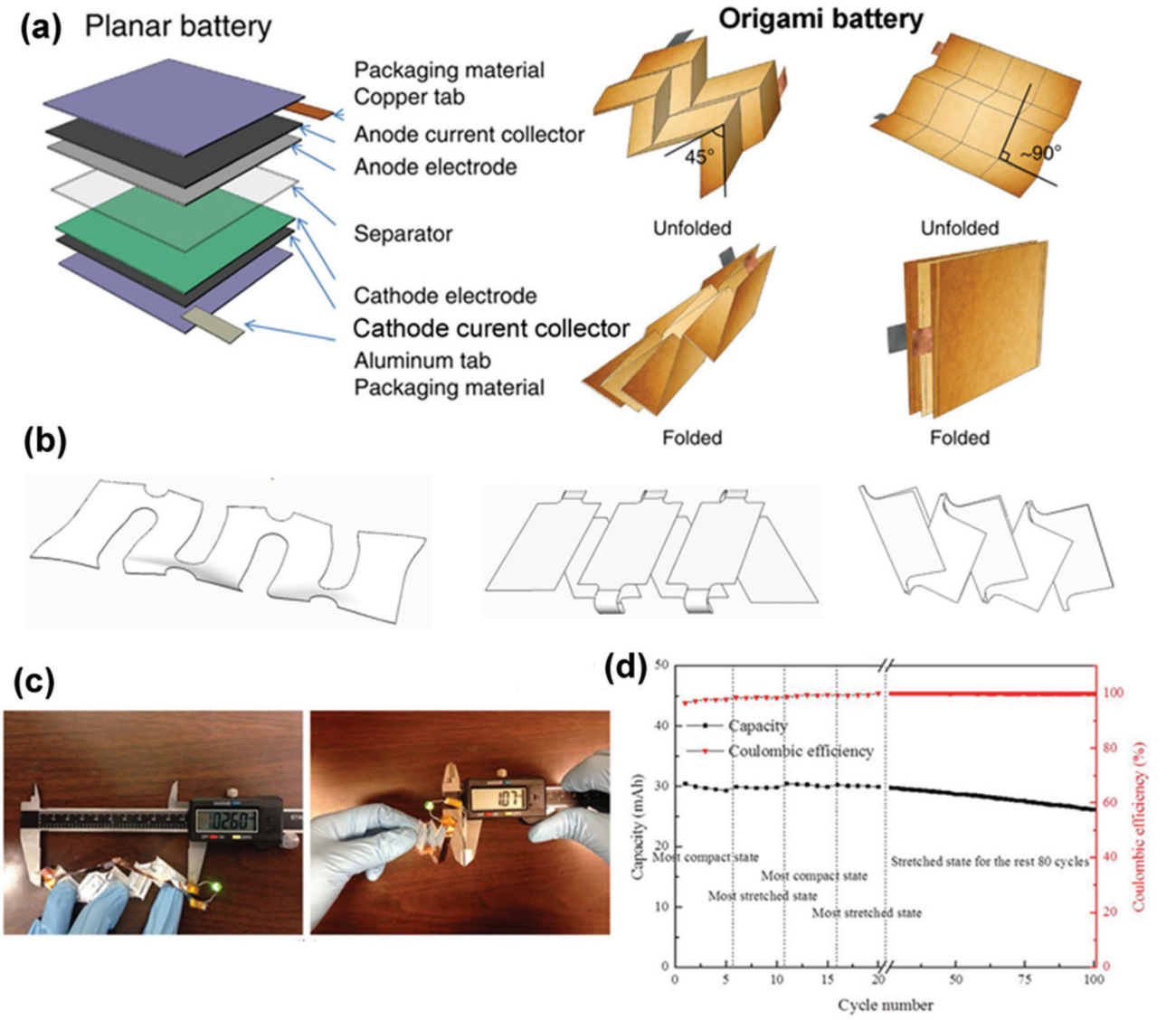

Figure 15. a) Illustration of the multilayer structure for conventional LIBs in the planar state. Two types of origami LIBs using Miura folding. Reproduced with permission.[10] Copyright 2014, Macmillan Publishers Limited. b) Illustrations of three kirigami patterns. c) Photograph of a LIB under its fully stretched and compact state. d) Energy capacity and Coulombic efficiency vs cycle number. b–d) Reproduced with permission.[10o] Copyright 2015, Macmillan Publishers Limited.

in modern society, which makes SCs one of the most promising technologies among various available battery chemistries. Flexible, bendable, foldable, stretchable are needed for SCs to achieve the increasing market requirement, representing a new direction in science and technology.[8] Compared with stretchable batteries, SCs have been developed rapidly due to relative easier fabrication and structure. Owing to the conventional materials for SCs including active electrode materials and polymer electrolyte usually sustain a small strain, various novel materials with intrinsic stretchability and new designs have been proposed to accommodate a high level of deformation for stretchable SCs. The following section, the common developed configurations as well as elastic polymer materials for stretchable SCs will be reviewed systematically.

3.2.1. Stretchable Configurations

Wavy/Buckled Configuration: One of the most simple and obvious idea structure designs for stretchability is wavy, buckled or wrinkle configuration, which has been developed widely. A pioneer work on stretchable SCs based on buckled structure was reported in 2009.[10a] Basically, SWNT macrofilm was laminated and aligned on the prestrained elastomeric PDMS substrate. A periodically buckled pattern could be formed by releasing the prestrained PDMS, owing to mechanical mismatch between the relatively stiff SWNT macrofilm and the compliant PDMS substrate. The results showed no significant change in the CVs of the stretchable SCs with 0 and 30% applied strains. The initial specific capacitance calculated based on the discharge slopes was found to reduce from 54 F g^{-1} to 52 F g^{-1} for the

Adv. Mater. 2016,
DOI: 10.1002/adma.201603436

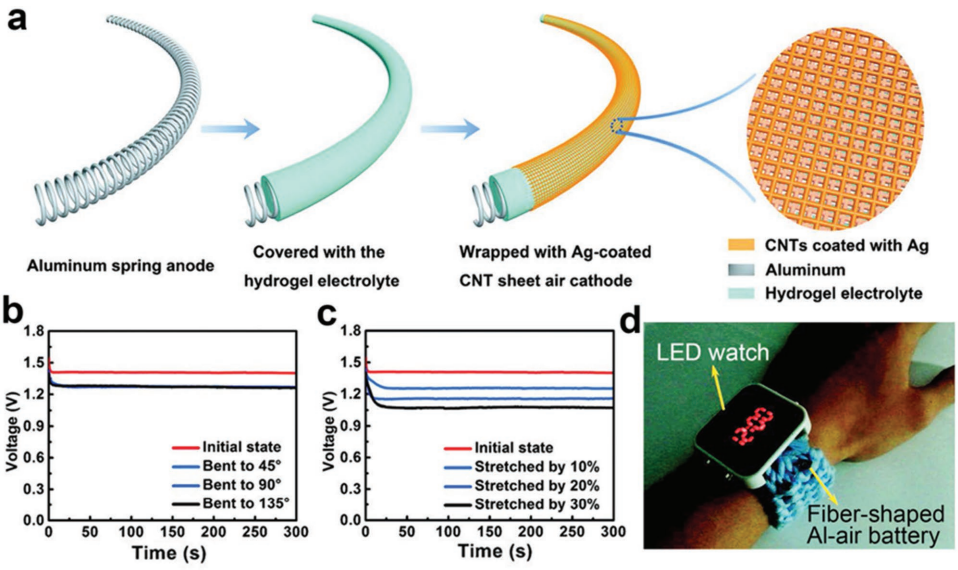

Figure 16. a) Fabrication of the fiber-shaped Al–air battery. b, c) Discharge curves of fiber-shaped Al–air batteries at different bending angles or stretching ratios at a discharge current of 1 mA. d) Photographs of a commercial LED watch powered by fiber-shaped Al–air batteries woven into a fabric. a–d) Reproduced with permission.[10s] Copyright 2016, Wiley-VCH.

stretchable SCs under 30% strain. It can be seen from this work that the stretchability of the SCs is only 30%, which limits their applications. Additionally, liquid electrolyte was employed, which would lead to electrochemical performance decay due to the possibility of leakage of harmful electrolytes, and the lamination between electrodes and separator could also decrease the performance of the stretchable SCs. Therefore, more effort on the development of high performance stretchable SCs have been devoted in recent years. Niu et al.[10f] demonstrated a highly stretchable SC prepared by directly growing SWCNT films with continuous reticulate architecture on prestrained PDMS. The stretchable electrodes were integrated with gel electrolyte of H_2SO_4/PVA. They indicated that the electrochemical performance of the stretchable SCs remained constant under 120% strain and also in the dynamic state of stretching.

Other carbon-based materials, for example, graphene, have also been adopted in stretchable SCs with wrinkle configuration. Zang et al.[10k] reported a simple and cost effective approach to prepare stretchable electrodes with high performance for SCs by using crumpled-graphene papers. The stretchable electrodes were obtained by transferring graphene paper onto the pre-strained elastomer film along one or two directions sequentially. The stretchable electrodes based on the crumpled graphene papers exhibited a high level stretchability of linear strain 300% and areal strain 800%, and high specific capacitance of 196 F g^{-1} and good reliability over 1000 stretch/release cycles. In addition, stretchable all-solid-state SCs with a uniform wavy shape were demonstrated, which consists of two wavy PANI/graphene electrodes and a H_3PO_4/PVA gel electrolyte.[141] Ni foam was employed as a catalyst for growing porous graphene. The flexible sheet was then manually folded into a wavy shape by using a steel rod. The stretchable SC exhibited a maximum specific capacitance of 261 F g^{-1} and good cycling stability of 89% capacitance retention over 1000 charge/discharge cycles at a current density of 1 mA cm^{-2}. Moreover, the results also showed that that the SC maintained both high mechanical properties and high capacitance, even under a 30% strain.

Recently, Xiaodong Chen's group from Nanyang Technological University developed an advanced wavy structure for stretchable SCs.[142] As shown in **Figure 17**a, compared with in-plane structure that would lead to cracks of the rigid electrodes under stretching, the wrinkled structure endows much higher stretchability that can accomodate the strain by changing its shape with an out-of-plane bend. However, the direction adhesion part between the electrodes and the stretchable substrate likely causes large stress in the electrode materials, which restricts the stretchability and electrochemical and mechanical stability of the system. Therefore, they discovered a novel wrinkled structure. The wrinkled electrodes were suspended on the stretchable substrate rather than direct attachment on it, which could significantly reduce the stress in the electrode materials during stretching. Chen's group developed suspended wavy graphene microribbons used in stretchable micro-SCs. The suspended electrode array was obtained by transferring graphene microribbons onto tripod-shaped PDMS substrate, as indicated in Figure 17b. Figure 17c indicates that the rGO microribbons were well bonded to the special PDMS substrate, without noticeable damages or defects. The cross-sectional optical image clearly indicated that these PDMS tripods were positioned with a sufficient gap for the bending of the PDMS film and the rGO microribbons. The results also showed stable electrochemical performance of the stretchable SCs under various strains (0–100%), as shown in Figure 17d. It also can be seen that the stretchable SC without or with 100% strain could light the LCD. Hence, this novel strategy supplies a promising approach for the stretchable SCs for in mobile and wearable electronic devices.

Wire-Like Configuration: In recent years, wire-shaped SCs that can afford high strained deformation have been developed rapidly. Huisheng Peng's group for the first time, developed a stretchable, fiber-shaped SCs with high electrochemical and

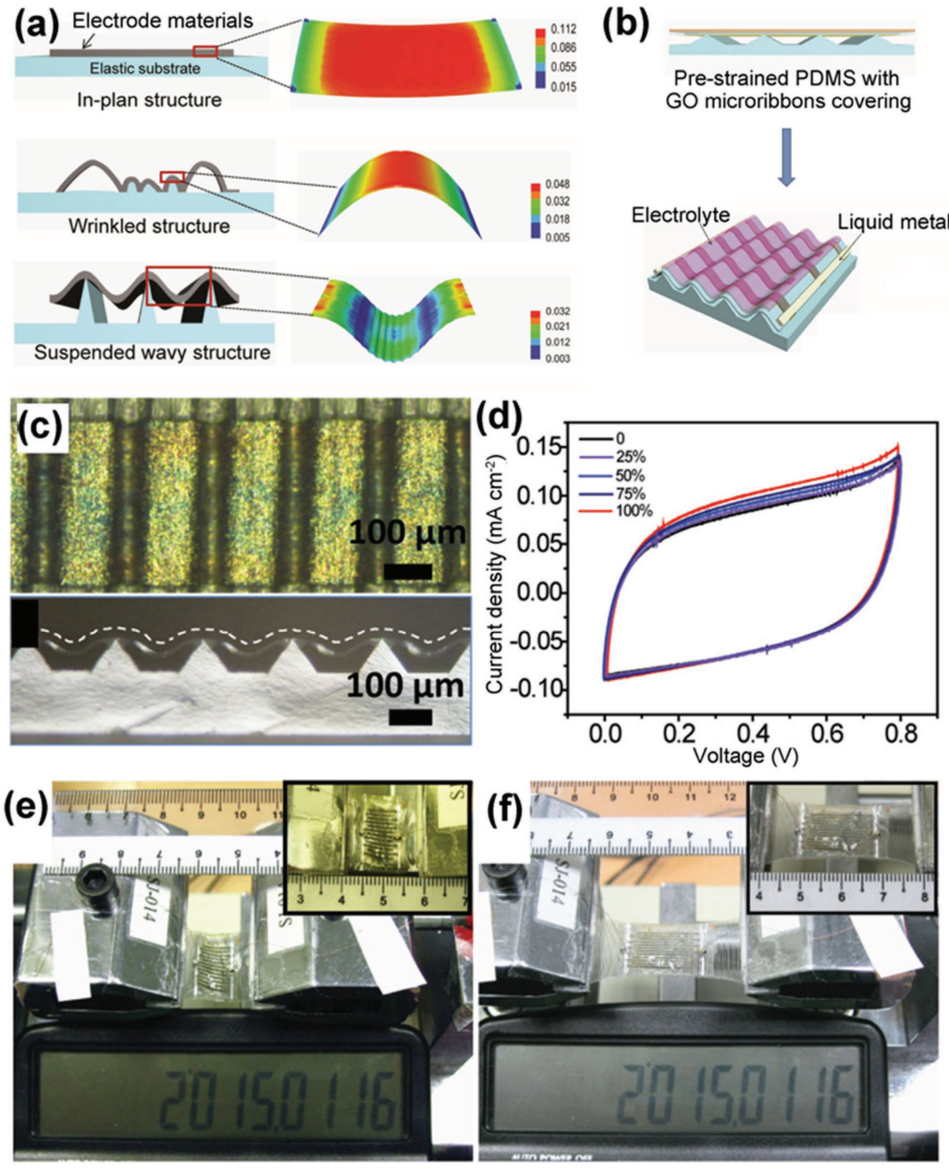

Figure 17. a) Schematic illustration of the different electrode arrays and the relevant strain distribution by the finite element modeling analysis. b) Schematic illustration of preparation process of the stretchable micro-SC. c) Optical images of the micro-SCs under released status together with its cross-sectional image. d) CV curves of the micro-SCs under various strains at scan rate of 500 mV s^{-1}. e,f) LCD lit by the stretchable micro-SCs under 0 (e) and 100% (f) strain. a–f) Reproduced with permission.[142] Copyright 2015, Wiley-VCH.

mechanical performances.[10g] The spinnable CNT arrays were first prepared by CVD. Serving as the electrodes, aligned CNT sheets were then wrapped on an elastic fiber coated with a thin layer of gel electrolyte. This stretchable wire-like SC showed specific capacitance of 19.2 F g^{-1} and it could be further enhanced to 41.4 F g^{-1} by introducing OMC components among aligned CNTs. The stretchable SC showed unchanged CV and charge/discharge curves at a 75% strain and the capacitance retention higher than 95% could be achieved after stretched by 100 cycles at a 75% strain. Accordingly, this wire-like SC with high stretchability demonstrates a promising potential. Later, Peng and co-workers reported a new superelastic fiber-shaped SC produced based on two aligned CNT/PANI composite sheets as electrodes, which showed more than 400% stretchability.[143a] An interesting result showed a high specific capacitance of about 79.4 F g^{-1} was well maintained by stretching under a 300% strain for 5000 cycles for this fiber-shaped SC.

Choi et al. reported stretchable, cable-like solid-state MnO_2/CNT/nylon fiber SCs.[143b] The elastic electrodes were prepared with giant inserted twist to coil a nylon sewing thread that was helically wrapped with a CNT sheet, and pseudocapacitive MnO_2 nanofibers were then electrochemically deposited. Excellent electrochemical performances and mechanical properties were observed for the wire-like SCs, which shows only 15% decrease capacitance when reversibly stretched to 150% along the fiber direction. The maximum linear capacitance of 5.4 mF cm^{-1} and areal capacitance of 40.9 mF cm^{-2} (based on active materials) and areal energy density of 2.6 mW h cm^{-2}

Adv. Mater. 2016,
DOI: 10.1002/adma.201603436

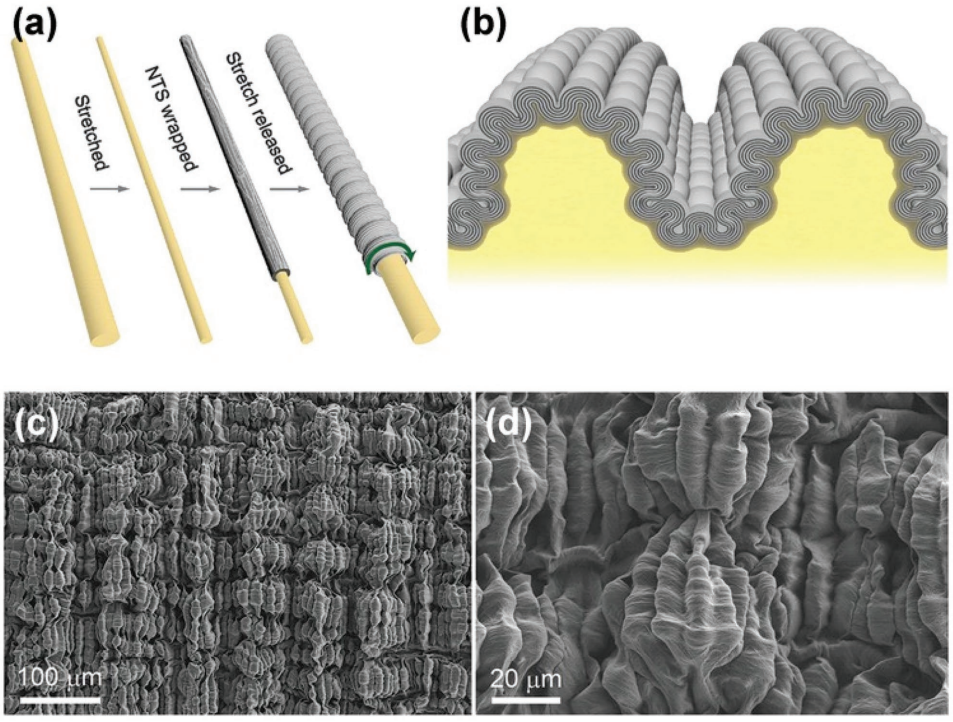

Figure 18. Two-dimensional, hierarchically buckled sheath–core fibers. a) Schematic illustration of fabrication process. b) Illustration of the structure of a longitudinal section of the sheath, showing 2D hierarchical buckling. c) Low- and d) high-resolution SEM images showing long- and short-period buckles for a fiber under 100% strain. a–d) Reproduced with permission.[10n] Copyright 2015, American Association for the Advancement of Science.

and power density of 66.9 mW cm^{-2} (based on overall SC dimensions) were achieved for the stretchable SCs.

In 2015, a super stretchable conducting fiber with up to 1320% stretchability was demonstrated, which was prepared by wrapping CNT sheets oriented in the wire direction on stretched rubber wire cores, resulting a sheath–core structure.[10n] This idea is based on the combination of buckled configuration and wire-like structure. As shown in **Figure 18**a, the rubber fiber core was highly stretched (1400% strain) during the wrapping of nanotube sheet (NTS) layers, resulted in the observed hierarchical 2D buckling-induced wavy surface architecture of CNT sheets. The designed structure showed distinct short- and long-period sheath buckling, which was able to be stretched reversibly out of phase in the axial as well as belt directions. A resistance change of less than 5% under 1000% strain was observed, which enables a various applications.

Textile Configuration: Textile is a porous and flexible, which is generally made by weaving natural or synthetic fibers, including cotton or polyester, which is flexible or even stretchable. For wearable electronic devices, an energy-storage system in a textile configuration is easy to be incorporated as a component. A pioneer work about stretchable SCs from our group demonstrated conformally coating SWNTs on cellulose and polyester fibers to form a porous and conductive textile as electrodes.[10b] The conductive textiles showed good flexibility and stretchability and had a strong adhesion between the SWNTs and the textiles. Stretchable SCs using these conductive textiles indicated high areal capacitance of 0.48 F cm^{-2}. Therefore, the highly conductive textiles could deliver a new direction for wearable electronics and energy storage several years ago.

Later, Jang Wook Choi's group explored a textile structure alternately interwoven with inelastic and elastic yarns, for which, strain up to 200% could be achieved via a tricot weave in diagonal directions.[144] **Figure 19**a presents the schematic illustration of the weaving structure of the tricot-weave textile. The textile consisted inelastic polyester yarns (green line) contributed the basic framework of the textile and elastic Spandex yarns (orange line) woven together by being wound around the polyester loops, constituting a repeating zigzag pattern. The stretchable SCs using this textile coated with MWCNTs showed consistent capacitance of 35 F g^{-1} at 0.25 A g^{-1} at different strains. Figure 19c indicates the CV profiles under both with and without dynamic strain operation, showing that two profiles strains fully overlapped each other, implying the good mechanical stability. The textile SCs were also tested under biaxial stretching mode. The results showed that the capacitance was well retained when the SCs were stretched at 50% strain in biaxial directions.

Other Configurations: Other configurations to achieve high-level stretchability for SCs have been also reported recently, including coating on stretchable substrate, embedding in stretchable materials, and serpentine metallic interconnections. Liming Dai's group demonstrated a stretchable all-solid-state SC with a good electrochemical and mechanical stability and transparent feature, using highly aligned CNT sheets on a PDMS substrate as the transparent and flexible current collector and active materials.[145] However, the electrochemical performance of the stretchable SCs was shown at only 30% strain. Bandodkar et al.[10l] demonstrated highly stretchable electrochemical devices, which were prepared by screen-printing

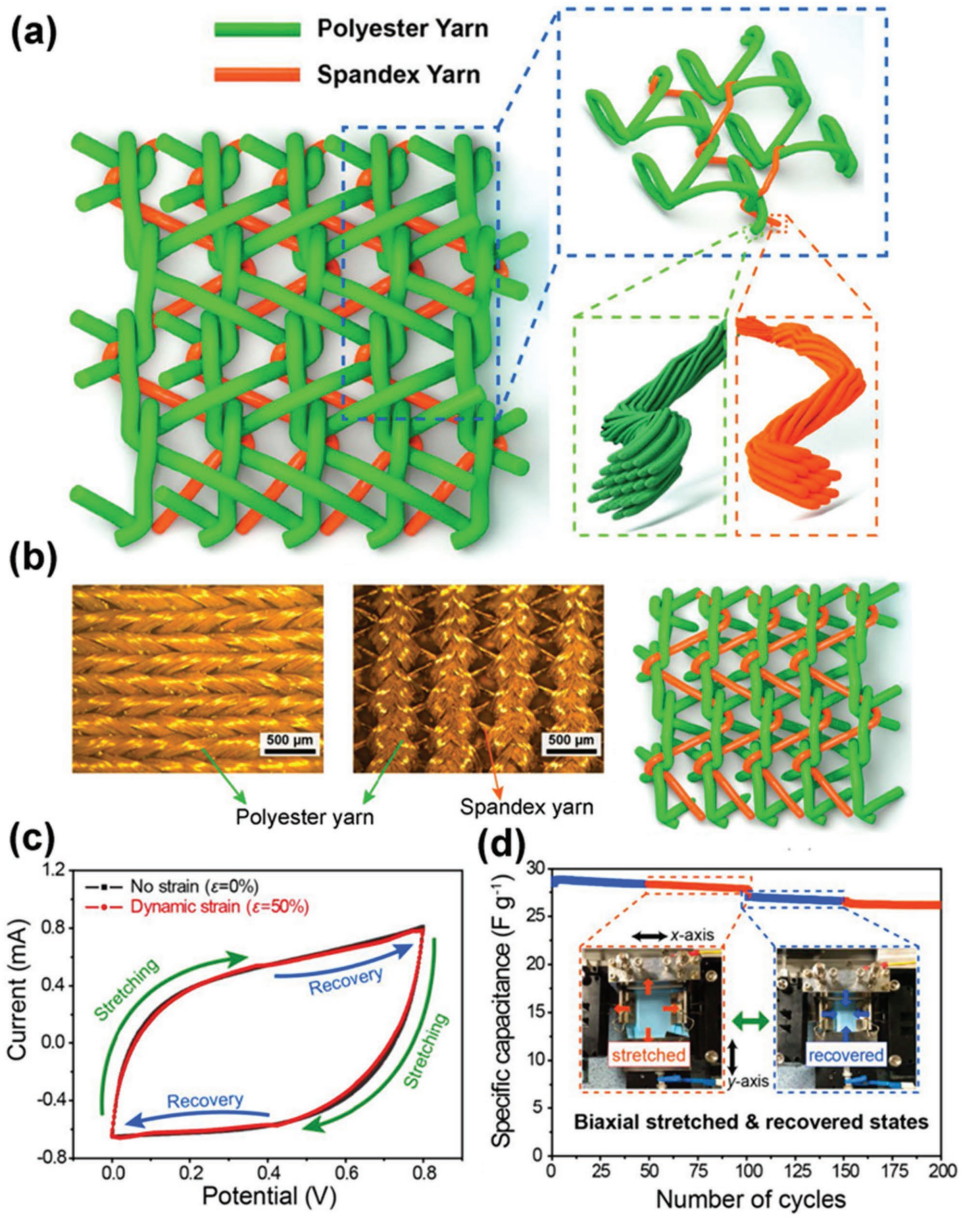

Figure 19. a) Schematic illustration of the tricot-weaving structure consisting of two kinds of yarn (green: polyester yarn, orange: Spandex yarn), a focused view of the weaving structure made of both yarns, a further zoomed-in view of the weaving point to illustrate that each yarn consists of a bundle of fibers. b) Optical microscopy images of the actual textile electrode from the front and the rear sides after Ag nanoparticles coating, along with a rear view schematic. c) CV curves under and without dynamic strain at a scan rate of 80 mV s^{-1}. d) The cycling performance under biaxially 50% strain and recovered states. a–d) Reproduced with permission.[144] Copyright 2015, American Chemical Society.

of conducting inks judiciously tailored with elastomer and surfactant by custom-designed stencils. The designed 2D serpentine interconnects was on the between the electrodes and contact pads enabled high levels of stretchability without failure.

3.2.2. Stretchable Electrolytes for Supercapacitors

Developing intrinsically stretchable materials for energy-storage devices presents a stiffer challenge. A handful of reports in the literature have focus on the stretchable electrolytes for SCs. Zhao et al.[146] reported a highly stretchable H_3PO_4/PVA polymer electrolyte achieved by modifying the polymer molecular weight and its weight ratio according to the conductivity and mechanical properties. The stretchable electrolyte showed a high conductivity of 3.4×10^{-3} S cm^{-1} and a high fracture strain at 410% elongation. A stretchable SC using this stretchable electrolyte and buckled polypyrrole electrodes was assembled, which showed good capacitance retention of 94.5% under 30% strain and capacitance retention of 81% after 1000 stretch/release cycles.

In addition, self-healing polymer has been an emerging area due to its amazing properties, for the development of many

DOI: 10.1002/adma.201603436

interesting and important applications such as electronic skin and energy-storage clothes. Recently, Huang et al.[10m] demonstrated an electrolyte prepared with poly(acrylic acid) dual crosslinked by hydrogen bonding and vinyl hybrid silica nanoparticles, which endows intrinsic self-healability and high stretchability. The SCs with this stretchable electrolyte and wavy electrodes attached to the electrolyte could stretched up to 600% strain and retain the capacitance completely even after 20 cycles of breaking/healing. The highly stretchable SCs with multifunctionality of self-healing indicate a significant step toward the potential and wide-scale applications such as wearablenergy-storagege devices.

4. Conclusions and Perspectives

Undeniably, LIBs and SCs have been employed in an extensive range of practical applications, changing the mode of production and lifestyle of the present world considerably. With a focus on flexible and stretchable energy storage, including LIBs and SCs, we have highlighted the advances and progress that have been achieved in recent years according to the materials exploration, structural designs, manufacture methods and integrated assembly. Different from the conventional structure and manufacture technology, to realize flexibility and stretchability, innovative concepts require the identification of each component in LIBs and SCs, including cathode, anode, separator/electrolyte, current collector and packaging materials. Two starting points can be concluded to achieve the function of flexibility and stretchability: carrying out novel configuration designs and exploring intrinsically flexible or stretchable materials. Carbon-based materials with outstanding performance including CNF, CNT, graphene, GO and their composites can be either used as conductive materials or active materials, which exhibit an irreplaceable role in the field of energy-storage systems. Together with other active electrode materials such as LCO, LTO, MnO_2, these inorganic materials are intrinsically inflexible, which promotes the development of various configurations for electrodes extensively. Electrode configurations such as paper-like, textile, sponge, wire-shape etc. can provide the realization of flexibility, and configurations such as porous framework, wavy/buckled structure, helically coiled spring shape etc. can enable the devices with stretchable feature. In addition to 2D electrode structure, 3D electrode designs using nanostructure materials of optimizing the ionic/electronic current paths, large surface area, better permeability, have also been widely exploited in LIBs and SCs with enhanced electrochemical performances. Moreover, the development of microbatteries and micro-SCs with enhanced energy/power densities also plays an interesting direction in micro energy harvesting, expanding the practical applications.

The recent advances and achievements have demonstrated the promising potential of flexible and stretchable energy-storage devices toward practical applications such as wearable electronics. However, lots of challenges remained to be addressed for realizing the practical applications and further studies are required to reach a full understanding on electrochemical performances and mechanical properties. Developing reliable materials with enhanced electrochemical and mechanical performances and improved safety for flexibility and stretchability electrodes, exploring large-scaled and industrial production technologies to lower the fabrication cost are urgent. By replacing conventional flammable liquid electrolyte, solid-state electrolytes can provide better safety and integrity and compatibility. However, study of flexible and stretchable solid electrolytes with comparable ionic conductivity with liquid electrolyte becomes an urgent problem to be solved. Additionally, improving the cycling stability of flexible and stretchable devices and subsequently lowering energy costs are also imperative. On other hand, currently the packaging materials with flexible and stretchable features have been attracted little attention, especially for stretchable packages. Therefore, optimizing device structure and modification reliable packaging materials to protect the integrity of energy storage under various deformed conditions should also be considered significantly. Fully flexible or stretchable integrated energy-storage systems can also expedite the future industrial production.

Gazing into the future, the field of flexible and stretchable energy-storage devices is absolutely exciting and fairly open-ended, providing researchers from various backgrounds to explore novel and interesting concepts and designs. Along with the technical breakthroughs in flexible and stretchable energy-storage systems, we believe novel devices that can change the lifestyle of the present world will be emerged in our daily lives in the near future.

Acknowledgements

This work was supported by Samsung Electronics. The authors thank Yongming Sun for discussion.

Received: June 29, 2016
Revised: July 27, 2016
Published online:

[1] a) P. G. Bruce, S. A. Freunberger, L. J. Hardwick, J. M. Tarascon, *Nat. Mater.* **2012**, *11*, 19; b) D. Larcher, J. M. Tarascon, *Nat. Chem.* **2015**, *7*, 19; c) C. Liu, F. Li, L. P. Ma, H. M. Cheng, *Adv. Mater.* **2010**, *22*, E28.
[2] M. Stoppa, A. Chiolerio, *Sensors* **2014**, *14*, 11957.
[3] a) X. Wang, X. Lu, B. Liu, D. Chen, Y. Tong, G. Shen, *Adv. Mater.* **2014**, *26*, 4763; b) L. Li, Z. Wu, S. Yuan, X.-B. Zhang, *Eng. Environ. Sci.* **2014**, *7*, 2101.
[4] a) T. Cheng, Y. Zhang, W. Y. Lai, W. Huang, *Adv. Mater.* **2015**, *27*, 3349; b) Y. Zhang, Y. Huang, J. A. Rogers, *Curr. Opin. Solid State Mater. Sci.* **2015**, *19*, 190.
[5] M. Armand, J. M. Tarascon, *Nature* **2008**, *451*, 652.
[6] a) B. E. Conway, *J. Electrochem. Soc.* **1991**, *138*, 1539; b) L. L. Zhang, X. S. Zhao, *Chem. Soc. Rev.* **2009**, *38*, 2520; c) Y. Sun, N. Liu, Y. Cui, *Nat. Energy* **2016**, 16071; d) Y. Yang, G. Zheng, Y. Cui, *Chem. Soc. Rev.* **2013**, *42*, 3018.
[7] B. Scrosati, *Electrochim. Acta* **2000**, *45*, 2461.
[8] A. Vlad, N. Singh, C. Galande, P. M. Ajayan, *Adv. Eng. Mater.* **2015**, *5*, 1402115.
[9] a) H. Nishide, K. Oyaizu, *Science* **2008**, *319*, 737; b) C. Yan, P. S. Lee, *Small* **2014**, *10*, 3443.
[10] a) C. Yu, C. Masarapu, J. Rong, B. Wei, H. Jiang, *Adv. Mater.* **2009**, *21*, 4793; b) L. Hu, M. Pasta, F. L. Mantia, L. Cui, S. Jeong, H. D. Deshazer, J. W. Choi, S. M. Han, Y. Cui, *Nano Lett.* **2010**,

10, 708; c) C. Wang, W. Zheng, Z. Yue, C. O. Too, G. G. Wallace, *Adv. Mater.* **2011**, *23*, 3580; d) A. M. Gaikwad, A. M. Zamarayeva, J. Rousseau, H. Chu, I. Derin, D. A. Steingart, *Adv. Mater.* **2012**, *24*, 5071; e) D. Kim, G. Shin, Y. J. Kang, W. Kim, J. S. Ha, *ACS Nano* **2013**, *7*, 7975; f) Z. Niu, H. Dong, B. Zhu, J. Li, H. H. Hng, W. Zhou, X. Chen, S. Xie, *Adv. Mater.* **2013**, *25*, 1058; g) Z. Yang, J. Deng, X. Chen, J. Ren, H. Peng, *Angew. Chem., Int. Ed.* **2013**, *52*, 13453; h) S. Xu, Y. Zhang, J. Cho, J. Lee, X. Huang, L. Jia, J. A. Fan, Y. Su, J. Su, H. Zhang, H. Cheng, B. Lu, C. Yu, C. Chuang, T. I. Kim, T. Song, K. Shigeta, S. Kang, C. Dagdeviren, I. Petrov, P. V. Braun, Y. Huang, U. Paik, J. A. Rogers, *Nat. Commun.* **2013**, *4*, 1543; i) Z. Song, T. Ma, R. Tang, Q. Cheng, X. Wang, D. Krishnaraju, R. Panat, C. K. Chan, H. Yu, H. Jiang, *Nat. Commun.* **2014**, *5*, 3140; j) C. Yan, X. Wang, M. Cui, J. Wang, W. Kang, C. Y. Foo, P. S. Lee, *Adv. Energy Mater.* **2014**, *4*, 1301396; k) J. Zang, C. Cao, Y. Feng, J. Liu, X. Zhao, *Sci. Rep.* **2014**, *4*, 6492; l) A. J. Bandodkar, R. Nunez-Flores, W. Jia, J. Wang, *Adv. Mater.* **2015**, *27*, 3060; m) Y. Huang, M. Zhong, Y. Huang, M. Zhu, Z. Pei, Z. Wang, Q. Xue, X. Xie, C. Zhi, *Nat. Commun.* **2015**, *6*, 10310; n) Z. F. Liu, S. Fang, F. A. Moura, J. N. Ding, N. Jiang, J. Di, M. Zhang, X. Lepró, D. S. Galvão, C. S. Haines, N. Y. Yuan, S. G. Yin, D. W. Lee, R. Wang, H. Y. Wang, W. Lv, C. Dong, R. C. Zhang, M. J. Chen, Q. Yin, Y. T. Chong, R. Zhang, X. Wang, M. D. Lima, R. Ovalle-Robles, D. Qian, H. Lu, R. H. Baughman, *Science* **2015**, *349*, 400; o) Z. Song, X. Wang, C. Lv, Y. An, M. Liang, T. Ma, D. He, Y. J. Zheng, S. Q. Huang, H. Yu, H. Jiang, *Sci. Rep.* **2015**, *5*, 10988; p) Y.-H. Lee, Y. Kim, T.-I. Lee, I. Lee, J. Shin, H. S. Lee, T.-S. Kim, J. W. Choi, *ACS Nano* **2015**, *9*, 12214; q) Y. Xu, Y. Zhang, Z. Guo, J. Ren, Y. Wang, H. Peng, *Angew. Chem., Int. Ed.* **2015**, *54*, 15390; r) W. Liu, Z. Chen, G. Zhou, Y. Sun, H. R. Lee, C. Liu, H. Yao, Z. Bao, Y. Cui, *Adv. Mater.* **2016**, *28*, 3578; s) Y. Xu, Y. Zhao, J. Ren, Y. Zhang, H. Peng, *Angew. Chem., Int. Ed.* **2016**, *55*, 7979.

[11] L. Nyholm, G. Nystrom, A. Mihranyan, M. Stromme, *Adv. Mater.* **2011**, *23*, 3751.

[12] M. F. De Volder, S. H. Tawfick, R. H. Baughman, A. J. Hart, *Science* **2013**, *339*, 535.

[13] L. Hu, H. Wu, F. La Mantia, Y. Yang, Y. Cui, *ACS Nano* **2011**, *4*, 5843.

[14] Z. Chen, J. W. F. To, C. Wang, Z. Lu, N. Liu, A. Chortos, L. Pan, F. Wei, Y. Cui, Z. Bao, *Adv. Eng. Mater.* **2014**, *4*, 400207; DOI: 10.1002/aenm.201400207.

[15] a) K. Fu, O. Yildiz, H. Bhanushali, Y. Wang, K. Stano, L. Xue, X. Zhang, P. D. Bradford, *Adv. Mater.* **2013**, *25*, 5109; b) L. Hu, N. Liu, M. Eskilsson, G. Zheng, J. McDonough, L. Wågberg, Y. Cui, *Nano Eng.* **2013**, *2*, 138; c) S. Luo, K. Wang, J. Wang, K. Jiang, Q. Li, S. Fan, *Adv. Mater.* **2012**, *24*, 2294; d) K. H. Choi, S. J. Cho, S. J. Chun, J. T. Yoo, C. K. Lee, W. Kim, Q. Wu, S. B. Park, D. H. Choi, S. Y. Lee, S. Y. Lee, *Nano Lett.* **2014**, *14*, 5677; e) Y. Xu, Y. Zhu, F. Han, C. Luo, C. Wang, *Adv. Energy Mater.* **2015**, *5*, 1400753; DOI: 10.1002/adma.201400753.

[16] a) J. Ji, Y. Li, W. Peng, G. Zhang, F. Zhang, X. Fan, *Adv. Mater.* **2015**, *27*, 5264; b) M. Mao, J. Hu, H. Liu, *Int. Energy Res.* **2015**, *39*, 727.

[17] C. Wang, D. Li, C. O. Too, G. G. Wallace, *Chem. Mater.* **2009**, *21*, 2604.

[18] L. Chen, G. Zhou, Z. Liu, X. Ma, J. Chen, Z. Zhang, X. Ma, F. Li, H. M. Cheng, W. Ren, *Adv. Mater.* **2016**, *28*, 510.

[19] a) D. A. Dikin, S. Stankovich, E. J. Zimney, R. D. Piner, G. H. Dommett, G. Evmenenko, S. T. Nguyen, R. S. Ruoff, *Nature* **2007**, *448*, 457; b) G. Eda, G. Fanchini, M. Chhowalla, *Nat. Nanotechnol.* **2008**, *3*, 270.

[20] B. Wang, X. Li, X. Zhang, B. Luo, M. Jin, M. Liang, S. A. Dayeh, S. T. Picraux, L. Zhi, *ACS Nano* **2013**, *7*, 1437.

[21] G. Zeng, N. Shi, M. Hess, X. Chen, W. Cheng, T. Fan, M. Niederberger, *ACS Nano* **2015**, *9*, 4227.

[22] C. Pang, H. Cui, G. Yang, C. Wang, *Nano Lett.* **2013**, *13*, 4708.

[23] Z. Chen, W. Ren, L. Gao, B. Liu, S. Pei, H. M. Cheng, *Nat. Mater.* **2011**, *10*, 424.

[24] N. Li, Z. Chen, W. Ren, F. Lia, H.-M. Cheng, *Proc. Natl. Acad. Sci. USA* **2012**, *109*, 17360.

[25] a) C. Botas, D. Carriazo, G. Singh, T. Rojo, *J. Mater. Chem. A* **2015**, *3*, 13402; b) D. Chao, X. Xia, J. Liu, Z. Fan, C. F. Ng, J. Lin, H. Zhang, Z. X. Shen, H. J. Fan, *Adv. Mater.* **2014**, *26*, 5794; c) M. Chen, J. Liu, D. Chao, J. Wang, J. Yin, J. Lin, H. J. Fan, Z. X. Shen, *Nano Eng.* **2014**, *9*, 364; d) H.-P. Cong, S. Xin, S.-H. Yu, *Nano Energy* **2015**, *13*, 482; e) J. Ji, J. Liu, L. Lai, X. Zhao, Y. Zhen, J. Lin, Y. Zhu, H. Ji, L. L. Zhang, R. S. Ruoff, *ACS Nano* **2015**, *9*, 8609; f) J. Luo, J. Liu, Z. Zeng, C. F. Ng, L. Ma, H. Zhang, J. Lin, Z. Shen, H. J. Fan, *Nano Lett.* **2013**, *13*, 6136; g) X. Shen, T. Qian, J. Zhou, N. Xu, T. Yang, C. Yan, *ACS Appl. Mater. Interfaces* **2015**, *7*, 25298; h) X. Wang, G. Li, F. M. Hassan, M. Li, K. Feng, X. Xiao, Z. Chen, *J. Mater. Chem. A* **2015**, *3*, 3962; i) M. Zou, Z. Ma, Q. Wang, Y. Yang, S. Wu, L. Yang, S. Hu, W. Xu, R. P. S. Han, R. Zou, A. Cao, *J. Mater. Chem. A* **2016**, *4*, 8204.

[26] L. Hu, H. Wu, Y. Gao, A. Cao, H. Li, J. McDough, X. Xie, M. Zhou, Y. Cui, *Adv. Eng. Mater.* **2011**, *1*, 523.

[27] K. Jost, G. Dion, Y. Gogotsi, *J. Mater. Chem. A* **2014**, *2*, 10776.

[28] a) L. Hu, F. La Mantia, H. Wu, X. Xie, J. McDonough, M. Pasta, Y. Cui, *Adv. Eng. Mater.* **2011**, *1*, 1012; b) M. Pasta, F. La Mantia, L. Hu, H. D. Deshazer, Y. Cui, *Nano Res.* **2010**, *3*, 452; c) G. Yu, L. Hu, M. Vosgueritchian, H. Wang, X. Xie, J. R. McDonough, X. Cui, Y. Cui, Z. Bao, *Nano Lett.* **2011**, *11*, 2905.

[29] G. Lui, G. Li, X. Wang, G. Jiang, E. Lin, M. Fowler, A. Yu, Z. Chen, *Nano Eng.* **2016**.

[30] X. Pu, L. Li, H. Song, C. Du, Z. Zhao, C. Jiang, G. Cao, W. Hu, Z. L. Wang, *Adv. Mater.* **2015**, *27*, 2472.

[31] a) J. H. Pikul, H. Gang Zhang, J. Cho, P. V. Braun, W. P. King, *Nat. Commun.* **2013**, *4*, 1732; b) M. Roberts, P. Johns, J. Owen, D. Brandell, K. Edstrom, G. El Enany, C. Guery, D. Golodnitsky, M. Lacey, C. Lecoeur, H. Mazor, E. Peled, E. Perre, M. M. Shaijumon, P. Simon, P.-L. Taberna, *J. Mater. Chem.* **2011**, *21*, 9876; c) X. H. Xia, D. L. Chao, Y. Q. Zhang, Z. X. Shen, H. J. Fan, *Nano Today* **2014**, *9*, 785.

[32] J. Liu, K. Song, P. A. van Aken, J. Maier, Y. Yu, *Nano Lett.* **2014**, *14*, 2597.

[33] H. Lin, W. Weng, J. Ren, L. Qiu, Z. Zhang, P. Chen, X. Chen, J. Deng, Y. Wang, H. Peng, *Adv. Mater.* **2014**, *26*, 1217.

[34] S. W. Kim, J. H. Yun, B. Son, Y. G. Lee, K. M. Kim, Y. M. Lee, K. Y. Cho, *Adv. Mater.* **2014**, *26*, 2977.

[35] C. K. Chan, H. Peng, G. Liu, K. McIlwrath, X. F. Zhang, R. A. Huggins, Y. Cui, *Nat. Nanotechnol.* **2008**, *3*, 31.

[36] A. Goyal, A. L. Reddy, P. M. Ajayan, *Small* **2011**, *7*, 1709.

[37] Y. Li, B. Tan, Y. Wu, *Nano Lett.* **2008**, *8*, 265.

[38] W. Zeng, F. Zheng, R. Li, Y. Zhan, Y. Li, J. Liu, *Nanoscale* **2012**, *4*, 2760.

[39] J. Y. Liao, D. Higgins, G. Lui, V. Chabot, X. Xiao, Z. Chen, *Nano Lett.* **2013**, *13*, 5467.

[40] a) S.-Y. Lee, K.-H. Choi, W.-S. Choi, Y. H. Kwon, H.-R. Jung, H.-C. Shin, J. Y. Kim, *Eng. Environ. Sci.* **2013**, *6*, 2414; b) W. Weng, P. Chen, S. He, X. Sun, H. Peng, *Angew. Chem., Int. Ed.* **2016**, *55*, 6140; c) H. Peng, *Fiber-Shaped Energy Harvesting and Storage Devices*, Springer Verlag, Berlin/Heidelberg, Germany **2014**.

[41] Y. Zhang, Y. Zhao, X. Cheng, W. Weng, J. Ren, X. Fang, Y. Jiang, P. Chen, Z. Zhang, Y. Wang, *Angew. Chem., Int. Ed.* **2015**, *54*, 11177.

[42] Y. H. Kwon, S.-W. Woo, H.-R. Jung, H. K. Yu, K. Kim, B. H. Oh, S. Ahn, S.-Y. Lee, S.-W. Song, J. Cho, H.-C. Shin, J. Y. Kim, *Adv. Mater.* **2012**, *24*, 5192.

[43] W. Weng, Q. Sun, Y. Zhang, H. Lin, J. Ren, X. Lu, M. Wang, H. Peng, *Nano Lett.* **2014**, *14*, 3432.
[44] J. Ren, Y. Zhang, W. Bai, X. Chen, Z. Zhang, X. Fang, W. Weng, Y. Wang, H. Peng, *Angew. Chem., Int. Ed.* **2014**, *53*, 7864.
[45] K. Wang, S. Luo, Y. Wu, X. He, F. Zhao, J. Wang, K. Jiang, S. Fan, *Adv. Funct. Mater.* **2013**, *23*, 846.
[46] M. H. Park, M. Noh, S. Lee, M. Ko, S. Chae, S. Sim, S. Choi, H. Kim, H. Nam, S. Park, J. Cho, *Nano Lett.* **2014**, *14*, 4083.
[47] J. S. Kim, D. Ko, D. J. Yoo, D. S. Jung, C. T. Yavuz, N. I. Kim, I. S. Choi, J. Y. Song, J. W. Choi, *Nano Lett.* **2015**, *15*, 2350.
[48] a) P. Knauth, *Solid State Ionics* **2009**, *180*, 911; b) E. Quartarone, P. Mustarelli, *Chem. Soc. Rev.* **2011**, *40*, 2525.
[49] a) N. Kamaya, K. Homma, Y. Yamakawa, M. Hirayama, R. Kanno, M. Yonemura, T. Kamiyama, Y. Kato, S. Hama, K. Kawamoto, A. Mitsui, *Nat. Mater.* **2011**, *10*, 682; b) Y. Wang, W. D. Richards, S. P. Ong, L. J. Miara, J. C. Kim, Y. Mo, G. Ceder, *Nat. Mater.* **2015**, *14*, 1026.
[50] J. F. Ihlefeld, P. G. Clem, B. L. Doyle, P. G. Kotula, K. R. Fenton, C. A. Apblett, *Adv. Mater.* **2011**, *23*, 5663.
[51] M. Koo, K. I. Park, S. H. Lee, M. Suh, D. Y. Jeon, J. W. Choi, K. Kang, K. J. Lee, *Nano Lett.* **2012**, *12*, 4810.
[52] Y. Seino, T. Ota, K. Takada, A. Hayashi, M. Tatsumisago, *Eng. Environ. Sci.* **2014**, *7*, 627.
[53] Y. J. Nam, S. J. Cho, D. Y. Oh, J. M. Lim, S. Y. Kim, J. H. Song, Y. G. Lee, S. Y. Lee, Y. S. Jung, *Nano Lett.* **2015**, *15*, 3317.
[54] R. C. Agrawal, G. P. Pandey, *J. Physics D: Appl. Phys.* **2008**, *41*, 223001.
[55] Y. Liu, S. Gorgutsa, C. Santato, M. Skorobogatiy, *J. Electrochem. Soc.* **2012**, *159*, A349.
[56] R. Bouchet, S. Maria, R. Meziane, A. Aboulaich, L. Lienafa, J.-P. Bonnet, T. N. T. Phan, D. Bertin, D. Gigmes, D. Devaux, R. Denoyel, M. Armand, *Nat. Mater.* **2013**, *12*, 452.
[57] A. Manuel Stephan, K. S. Nahm, *Polymer* **2006**, *47*, 5952.
[58] W. Liu, N. Liu, J. Sun, P. C. Hsu, Y. Li, H. W. Lee, Y. Cui, *Nano Lett.* **2015**, *15*, 2740.
[59] M. Kammoun, S. Berg, H. Ardebili, *Nanoscale* **2015**, *7*, 17516.
[60] K. K. Fu, Y. Gong, J. Dai, A. Gong, X. Han, Y. Yao, C. Wang, Y. Wang, Y. Chen, C. Yan, Y. Li, E. D. Wachsman, L. Hu, *Proc. Natl. Acad. Sci. USA* **2016**, *113*, 7094.
[61] R. E. Sousa, C. M. Costa, S. Lanceros-Mendez, *ChemSusChem* **2015**, *8*, 3539.
[62] S. H. Kim, K. H. Choi, S. J. Cho, S. Choi, S. Park, S. Y. Lee, *Nano Lett.* **2015**, *15*, 5168.
[63] E. H. Kil, K. H. Choi, H. J. Ha, S. Xu, J. A. Rogers, M. R. Kim, Y. G. Lee, K. M. Kim, K. Y. Cho, S. Y. Lee, *Adv. Mater.* **2013**, *25*, 1395.
[64] a) J. W. Choi, D. Aurbach, *Nat. Rev. Mater.* **2016**, *1*, 16013; b) G. Zheng, S. W. Lee, Z. Liang, H. W. Lee, K. Yan, H. Yao, H. Wang, W. Li, S. Chu, Y. Cui, *Nat. Nanotechnol.* **2014**, *9*, 618; c) Z. Liang, D. Lin, J. Zhao, Z. Lu, Y. Liu, C. Liu, Y. Lu, H. Wang, K. Yan, X. Tao, Y. Cui, *Proc. Natl. Acad. Sci. USA* **2016**, *113*, 2862; d) D. Lin, Y. Liu, Z. Liang, H. W. Lee, J. Sun, H. Wang, K. Yan, J. Xie, Y. Cui, *Nat. Nanotechnol.* **2016**, *11*, 626; e) Y. Liu, D. Lin, Z. Liang, J. Zhao, K. Yan, Y. Cui, *Nat. Commun.* **2016**, *7*, 10992; f) K. Yan, H. W. Lee, T. Gao, G. Zheng, H. Yao, H. Wang, Z. Lu, Y. Zhou, Z. Liang, Z. Liu, S. Chu, Y. Cui, *Nano Lett.* **2014**, *14*, 6016; g) K. Yan, Z. Lu, H.-W. Lee, F. Xiong, P.-C. Hsu, Y. Li, J. Zhao, S. Chu, Y. Cui, *Nat. Energy* **2016**, *1*, 16010.
[65] a) G. Zhou, D.-W. Wang, F. Li, P.-X. Hou, L. Yin, C. Liu, G. Q. Lu, I. R. Gentle, H.-M. Cheng, *Eng. Environ. Sci.* **2012**, *5*, 8901; b) G. Zhou, L. Li, C. Ma, S. Wang, Y. Shi, N. Koratkar, W. Ren, F. Li, H.-M. Cheng, *Nano Energy* **2015**, *11*, 356; c) G. Zhou, L. Li, D. W. Wang, X. Y. Shan, S. Pei, F. Li, H. M. Cheng, *Adv. Mater.* **2015**, *27*, 641.
[66] C. Wang, X. Wang, Y. Yang, A. Kushima, J. Chen, Y. Huang, J. Li, *Nano Lett.* **2015**, *15*, 1796.
[67] L. Li, Z. P. Wu, H. Sun, D. Chen, J. Gao, S. Suresh, P. Chow, C. V. Singh, N. Koratkar, *ACS Nano* **2015**, *9*, 11342.
[68] H. Wang, W. Zhang, H. Liu, Z. Guo, *Angew. Chem., Int. Ed.* **2016**, *55*, 3992.
[69] Q. C. Liu, L. Li, J. J. Xu, Z. W. Chang, D. Xu, Y. B. Yin, X. Y. Yang, T. Liu, Y. S. Jiang, J. M. Yan, X. B. Zhang, *Adv. Mater.* **2015**, *27*, 8095.
[70] Q. C. Liu, J. J. Xu, D. Xu, X. B. Zhang, *Nat. Commun.* **2015**, *6*, 7892.
[71] Y. Zhang, L. Wang, Z. Guo, Y. Xu, Y. Wang, H. Peng, *Angew. Chem., Int. Ed.* **2016**, *55*, 4487.
[72] a) L. David, R. Bhandavat, G. Singh, *ACS Nano* **2014**, *8*, 1759; b) J.-K. Kim, Y. J. Lim, H. Kim, G.-B. Cho, Y. Kim, *Eng. Environ. Sci.* **2015**, *8*, 3589; c) X. Xiong, W. Luo, X. Hu, C. Chen, L. Qie, D. Hou, Y. Huang, *Sci. Rep.* **2015**, *5*, 9254.
[73] J. Fu, D. U. Lee, F. M. Hassan, L. Yang, Z. Bai, M. G. Park, Z. Chen, *Adv. Mater.* **2015**, *27*, 5617.
[74] A. M. Gaikwad, G. L. Whiting, D. A. Steingart, A. C. Arias, *Adv. Mater.* **2011**, *23*, 3251.
[75] P. Simon, Y. Gogotsi, *Nat. Mater.* **2008**, *7*, 845.
[76] L. Huang, D. Chen, Y. Ding, S. Feng, Z. L. Wang, M. Liu, *Nano Lett.* **2013**, *13*, 3135.
[77] J. Xiao, L. Wan, S. Yang, F. Xiao, S. Wang, *Nano Lett.* **2014**, *14*, 831.
[78] Y. Sun, R. B. Sills, X. Hu, Z. W. Seh, X. Xiao, H. Xu, W. Luo, H. Jin, Y. Xin, T. Li, Z. Zhang, J. Zhou, W. Cai, Y. Huang, Y. Cui, *Nano Lett.* **2015**, *15*, 3899.
[79] Y. J. Kang, H. Chung, C.-H. Han, W. Kim, *Nanotechnology* **2012**, *23*, 289501.
[80] X. Xiao, X. Peng, H. Jin, T. Li, C. Zhang, B. Gao, B. Hu, K. Huo, J. Zhou, *Adv. Mater.* **2013**, *25*, 5091.
[81] a) D. L. a. R. B. Kaner, *Nat. Nanotechnol.* **2008**, *3*, 101; b) Y. Shao, M. F. El-Kady, L. J. Wang, Q. Zhang, Y. Li, H. Wang, M. F. Mousavi, R. B. Kaner, *Chem. Soc. Rev.* **2015**, *44*, 3639.
[82] A. Yu, I. Roes, A. Davies, Z. Chen, *Appl. Phys. Lett.* **2010**, *96*, 253105.
[83] F. Liu, S. Song, D. Xue, H. Zhang, *Adv. Mater.* **2012**, *24*, 1089.
[84] K. Parvez, Z. S. Wu, R. Li, X. Liu, R. Graf, X. Feng, K. Mullen, *J. Am. Chem. Soc.* **2014**, *136*, 6083.
[85] a) L. L. Zhang, X. Zhao, M. D. Stoller, Y. Zhu, H. Ji, S. Murali, Y. Wu, S. Perales, B. Clevenger, R. S. Ruoff, *Nano Lett.* **2012**, *12*, 1806; b) F. Xiao, S. Yang, Z. Zhang, H. Liu, J. Xiao, L. Wan, J. Luo, S. Wang, Y. Liu, *Sci. Rep.* **2015**, *5*, 9359; c) L. Liu, Z. Niu, L. Zhang, W. Zhou, S. Xie, *Adv. Mater.* **2014**, *26*, 4855; d) J. Chen, X. Wang, J. Wang, P. S. Lee, *Adv. Energy Mater.* **2016**, *6*, 501745; DOI: 10.1002/aenm.201501745.
[86] Y. He, W. Chen, X. Li, Z. Zhang, J. Fu, C. Zhao, E. Xie, *ACS Nano* **2013**, *7*, 174.
[87] C. Meng, C. Liu, L. Chen, C. Hu, S. Fan, *Nano Lett.* **2010**, *10*, 4025.
[88] Z. Ling, C. E. Ren, M. Q. Zhao, J. Yang, J. M. Giammarco, J. Qiu, M. W. Barsoum, Y. Gogotsi, *Proc. Natl. Acad. Sci. USA* **2014**, *111*, 16676.
[89] M. Acerce, D. Voiry, M. Chhowalla, *Nat. Nanotechnol.* **2015**, *10*, 313.
[90] C. Wu, X. Lu, L. Peng, K. Xu, X. Peng, J. Huang, G. Yu, Y. Xie, *Nat. Commun.* **2013**, *4*, 2431.
[91] C. Hao, B. Yang, F. Wen, J. Xiang, L. Li, W. Wang, Z. Zeng, B. Xu, Z. Zhao, Z. Liu, Y. Tian, *Adv. Mater.* **2016**, *28*, 3194.
[92] W. Chen, R. B. Rakhi, L. Hu, X. Xie, Y. Cui, H. N. Alshareef, *Nano Lett.* **2011**, *11*, 5165.
[93] P. Li, C. Kong, Y. Shang, E. Shi, Y. Yu, W. Qian, F. Wei, J. Wei, K. Wang, H. Zhu, A. Cao, D. Wu, *Nanoscale* **2013**, *5*, 8472.
[94] S. Chen, G. He, H. Hu, S. Jin, Y. Zhou, Y. He, S. He, F. Zhao, H. Hou, *Eng. Environ. Sci.* **2013**, *6*, 2435.

[95] L. Shen, J. Wang, G. Xu, H. Li, H. Dou, X. Zhang, *Adv. Energy Mater.* **2015**, *5*, 400977; DOI: 10.1002/aenm.201400977.
[96] J. Liu, L. Zhang, H. B. Wu, J. Lin, Z. Shen, X. W. Lou, *Eng. Environ. Sci.* **2014**, *7*, 3709.
[97] X.-L. Wu, H.-L. Guo, S. Yang, X. Wang, A.-W. Xu, *ACS Nano* **2013**, *7*, 3589.
[98] L. Hu, X. Xie, N. Liu, Y. Yang, H. Wu, Y. Yao, M. Pasta, Y. Cui, H. N. Alshareef, *ACS Nano* **2011**, *5*, 8904.
[99] Q. Lv, S. Wang, H. Sun, J. Luo, J. Xiao, J. Xiao, F. Xiao, S. Wang, *Nano Lett.* **2016**, *16*, 40.
[100] L. Dong, C. Xu, Y. Li, C. Wu, B. Jiang, Q. Yang, E. Zhou, F. Kang, Q. H. Yang, *Adv. Mater.* **2016**, *28*, 1675.
[101] a) W. Wang, W. Liu, Y. Zeng, Y. Han, M. Yu, X. Lu, Y. Tong, *Adv. Mater.* **2015**, *27*, 3572; b) Q. Liao, S. Jin, G. Yang, C. Wang, *ACS Nano* **2015**, *9*, 5310.
[102] a) D. Pech, M. Brunet, H. Durou, P. Huang, V. Mochalin, Y. Gogotsi, P. L. Taberna, P. Simon, *Nat. Nanotechnol.* **2010**, *5*, 651; b) M. Beidaghi, Y. Gogotsi, *Eng. Environ. Sci.* **2014**, *7*, 867.
[103] Z. S. Wu, K. Parvez, X. Feng, K. Mullen, *Nat. Commun.* **2013**, *4*, 2487.
[104] K. Wang, W. Zou, B. Quan, A. Yu, H. Wu, P. Jiang, Z. Wei, *Adv. Energy. Mater.* **2011**, *1*, 1068.
[105] J. J. Yoo, K. Balakrishnan, J. Huang, V. Meunier, B. G. Sumpter, A. Srivastava, M. Conway, A. L. Reddy, J. Yu, R. Vajtai, P. M. Ajayan, *Nano Lett.* **2011**, *11*, 1423.
[106] I. Nam, S. Park, G.-P. Kim, J. Park, J. Yi, *Chem. Sci.* **2013**, *4*, 1663.
[107] J. Lin, C. Zhang, Z. Yan, Y. Zhu, Z. Peng, R. H. Hauge, D. Natelson, J. M. Tour, *Nano Lett.* **2013**, *13*, 72.
[108] Z. Liu, Z. S. Wu, S. Yang, R. Dong, X. Feng, K. Mullen, *Adv. Mater.* **2016**, *28*, 2217.
[109] J. Zhang, X. S. Zhao, *ChemSusChem* **2012**, *5*, 818.
[110] K. Wang, H. Wu, Y. Meng, Z. Wei, *Small* **2014**, *10*, 14.
[111] J. Huang, K. Wang, Z. Wei, *J. Mater. Chem.* **2010**, *20*, 1117.
[112] C. Zhou, Y. Zhang, Y. Li, J. Liu, *Nano Lett.* **2013**, *13*, 2078.
[113] K. Wang, P. Zhao, X. Zhou, H. Wu, Z. Wei, *J. Mater. Chem.* **2011**, *21*, 16373.
[114] Q. W. Jing Xu, X. Wang, Q. Xiang, B. Liang, D. Chen, G. Shen, *ACS Nano* **2013**, *7*, 5453.
[115] D. Yu, Q. Qian, L. Wei, W. Jiang, K. Goh, J. Wei, J. Zhang, Y. Chen, *Chem. Soc. Rev.* **2015**, *44*, 647.
[116] J. Bae, M. K. Song, Y. J. Park, J. M. Kim, M. Liu, Z. L. Wang, *Angew. Chem., Int. Ed.* **2011**, *50*, 1683.
[117] L. Liu, Y. Yu, C. Yan, K. Li, Z. Zheng, *Nat. Commun.* **2015**, *6*, 7260.
[118] a) Y. Fu, X. Cai, H. Wu, Z. Lv, S. Hou, M. Peng, X. Yu, D. Zou, *Adv. Mater.* **2012**, *24*, 5713; b) Y. H. Yang Huang, M. Zhu, W. Meng, Z. Pei, C. Liu, H. Hu, C. Zhi, *ACS Nano* **2015**, *9*, 6242.
[119] X. Xiao, P. Yang, Y. Gao, H. Jin, W. Ni, W. Zhan, X. Zhang, Y. Cao, L. Gong, W.-C. Yen, W. Mai, J. Chen, K. Huo, Z. L. Wang, Y.-L. Chueh, J. Zhou, *ACS Nano* **2012**, *6*, 9200.
[120] X. Dong, Z. Guo, Y. Song, M. Hou, J. Wang, Y. Wang, Y. Xia, *Adv. Funct. Mater.* **2014**, *24*, 3405.
[121] Y. Meng, Y. Zhao, C. Hu, H. Cheng, Y. Hu, Z. Zhang, G. Shi, L. Qu, *Adv. Mater.* **2013**, *25*, 2326.
[122] Y. Xue, J. Niu, Z. Xia, A. Roy, H. Chen, J. Qu, Z. L. Wang, *Sci. Adv.* **2015**, *1*, e1400198.
[123] G. Qu, J. Cheng, X. Li, D. Yuan, P. Chen, X. Chen, B. Wang, H. Peng, *Adv. Mater.* **2016**, *28*, 3646.
[124] Y. Huang, M. Zhu, Z. Pei, Q. Xue, Y. Huang, C. Zhi, *J. Mater. Chem. A* **2016**, *4*, 1290.
[125] D. Son, J. Lee, S. Qiao, R. Ghaffari, J. Kim, J. E. Lee, C. Song, S. J. Kim, D. J. Lee, S. W. Jun, S. Yang, M. Park, J. Shin, K. Do, M. Lee, K. Kang, C. S. Hwang, N. Lu, T. Hyeon, D. H. Kim, *Nat. Nanotechnol.* **2014**, *9*, 397.
[126] a) D.-H. Kim, N. Lu, R. Ma, Y.-S. Kim, R.-H. Kim, S. Wang, J. Wu, S. M. Won, H. Tao, A. Islam, K. J. Yu, T.-i. Kim, R. Chowdhury, M. Ying, L. Xu, M. Li, H.-J. Chung, H. Keum, M. McCormick, P. Liu, Y.-W. Zhang, F. G. Omenetto, Y. Huang, T. Coleman, J. A. Rogers, *Science* **2011**, *333*, 838; b) S. Xu, Y. Zhang, L. Jia, K. E. Mathewson, K.-I. Jang, J. Kim, H. Fu, X. Huang, P. Chava, R. Wang, S. Bhole, L. Wang, Y. J. Na, Y. Guan, M. Flavin, Z. Han, Y. Huang, J. A. Rogers, *Science* **2014**, *344*, 70; c) S. Bauer, S. Bauer-Gogonea, I. Graz, M. Kaltenbrunner, C. Keplinger, R. Schwodiauer, *Adv. Mater.* **2014**, *26*, 149.
[127] L. Wen, F. Li, H. M. Cheng, *Adv. Mater.* **2016**, *28*, 4306.
[128] a) H. Lee, J.-K. Yoo, J.-H. Park, J. H. Kim, K. Kang, Y. S. Jung, *Adv. Energy Mater.* **2012**, *2*, 976; b) Q. Xiao, Q. Zhang, Y. Fan, X. Wang, R. A. Susantyoko, *Eng. Environ. Sci.* **2014**, *7*, 2261.
[129] W. Weng, Q. Sun, Y. Zhang, S. He, Q. Wu, J. Deng, X. Fang, G. Guan, J. Ren, H. Peng, *Adv. Mater.* **2015**, *27*, 1363.
[130] a) Y. Zhang, W. Bai, J. Ren, W. Weng, H. Lin, Z. Zhang, H. Peng, *J. Mater. Chem. A* **2014**, *2*, 11054; b) Y. Zhang, W. Bai, X. Cheng, J. Ren, W. Weng, P. Chen, X. Fang, Z. Zhang, H. Peng, *Angew. Chem.* **2014**, *53*, 14564.
[131] a) Y. Yang, S. Jeong, L. Hu, H. Wu, S. W. Lee, Y. Cui, *Proc. Natl. Acad. Sci. USA* **2011**, *108*, 13013; b) Y. Zhang, C. J. Sheehan, J. Zhai, G. Zou, H. Luo, J. Xiong, Y. T. Zhu, Q. X. Jia, *Adv. Mater.* **2010**, *22*, 3027.
[132] a) Z. Wang, A. A. Volinsky, N. D. Gallant, *J. Appl. Polymer Sci.* **2014**, *131*, 41050; DOI: 10.1002/app.41050; b) F. Liu, N. A. Hashim, Y. Liu, M. R. M. Abed, K. Li, *J. Membrane Sci.* **2011**, *375*, 1.
[133] O. Kriha, M. Becker, M. Lehmann, D. Kriha, J. Krieglstein, M. Yosef, S. Schlecht, R. B. Wehrspohn, J. H. Wendorff, A. Greiner, *Adv. Mater.* **2007**, *19*, 2483.
[134] a) Y. Sun, W. M. Choi, H. Jiang, Y. Y. Huang, J. A. Rogers, *Nat. Nanotechnol.* **2006**, *1*, 201; b) J. A. Rogers, T. Someya, Y. Huang, *Science* **2010**, *327*, 1603.
[135] Y. Wang, W.-H. Zhong, *ChemElectroChem* **2015**, *2*, 22.
[136] L. Porcarelli, C. Gerbaldi, F. Bella, J. R. Nair, *Sci. Rep.* **2016**, *6*, 19892.
[137] Y. Wang, B. Li, J. Ji, A. Eyler, W.-H. Zhong, *Adv. Energy Mater.* **2013**, *3*, 1557.
[138] H. Zhang, C. Liu, L. Zheng, W. Feng, Z. Zhou, J. Nie, *Electrochim. Acta* **2015**, *159*, 93.
[139] T. Kelly, B. M. Ghadi, S. Berg, H. Ardebili, *Sci. Rep.* **2016**, *6*, 20128.
[140] X. Ji, L. F. Nazar, *J. Mater. Chem.* **2010**, *20*, 9821.
[141] Y. Xie, Y. Liu, Y. Zhao, Y. H. Tsang, S. P. Lau, H. Huang, Y. Chai, *J. Mater. Chem. A* **2014**, *2*, 9142.
[142] D. Qi, Z. Liu, Y. Liu, W. R. Leow, B. Zhu, H. Yang, J. Yu, W. Wang, H. Wang, S. Yin, X. Chen, *Adv. Mater.* **2015**, *27*, 5559.
[143] a) Z. Zhang, J. Deng, X. Li, Z. Yang, S. He, X. Chen, G. Guan, J. Ren, H. Peng, *Adv. Mater.* **2015**, *27*, 356; b) C. Choi, S. H. Kim, H. J. Sim, J. A. Lee, A. Y. Choi, Y. T. Kim, X. Lepró, G. M. Spinks, R. H. Baughman, S. J. Kim, *Sci. Rep.* **2015**, *5*, 9387; DOI: 10.1038/srep09387.
[144] Y.-H. Lee, T.-I. Lee, I. Lee, H. S. Lee, T.-S. Kim, J. W. Choi, *ACS Nano* **2015**, *9*, 12214.
[145] T. Chen, H. Peng, M. Durstock, L. Dai, *Sci. Rep.* **2014**, *4*, 3612.
[146] C. Zhao, C. Wang, Z. Yue, K. Shu, G. G. Wallace, *ACS Appl. Mater. Interfaces* **2013**, *5*, 9008.